Notes on

High Voltage Fields

by

Sivaji Chakravorti

Numerical Computation of Electric Field

Introduction

The design of the insulation of high voltage apparatus between phases and earth and also between the phases is based on the knowledge of electric field distribution and the dielectric properties of the combination of insulating materials used in the system. The principal aim is that the insulation should withstand the electric stresses with adequate reliability and at the same time the insulation should not be over dimensioned.
It is well known that the withstand voltage of the external insulation of apparatus designed with non-self restoring insulation is determined by the maximum value of electric field intensity within the insulation system. Further, corona discharges are eliminated by proper design of high voltage shielding electrodes. Thus a comprehensive study of the electric field distribution in and around high voltage equipment is of great practical importance.
High voltage equipments, in practice, are in most of the cases subjected to a.c. field of frequency 50Hz or 60Hz. These fields may be approximated as quasi-static as the wavelength is much longer compared to the dimension of the components involved. Because of this, the electrostatic field calculation is possible by the different methods in use.

Mathematically, an electric field calculation problem may be formulated as follows:

The purpose is to determine, at each point within the field region of interest, the value of potential $\phi(x,y,z)$ and that of the electric field intensity $\vec{E}(x,y,z)$ are to be determined, which are related as

$$\vec{E}(x,y,z) = -\vec{\nabla}\phi \qquad \text{…. 13.1}$$

In order to do that either the Laplace's Equation for systems without any source of charge in the field region,

$$\vec{\nabla}^2\phi = 0 \qquad \text{…. 13.2}$$

or, the Poisson's Equation for systems with sources of charge in the field region,

$$\vec{\nabla}^2\phi = -\frac{\rho_v}{\varepsilon} \qquad \text{…. 13.3}$$

are required to be solved.

The solutions of these equations are called Boundary Value problems, whereby the boundary conditions are specified by means of the given potential of electrode (Dirichlet's Problem) or by the given value of electric field intensity (Neumann's Problem).

Methods of Determination of Electric Field Distribution

The methods that are employed for determination of electric field are detailed in Fig.13.1.

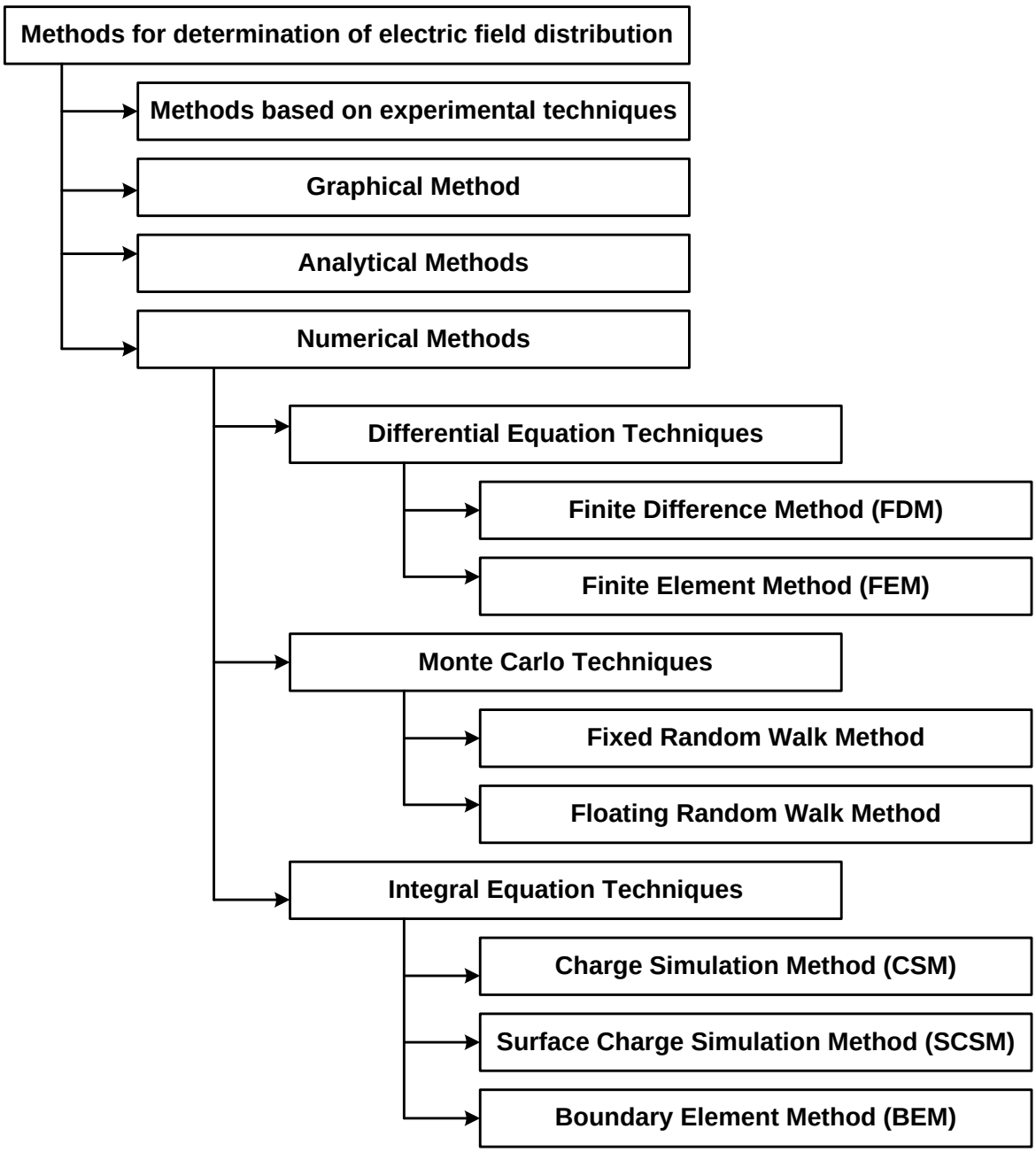

Fig. 13.1 Different methods for determination of electric field distribution

The analytical methods can only be applied to the cases, where the electrode or dielectric boundaries are of simple geometrical forms such as cylinders, spheres etc. In other words, in this method the boundaries are required to be defined exclusively by known mathematical functions. The results obtained are very accurate. But, as it is obvious, this method cannot be applied to complex problems. However, the results obtained by analytical methods for standard configurations are used still today to validate the results obtained by some other approximate methods such as numerical methods.

Earlier the experimental as well as the graphical methods were used to get a fair idea about the nature of field distribution in some practical cases. However, these methods are greatly limited in their areas of usage and the errors involved are usually very high for any complex problem to be taken directly for design purposes.

In more and more engineering problems now-a-days, it is found that it is necessary to obtain approximate numerical solutions rather than exact closed-form solutions. The governing

equations and boundary conditions for these problems could be written without too much effort, but it may be seen immediately that no simple analytical solution can be found. The difficulty in these engineering problems lies in the fact that either the geometry or some other feature of the problem is irregular. Analytical solutions to this type of problems seldom exist; yet these are the kinds of problems that engineers need to solve.

There are several alternatives to overcome this dilemma. One possibility is to make simplifying assumptions ignoring the difficulties to reduce the problem to one that can be easily handled. Sometimes this approach works; but, more often than not, it leads to serious inaccuracies. With the availability of computers today, a more viable alternative is to retain the complexities of the problem and find an approximate numerical solution.

Several approximate numerical analysis methods have evolved over the years as shown in Fig.13.1. For each practical field problem, depending upon the dielectric properties, complexity of contours and boundary conditions, one or the other numerical method is more suited.

Uniqueness Theorem

It states that once any method of solving Poisson's or Laplace's equations subject to given boundary conditions has been found, the problem has been solved once and for all. No other method can ever give a different solution.

Proof:

Consider a volume V bounded by a surface S. Also consider that there is a charge density ρ_v throughout the volume V, and the value of the scalar electric potential on the surface S is ϕ_s. Assume that there are two solutions of Poisson's equation, viz. ϕ_1 and ϕ_2. Then

$$\vec{\nabla}^2\phi_1 = -\frac{\rho_v}{\varepsilon} \quad \text{and} \quad \vec{\nabla}^2\phi_2 = -\frac{\rho_v}{\varepsilon}$$

So, $\vec{\nabla}^2(\phi_1 - \phi_2) = 0$ …. 13.4

Now, each solution must also satisfy the boundary conditions. It is to be noted here that one particular point can not have two different electric potentials, as the work done to move a unit positive charge from infinity to that point is unique. Let, the value of ϕ_1 on the boundary is ϕ_{1s} and the value of ϕ_2 on the boundary is ϕ_{2s} and they must be identical to ϕ_s.

Therefore, $\phi_{1s} = \phi_{2s} = \phi_s$

or, $\phi_{1s} - \phi_{2s} = 0$

For any scalar ϕ and any vector $\vec{D}$, the following vector identity can be written.

$$\vec{\nabla}(\phi\vec{D}) \equiv \phi(\vec{\nabla}.\vec{D}) + \vec{\nabla}\phi.\vec{D} \quad \text{…. 13.5}$$

Consider the scalar as $(\phi_1 - \phi_2)$ and the vector as $\vec{\nabla}(\phi_1 - \phi_2)$. Then from identity (13.5),

$$\vec{\nabla}.\left[(\phi_1 - \phi_2)\vec{\nabla}(\phi_1 - \phi_2)\right] \equiv (\phi_1 - \phi_2)\left[\vec{\nabla}.\vec{\nabla}(\phi_1 - \phi_2)\right] + \vec{\nabla}(\phi_1 - \phi_2).\vec{\nabla}(\phi_1 - \phi_2) \quad \text{…. 13.6}$$

Now, integrating throughout the volume V enclosed by the boundary surface S,

$$\int_V \vec{\nabla}.\left[(\phi_1 - \phi_2)\vec{\nabla}(\phi_1 - \phi_2)\right]dv \equiv \int_V (\phi_1 - \phi_2)\left[\vec{\nabla}.\vec{\nabla}(\phi_1 - \phi_2)\right]dv + \int_V \vec{\nabla}(\phi_1 - \phi_2).\vec{\nabla}(\phi_1 - \phi_2)dv$$

$$\equiv \int_V (\phi_1 - \phi_2)\left[\vec{\nabla}^2(\phi_1 - \phi_2)\right]dv + \int_V \left[\vec{\nabla}(\phi_1 - \phi_2)\right]^2 dv \quad \text{…. 13.7}$$

Applying divergence theorem to the L.H.S of identity (13.7),

$$\int_V \vec{\nabla}.\left[(\phi_1-\phi_2)\vec{\nabla}(\phi_1-\phi_2)\right]dv = \int_S (\phi_{1S}-\phi_{2S})\vec{\nabla}(\phi_1-\phi_2)ds = 0 \quad \text{…. 13.8}$$

as $\phi_{1s} = \phi_{2s}$ on the specified surface *S*.

On the RHS of identity (13.7), $\vec{\nabla}^2(\phi_1-\phi_2) = 0$ from eqn.(13.4). Hence, identity (13.7) reduces to

$$\int_V \left[\vec{\nabla}(\phi_1-\phi_2)\right]^2 dv = 0 \quad \text{…. 13.9}$$

Since, $\left[\vec{\nabla}(\phi_1-\phi_2)\right]^2$ cannot be negative, hence the integrand must be zero everywhere so that the integral may be zero.

Hence,

$$\left[\vec{\nabla}(\phi_1-\phi_2)\right]^2 = 0 \qquad \text{or, } \vec{\nabla}(\phi_1-\phi_2) = 0 \quad \text{…. 13.10}$$

Again, if the gradient of $(\phi_1 - \phi_2)$ is zero everywhere, then

$$\phi_1 - \phi_2 = Constant \quad \text{…. 13.11}$$

This constant may be evaluated by considering a point on the boundary surface *S*. So that,

$$\phi_1 - \phi_2 = \phi_{1s} - \phi_{2s} = 0$$

or, $\phi_1 = \phi_2$

which means that the two solutions are identical.

However, in practice if the same problem is solved by using different numerical techniques the results are not exactly the same. This is due to the fact that the errors in a particular numerical method are often problem dependent and hence the results are not exactly same in all the methods. So, this is not a violation of the Uniqueness theorem.

Procedural Steps in Numerical Electric Field Computation

The following are the procedural steps that need to be followed not only for FDM but for most of the numerical electric field computation methods.

At first, the Region of Interest (ROI) needs to be identified. ROI is the region where the solution for electric field is to be obtained. For example, normally the field solution is not needed within the electrode volume or below the earth surface. Hence, for an isolated electrode and the earth surface, the ROI will be region between the electrode surface and the earth surface as shown in Fig.13.2. Before the ROI is identified, the geometries of the components that comprise the field system need to be defined. This step is now-a-days done with the help of CAD software.

The subsequent procedural step is to discretize the entire ROI or the boundaries to create the nodes where the solution of field will be obtained. Ideally one should find the field solution at each and every point within the ROI. But it will result in immense computational burden and hence the field solution is obtained at discrete nodes. This step is called Discretization and is often done with the help of mesh generators, which are software modules that create the mesh within the entire ROI or on the boundaries. In order that the electric field solution can be obtained at any specific location within the ROI, a pre-defined variation of electric field between successive nodes is assumed. In fact, this assumption is a root cause of inaccuracy of the numerical method.

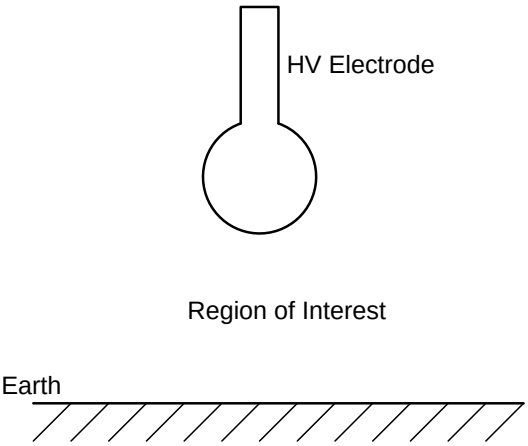

Fig. 13.2 Depiction of Region of Interest for Electric Field Computation

The next step is to create the system of equations based on the numerical method that is being employed. Subsequently, the system of equations is solved using a suitable solver. The solver needs to be chosen depending upon the nature of the coefficient matrix that is being created by the specific numerical method. This solution gives the results for the unknown field quantities at the pre-defined nodes. Finally the results at any desired location is computed using the assumed variation of electric field between the nodes, which is termed as post processing of results. The procedural steps are depicted in Fig.13.3.

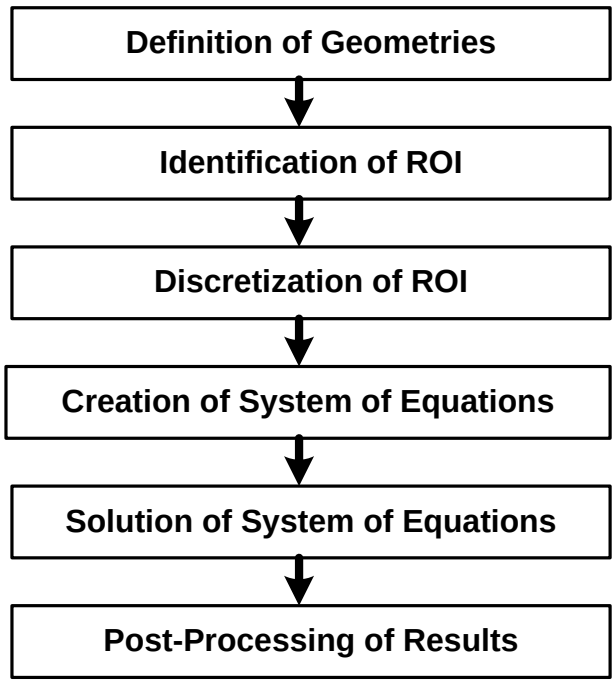

Fig. 13.3 Procedural steps in numerical electric field computation

Numerical Computation of HV Field by Finite Difference Method (FDM)

Introduction

The principle of Finite Difference Method (FDM) is to discretize the entire region under study and solve for unknown potentials a set of coupled simultaneous linear equations which approximate Laplace's or Poisson's equation. In fact this is the objective of most of the numerical field computation techniques that are being used at present.
In Finite Difference Method, for two-dimensional system the entire region of interest is discretized using either rectangles or squares. In 3-dimensional system, the discretization is done using either rectangular parallelepipeds or cubes. Most commonly electric potential is assumed to vary linearly between two successive nodes. However, this is not mandatory. Any other type variation, e.g. quadratic or polynomial, may also be assumed. But, a complex nature of potential variation increases the computational burden greatly and may not always give improved accuracy. If the electric potential is assumed to vary linearly, as it is commonly considered, then the nodes need to be closely spaced where the field varies significantly in space. This is generally the case near the electrodes or dielectric boundaries, particularly in the cases of contours having sharp corners. On the other hand, in the region away from the electrodes or dielectric boundaries, where the field does not change rapidly in space, the nodes may be spaced relatively widely apart.
For multi-dielectric problems, care should be taken during discretization to make sure that only one dielectric is present between two consecutive nodes. This is achieved by arranging one layer of nodes along the dielectric-dielectric interface. This aspect will be taken up in more details in a later section in this chapter.

FDM Equations in 3-D System for Single Dielectric Medium

As stated earlier, in three-dimensional system, discretization is done using either rectangular parallelepipeds or cubes. In such cases, one particular node is connected to six neighboring nodes as shown in Fig. 14.1. As it is assumed that electric potential varies linearly between two successive nodes, it is obvious that potential of that particular node will be related to potentials of the six connected nodes. FDM equation for any unknown node potential is developed in terms of potentials of the connected nodes by satisfying the Laplace's equation. The FDM equation thus developed is a linear equation, which is an approximation of the Laplace's equation that is a second order partial differential equation.
Since the nodal distances in a practical system are unequal, the following approach is normally taken for development of the FDM equations. After discretization, the largest nodal distance (h) is identified within the ROI. Then all the other nodal distances are represented as a fraction of that largest nodal distance as $s_x h$, where $s_x<1$. This is done because the factor s_x is a dimensionless quantity and the FDM equation is developed in terms of potentials of the six connected nodes and the dimensionless factors s_x. Therefore, the developed FDM equation becomes a linear equation involving electric potential only.

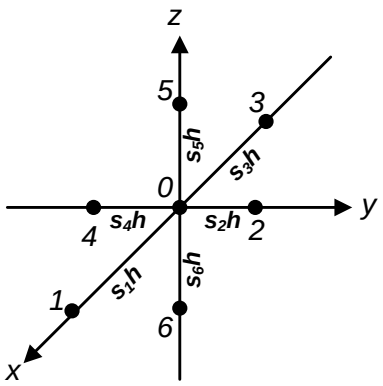

Fig. 14.1 Unequal nodal distances for FDM equation development in 3-D system

As shown in Fig. 14.1, the unknown potential of *node-0* will be formulated in terms of potentials of the six connected nodes *1* through *6*. Electric potential being a continuous function within the ROI and the nodal distances being not large, Taylor series can be applied for the determination of potential of any one connected node from the potential of *node-0*. Taylor series in 3-D system is expressed as follows:

$$f(x+a,y+b,z+c)= f(x,y,z)+a\frac{\partial}{\partial x}f(x,y,z)+b\frac{\partial}{\partial y}f(x,y,z)+c\frac{\partial}{\partial z}f(x,y,z)+ \frac{a^2}{2!}\frac{\partial^2}{\partial x^2}f(x,y,z)+\frac{b^2}{2!}\frac{\partial^2}{\partial y^2}f(x,y,z)+\frac{c^2}{2!}\frac{\partial^2}{\partial z^2}f(x,y,z)+..... \quad \text{... 14.1}$$

Applying Taylor series expansion between the nodes *1* and *0* considering the potential of *node-0* (V_0) as $f(x,y,z)$ and the node potential of *node-1* (V_1) as $f(x+a,y+b,z+c)$ so that $a=s_1h$, $b=c=0$ and neglecting higher order terms,

$$V_1=V_0+s_1h\frac{\partial V}{\partial x}\bigg|_0+\frac{(s_1h)^2}{2}\frac{\partial^2 V}{\partial x^2}\bigg|_0 \quad \text{… 14.2}$$

Similarly, applying Taylor series expansion between the nodes *0* and *3*, such that $a= -s_3h$, $b=c=0$.

$$V_3=V_0-s_3h\frac{\partial V}{\partial x}\bigg|_0+\frac{(s_3h)^2}{2}\frac{\partial^2 V}{\partial x^2}\bigg|_0 \quad \text{… 14.3}$$

Eliminating $\frac{\partial V}{\partial x}$ from eqns. (14.2) and (14.3),

$$\frac{\partial^2 V}{\partial x^2}\bigg|_0=\frac{\left(\frac{V_1}{s_1}+\frac{V_3}{s_3}\right)-V_0\left(\frac{1}{s_1}+\frac{1}{s_3}\right)}{\frac{h^2(s_1+s_3)}{2}} \quad \text{… 14.4}$$

Similarly, between the nodes *2* and *4* in the *y*-direction,

$$\frac{\partial^2 V}{\partial y^2}\bigg|_0=\frac{\left(\frac{V_2}{s_2}+\frac{V_4}{s_4}\right)-V_0\left(\frac{1}{s_2}+\frac{1}{s_4}\right)}{\frac{h^2(s_2+s_4)}{2}} \quad \text{… 14.5}$$

and between the nodes *5* and *6* in the *z*-direction,

$$\left.\frac{\partial^2 V}{\partial z^2}\right|_0 = \frac{\left(\frac{V_5}{s_5}+\frac{V_6}{s_6}\right) - V_0\left(\frac{1}{s_5}+\frac{1}{s_6}\right)}{\frac{h^2\left(s_5+s_6\right)}{2}} \qquad \ldots 14.6$$

Now, Laplace's equation in Cartesian coordinates at *node-0*,

$$\left.\frac{\partial^2 V}{\partial x^2}\right|_0 + \left.\frac{\partial^2 V}{\partial y^2}\right|_0 + \left.\frac{\partial^2 V}{\partial z^2}\right|_0 = 0 \qquad \ldots 14.7$$

So, from eqns. (14.4) through (14.7), eliminating *h*, the FDM equation for the unknown node potential V_0 is obtained as

$$V_0 = \frac{\frac{1}{s_1+s_3}\left(\frac{V_1}{s_1}+\frac{V_3}{s_3}\right)+\frac{1}{s_2+s_4}\left(\frac{V_2}{s_2}+\frac{V_4}{s_4}\right)+\frac{1}{s_5+s_6}\left(\frac{V_5}{s_5}+\frac{V_6}{s_6}\right)}{\frac{1}{s_1 s_3}+\frac{1}{s_2 s_4}+\frac{1}{s_5 s_6}} \qquad \ldots 14.8$$

For equal nodal distances in 3-D system, $s_1 = s_2 = s_3 = s_4 = s_5 = s_6 = 1$. So eqn.(14.8) reduces to

$$V_0 = \frac{1}{6}\left(V_1+V_2+V_3+V_4+V_5+V_6\right) \qquad \ldots 14.9$$

For 2-D system with unequal nodal distances, the FDM equation of (14.8) reduces to

$$V_0 = \frac{\frac{1}{s_1+s_3}\left(\frac{V_1}{s_1}+\frac{V_3}{s_3}\right)+\frac{1}{s_2+s_4}\left(\frac{V_2}{s_2}+\frac{V_4}{s_4}\right)}{\frac{1}{s_1 s_3}+\frac{1}{s_2 s_4}} \qquad \ldots 14.10$$

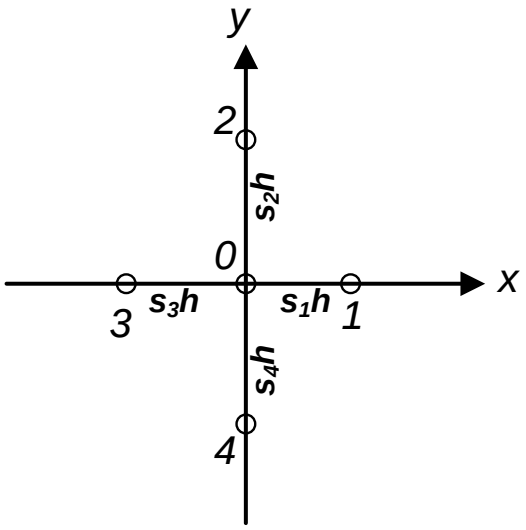

Fig. 14.2 Unequal nodal distances for FDM equation development in 2-D system

For equal nodal distances in 2-D system, the FDM equation of (14.10) reduces to

$$V_0 = \frac{1}{4}\left(V_1+V_2+V_3+V_4\right) \qquad \ldots 14.11$$

Problem 14.1

Consider the 3-D arrangement with single-dielectric having six given planes *a,b,c,d,e,f* as shown in Fig. 14.3. Write the FDM equations for the unknown node potentials V_{01} and V_{02}. Given $h_2=0.6\ h_1$.

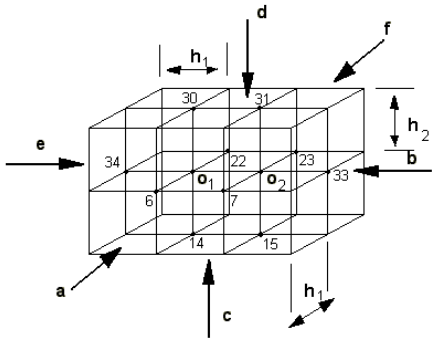

Fig. 14.3 3-D arrangement with two nodes having unknown potentials

Solution:

In this case, for both the nodes 0_1 and 0_2, $s_1= s_2= s_3 = s_4=1$ *and* $s_5= s_6=(h_2/h_1)=0.6$.

$$V_{01}=\frac{\frac{1}{1+1}\left(\frac{V_6}{1}+\frac{V_{22}}{1}\right)+\frac{1}{1+1}\left(\frac{V_{02}}{1}+\frac{V_{34}}{1}\right)+\frac{1}{0.6+0.6}\left(\frac{V_{30}}{0.6}+\frac{V_{14}}{0.6}\right)}{\frac{1}{1}+\frac{1}{1}+\frac{1}{0.6\times 0.6}} \qquad \ldots 14.12$$

and

$$V_{02}=\frac{\frac{1}{1+1}\left(\frac{V_7}{1}+\frac{V_{23}}{1}\right)+\frac{1}{1+1}\left(\frac{V_{33}}{1}+\frac{V_{01}}{1}\right)+\frac{1}{0.6+0.6}\left(\frac{V_{31}}{0.6}+\frac{V_{15}}{0.6}\right)}{\frac{1}{1}+\frac{1}{1}+\frac{1}{0.6\times 0.6}} \qquad \ldots 14.13$$

Problem 14.2

For the 2-D system with single-dielectric as shown in Fig. 14.4, write the FDM equations for the unknown node potentials. Boundary node potentials are given in the figure.

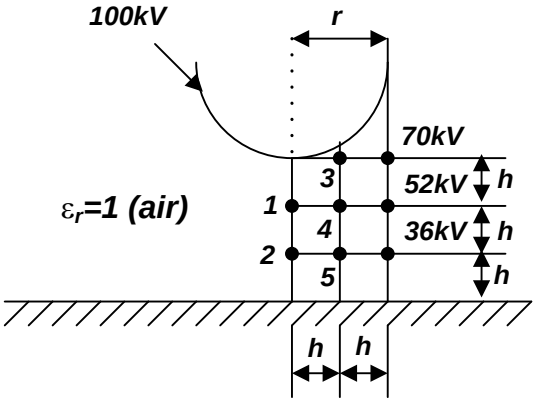

Fig. 14.4 2-D arrangement with nodes having unknown potentials

Solution:

From Fig. 14.4 it may be seen that for the nodes *1, 2, 4* and *5* the nodal distances are equal, i.e. $h = r/2$. For the node *3*, $s_1= s_3= s_4= 1$ and s_2 can be computed trigonometrically as 0.268, as $s_2 h=(r-r\cos\theta)$ *and* $\sin\theta=(h/r)$. Moreover, for the nodes *1* and *2*, symmetry wrt the

central plane is to be considered, such that for the node *1* another node on the LHS has to be considered whose potential will be equal to V_4 and similarly for *node-2*.

$$V_1 = \frac{1}{4}\left(V_4 + 100 + V_4 + V_2\right)$$

$$V_2 = \frac{1}{4}\left(V_5 + V_1 + V_5 + 0\right)$$

$$V_3 = \frac{\frac{1}{1+1}\left(\frac{70}{1} + \frac{100}{1}\right) + \frac{1}{0.268+1}\left(\frac{100}{0.268} + \frac{V_4}{1}\right)}{\frac{1}{1} + \frac{1}{0.268 \times 1}} \qquad \ldots 14.14$$

$$V_4 = \frac{1}{4}\left(52 + V_3 + V_1 + V_5\right)$$

$$V_5 = \frac{1}{4}\left(36 + V_4 + V_2 + 0\right)$$

FDM Equations in Axi-symmetric System for Single Dielectric Medium

When the field is expressed in cylindrical co-ordinates (r, θ, z) and the field distribution is independent of 'θ', then the field distribution is said to be axi-symmetric or rotationally symmetric, e.g. insulators, bushings etc. A typical diagram of an axi-symmetric object is shown in Fig. 14.5.

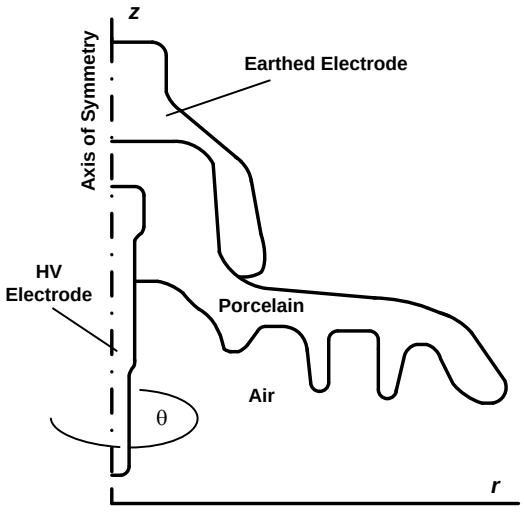

Fig. 14.5 Typical Axi-symmetric insulator geometry

To determine the electric field distribution in axi-symmetric system, Laplace's equation in cylindrical coordinates, as given below, needs to be solved.

$$\frac{\partial^2 V}{\partial r^2} + \frac{1}{r}\frac{\partial V}{\partial r} + \frac{1}{r^2}\frac{\partial^2 V}{\partial \theta^2} + \frac{\partial^2 V}{\partial z^2} = 0 \qquad \ldots 14.15$$

In axi-symmetric system, V is independent of θ, so that eqn.(14.15) reduces to

$$\frac{\partial^2 V}{\partial r^2} + \frac{1}{r}\frac{\partial V}{\partial r} + \frac{\partial^2 V}{\partial z^2} = 0 \qquad \ldots 14.16$$

FDM equation for a node lying away from the axis of symmetry

In Finite Difference Method, for axi-symmetric system the ROI is discretized using either rectangles or squares. In such cases, one particular node is connected to four neighboring nodes as shown in Fig. 14.6. As it is assumed that electric potential varies linearly between two successive nodes, it is obvious that the potential of that particular node will be related to potentials of the four connected nodes. FDM equation for any unknown node potential is developed in terms of potentials of the connected nodes by satisfying the Laplace's equation in cylindrical coordinates. Fig. 14.6 shows the *node-0* with unknown potential lying at a certain distance away from the axis of symmetry. In such a case, the radial distance of the *node-0* from the axis of symmetry is also taken as multiple (*sh*) of the largest nodal distance *h*.

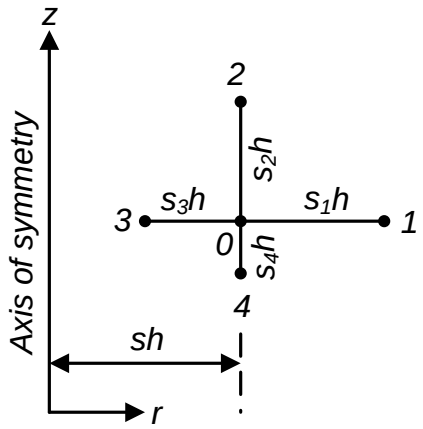

Fig. 14.6 Unequal nodal distances for FDM equation development in axi-symmetric system for a node lying away from the axis of symmetry

From Taylor series expansion between the nodes *1* and *0* in the *r*-direction, neglecting higher order terms,

$$V_1 = V_0 + s_1 h \left.\frac{\partial V}{\partial r}\right|_0 + \frac{(s_1 h)^2}{2} \left.\frac{\partial^2 V}{\partial r^2}\right|_0 \quad \ldots 14.17$$

Similarly, from Taylor series expansion between the nodes *0* and *3* in the *r*-direction,

$$V_3 = V_0 - s_3 h \left.\frac{\partial V}{\partial r}\right|_0 + \frac{(s_3 h)^2}{2} \left.\frac{\partial^2 V}{\partial r^2}\right|_0 \quad \ldots 14.18$$

Eliminating $\frac{\partial V}{\partial r}$ from eqns. (14.17) and (14.18),

$$\left.\frac{\partial^2 V}{\partial r^2}\right|_0 = \frac{\left(\frac{V_1}{s_1} + \frac{V_3}{s_3}\right) - V_0\left(\frac{1}{s_1} + \frac{1}{s_3}\right)}{\frac{h^2 (s_1 + s_3)}{2}} \quad \ldots 14.19$$

Eliminating $\frac{\partial^2 V}{\partial r^2}$ from eqns. (14.17) and (14.18),

$$\left.\frac{\partial V}{\partial r}\right|_0 = \frac{\dfrac{V_1}{s_1^2} - \dfrac{V_3}{s_3^2} - V_o\left(\dfrac{1}{s_1^2} - \dfrac{1}{s_3^2}\right)}{h\left(\dfrac{1}{s_1} + \dfrac{1}{s_3}\right)} \qquad \ldots 14.20$$

Considering the fact that the radial distance of *node-0* from the axis of symmetry is $r = sh$,

$$\left.\frac{1}{r}\frac{\partial V}{\partial r}\right|_0 = \left.\frac{1}{sh}\frac{\partial V}{\partial r}\right|_0 = \frac{\dfrac{V_1}{s_1^2} - \dfrac{V_3}{s_3^2} - V_o\left(\dfrac{1}{s_1^2} - \dfrac{1}{s_3^2}\right)}{sh^2\left(\dfrac{1}{s_1} + \dfrac{1}{s_3}\right)} \qquad \ldots 14.21$$

Similarly, between the nodes *2* and *4* in the *z*-direction,

$$\left.\frac{\partial^2 V}{\partial z^2}\right|_0 = \frac{\left(\dfrac{V_2}{s_2} + \dfrac{V_4}{s_4}\right) - V_0\left(\dfrac{1}{s_2} + \dfrac{1}{s_4}\right)}{\dfrac{h^2\left(s_2 + s_4\right)}{2}} \qquad \ldots 14.22$$

Putting the relevant expressions from eqns. (14.19), (14.21) and (14.22) in the Laplace's equation of (14.16), the FDM equation for the unknown node potential V_0 can be obtained as

$$V_o = \frac{\dfrac{1}{s_1 + s_3}\left\{\left(\dfrac{2s + s_3}{s_1}\right)V_1 + \left(\dfrac{2s - s_1}{s_3}\right)V_3\right\} + \dfrac{2s}{s_2 + s_4}\left(\dfrac{V_2}{s_2} + \dfrac{V_4}{s_4}\right)}{\dfrac{2s + s_3 - s_1}{s_1 s_3} + \dfrac{2s}{s_2 s_4}} \qquad \ldots 14.23$$

For an axi-symmetric arrangement with equal nodal distances, i.e. $s_1 = s_2 = s_3 = s_4 = 1$, eqn. (14.23) reduces to

$$V_o = \frac{1}{4}\left(V_1 + V_2 + V_3 + V_4\right) + \frac{V_1 - V_3}{8s} \qquad \ldots 14.24$$

It may be seen from the above equation that for a node lying on the axis of symmetry, i.e. for *s=0*, eqn. (14.24) is not valid. Hence, the FDM equation for a node lying on the axis of symmetry needs to be developed separately.

FDM equation for a node lying on the axis of symmetry

Fig. 14.7 shows an axi-symmetric nodal arrangement with unequal nodal distances where the *node-0* having unknown node potential is lying on the axis of symmetry.

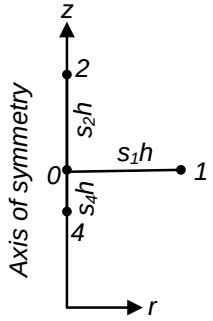

Fig. 14.7 Axi-symmetric system with unequal nodal distances with a node lying on the axis of symmetry

For an axi-symmetric system, along the axis of symmetry the electric flux lines are tangent to the axis. In other words, as $r \to 0, \frac{\partial V}{\partial r} \to 0$.

So, applying L-Hospital's rule, $\underset{r \to 0}{Lt} \frac{1}{r} \frac{\partial V}{\partial r} = \frac{\partial^2 V}{\partial r^2}$.

Hence, for a node lying on the axis of symmetry, Laplace's equation of (14.16) is modified to

$$2 \frac{\partial^2 V}{\partial r^2} + \frac{\partial^2 V}{\partial z^2} = 0 \qquad \ldots 14.25$$

From Taylor series expansion between the nodes *1* and *0* in the *r*-direction, neglecting higher order terms,

$$V_1 = V_0 + s_1 h \frac{\partial V}{\partial r}\bigg|_0 + \frac{(s_1 h)^2}{2} \frac{\partial^2 V}{\partial r^2}\bigg|_0 \qquad \ldots 14.26$$

But, as $r \to 0, \frac{\partial V}{\partial r} \to 0$. So, from eqn. (14.26)

$$\frac{\partial^2 V}{\partial r^2}\bigg|_0 = \frac{2(V_1 - V_o)}{(s_1 h)^2} \qquad \ldots 14.27$$

Following eqn. (14.22) applying Taylor series between the nodes *2, 0* and *4* in the *z*-direction,

$$\frac{\partial^2 V}{\partial z^2}\bigg|_0 = \frac{\left(\frac{V_2}{s_2} + \frac{V_4}{s_4}\right) - V_0\left(\frac{1}{s_2} + \frac{1}{s_4}\right)}{\frac{h^2 (s_2 + s_4)}{2}} \qquad \ldots 14.28$$

Then satisfying the Laplace's equation of (14.25) with the help of eqns. (14.27) and (14.28), the FDM equation for a node lying on the axis of symmetry can be obtained as follows

$$V_o = \frac{\frac{2V_1}{s_1^2} + \frac{1}{s_2 + s_4}\left(\frac{V_2}{s_2} + \frac{V_4}{s_4}\right)}{\frac{2}{s_1^2} + \frac{1}{s_2 s_4}} \qquad \ldots 14.29$$

For equal nodal distances, i.e. for $s_1 = s_2 = s_4 = 1$, eqn. (14.29) reduces to

$$V_0 = \frac{1}{6}(4V_1 + V_2 + V_4) \qquad \ldots 14.30$$

Problem 14.3

For the axi-symmetric arrangement with equal nodal distances as shown in Fig. 14.8, write the FDM equations for the unknown node potentials.

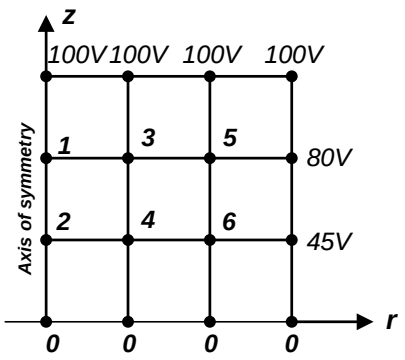

Fig. 14.8 Nodal arrangement pertaining to problem 14.3

Solution:

It may be noted from Fig. 14.8 that the nodes *1* and *2* lie on the axis of symmetry, while the nodes *3, 4, 5* and *6* lie away from the axis of symmetry.

$$V_1 = \frac{1}{6}\left(4V_3 + 100 + V_2\right)$$

$$V_2 = \frac{1}{6}\left(4V_4 + V_1 + 0\right)$$

$$V_3 = \frac{1}{4}\left(V_5 + 100 + V_1 + V_4\right) + \frac{V_5 - V_1}{8 \times 1} \quad \text{as } s = 1$$

$$V_4 = \frac{1}{4}\left(V_6 + V_3 + V_2 + 0\right) + \frac{V_6 - V_2}{8 \times 1} \quad \text{as } s = 1$$

$$V_5 = \frac{1}{4}\left(80 + 100 + V_3 + V_6\right) + \frac{80 - V_3}{8 \times 2} \quad \text{as } s = 2$$

$$V_6 = \frac{1}{4}\left(45 + V_5 + V_4 + 0\right) + \frac{45 - V_4}{8 \times 2} \quad \text{as } s = 2$$

Problem 14.4

For the axi-symmetric system with single-dielectric as shown in Fig. 14.9, write the FDM equations for the unknown node potentials. Boundary node potentials are given in the figure.

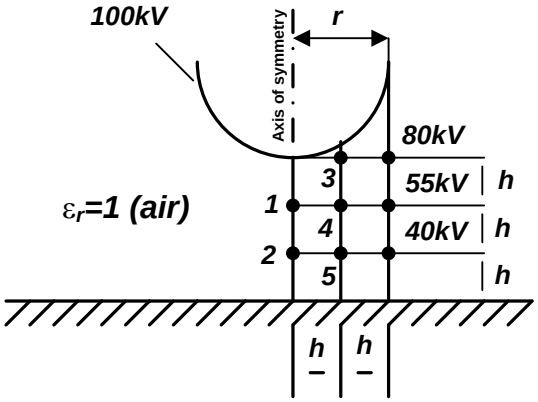

Fig. 14.9 Nodal arrangement pertaining to problem 14.4

Solution:

It may be noted from Fig. 14.9 that for the nodes *1,2,4* and *5* the nodal distances are equal, out of which the nodes *1* and *2* lie on the axis of symmetry. Nodes *3*, *4* and *5* lie away from the axis of symmetry, out of which the nodal distances for *node-3* are unequal such that $s_1 = s_3 = s_4 = 1$ and $s_2 = 0.268$.

$$V_1 = \frac{1}{6}\left(4V_4 + 100 + V_2\right)$$

$$V_2 = \frac{1}{6}\left(4V_5 + V_1 + 0\right)$$

$$V_3 = \frac{\dfrac{1}{1+1}\left\{\left(\dfrac{2\times1+1}{1}\right)80 + \left(\dfrac{2\times1-1}{1}\right)100\right\} + \dfrac{2\times1}{0.268+1}\left(\dfrac{100}{0.268} + \dfrac{V_4}{1}\right)}{\dfrac{2\times1+1-1}{1\times1} + \dfrac{2\times1}{0.268\times1}}$$

$$V_4 = \frac{1}{4}\left(55 + V_3 + V_1 + V_5\right) + \frac{55 - V_1}{8 \times 1} \quad \text{as } s = 1$$

$$V_5 = \frac{1}{4}\left(40 + V_4 + V_2 + 0\right) + \frac{40 - V_2}{8 \times 1} \qquad \text{as } s = 1$$

FDM Equations in Three-Dimensional System for Multi-Dielectric Media

Since the commonly used assumption in finite difference method is linear variation of electric potential between two successive nodes, hence it is imperative that there should not be two different dielectric media between two successive nodes. In other words, during discretization it should be ensured that one set of nodes will always be on the dielectric interface. Fig.14.10 shows one such nodal distribution with unequal nodal distances. The *y-z* plane is considered to be the dielectric interface and one set of nodes is on the dielectric interface. For all the nodes that lie within either medium *1* or medium *2* there will be only that dielectric between any two successive nodes and hence the FDM equations for single-dielectric medium could be used for such nodes. But for the nodes lying on the dielectric interface it is not the case. As shown in Fig.14.10 between the nodes *0* and *1* there is medium-*1* and between *0* and *3* there is medium-*2*. So FDM equation needs to be developed for the nodes that lie on the dielectric interface applying suitable boundary conditions.

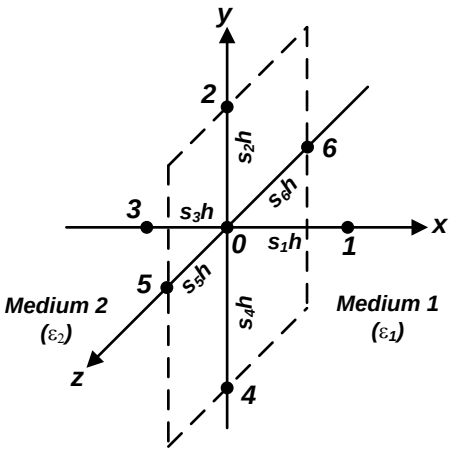

Fig. 14.10 Nodal arrangement for FDM equation development in 3-D system with multi-dielectric media

For Laplacian field, i.e. considering that the dielectric boundary does not have any free charge present on it, the necessary boundary condition is that the normal component of flux density remains constant on both the sides of the dielectric interface. For the nodal arrangement shown in Fig. 14.10, the *x*-component of electric flux density is the normal component on the dielectric interface as the *y-z* plane is the dielectric interface. Hence,

$$\vec{D}_x = \vec{D}'_x$$

$$or, \quad \varepsilon_1 \vec{E}_x = \varepsilon_2 \vec{E}'_x$$

$$or, \quad -\varepsilon_1 \frac{\partial V}{\partial x} = -\varepsilon_2 \frac{\partial V'}{\partial x} \qquad \ldots 14.31$$

$$or, \quad \frac{\partial V'}{\partial x} = \frac{\varepsilon_1}{\varepsilon_2} \frac{\partial V}{\partial x} = K \frac{\partial V}{\partial x}$$

$$where\ K = \frac{\varepsilon_1}{\varepsilon_2}$$

Here, it is to be noted that two potential functions need to be considered on the two sides of the dielectric interface as shown in eqn. (14.31). The potential function V is valid for medium-*1* and V' is valid for medium-*2*.

Accordingly two Laplace's equation, one with V and the other with V', need to be satisfied in this case, as given in eqn. (14.32a) and (14.32b). Eqn. (14.32a) is valid for medium-*1*, while eqn. (14.32b) is valid for medium-*2*.

$$\frac{\partial^2 V}{\partial x^2}+\frac{\partial^2 V}{\partial y^2}+\frac{\partial^2 V}{\partial z^2}=0 \qquad \ldots 14.32a$$

$$\frac{\partial^2 V'}{\partial x^2}+\frac{\partial^2 V'}{\partial y^2}+\frac{\partial^2 V'}{\partial z^2}=0 \qquad \ldots 14.32b$$

Now, from Taylor series expansion between the pair of nodes, the following expressions are obtained

$$V_1 = V_0 + s_1 h\frac{\partial V}{\partial x}\bigg|_0 + \frac{s_1^2 h^2}{2}\frac{\partial^2 V}{\partial x^2}\bigg|_0 \quad \text{between the nodes } 1 \text{ and } 0 \qquad \ldots 14.33a$$

$$V_3 = V_0 - s_3 h\frac{\partial V'}{\partial x}\bigg|_0 + \frac{s_3^2 h^2}{2}\frac{\partial^2 V'}{\partial x^2}\bigg|_0 \quad \text{between the nodes } 0 \text{ and } 3 \qquad \ldots 14.33b$$

$$V_2 = V_0 + s_2 h\frac{\partial V}{\partial y}\bigg|_0 + \frac{s_2^2 h^2}{2}\frac{\partial^2 V}{\partial y^2}\bigg|_0 \quad \text{between the nodes } 2 \text{ and } 0 \qquad \ldots 14.33c$$

$$V_4 = V_0 - s_4 h\frac{\partial V}{\partial y}\bigg|_0 + \frac{s_4^2 h^2}{2}\frac{\partial^2 V}{\partial y^2}\bigg|_0 \quad \text{between the nodes } 0 \text{ and } 4 \qquad \ldots 14.33d$$

$$V_5 = V_0 + s_5 h\frac{\partial V}{\partial z}\bigg|_0 + \frac{s_5^2 h^2}{2}\frac{\partial^2 V}{\partial z^2}\bigg|_0 \quad \text{between the nodes } 5 \text{ and } 0 \qquad \ldots 14.33e$$

$$V_6 = V_0 - s_6 h\frac{\partial V}{\partial z}\bigg|_0 + \frac{s_6^2 h^2}{2}\frac{\partial^2 V}{\partial z^2}\bigg|_0 \quad \text{between the nodes } 0 \text{ and } 6 \qquad \ldots 14.33f$$

It is to be mentioned here that the nodes *0*, *2*, *4*, *5* and *6* lie on the dielectric interface. According to the boundary conditions on dielectric-dielectric interface, electric potential and tangential component of electric field remain constant on the dielectric interface.

From eqn. (14.33a)
$$\frac{\partial^2 V}{\partial x^2}\bigg|_0 = \frac{V_1 - V_0 - s_1 h\dfrac{\partial V}{\partial x}\bigg|_0}{\dfrac{s_1^2 h^2}{2}} \qquad \ldots 14.34$$

and from eqn. (14.33b)
$$\frac{\partial^2 V'}{\partial x^2}\bigg|_0 = \frac{V_3 - V_0 + s_3 h\dfrac{\partial V'}{\partial x}\bigg|_0}{\dfrac{s_3^2 h^2}{2}} = \frac{V_3 - V_0 + s_3 hK\dfrac{\partial V}{\partial x}\bigg|_0}{\dfrac{s_3^2 h^2}{2}} \qquad \ldots 14.35$$

From eqns. (14.33c) and (14.33d) along the *y*-direction on the *y*-*z* plane,

$$\frac{\partial^2 V}{\partial y^2}\bigg|_0 = \frac{\left(\dfrac{V_2}{s_2}+\dfrac{V_4}{s_4}\right) - V_0\left(\dfrac{1}{s_2}+\dfrac{1}{s_4}\right)}{\dfrac{h^2\left(s_2+s_4\right)}{2}} = \frac{\partial^2 V'}{\partial y^2}\bigg|_0 \qquad \ldots 14.36$$

and from eqns. (14.33e) and (14.33f) along the *z*-direction on the *y*-*z* plane,

$$\left.\frac{\partial^2 V}{\partial z^2}\right|_0 = \frac{\left(\frac{V_5}{s_5}+\frac{V_6}{s_6}\right) - V_0\left(\frac{1}{s_5}+\frac{1}{s_6}\right)}{\frac{h^2\left(s_5+s_6\right)}{2}} = \left.\frac{\partial^2 V'}{\partial z^2}\right|_0 \qquad \ldots 14.37$$

From eqn. (14.32a), i.e. the Laplace's equation that is valid for medium-*1*,

$$\frac{V_1 - V_0 - s_1 h\left.\frac{\partial V}{\partial x}\right|_0}{\frac{s_1^2 h^2}{2}} + \frac{\left(\frac{V_2}{s_2}+\frac{V_4}{s_4}\right) - V_0\left(\frac{1}{s_2}+\frac{1}{s_4}\right)}{\frac{h^2\left(s_2+s_4\right)}{2}} + \frac{\left(\frac{V_5}{s_5}+\frac{V_6}{s_6}\right) - V_0\left(\frac{1}{s_5}+\frac{1}{s_6}\right)}{\frac{h^2\left(s_5+s_6\right)}{2}} = 0 \qquad \ldots 14.38$$

and from eqn. (14.32b), i.e. the Laplace's equation that is valid for medium-*2*,

$$\frac{V_3 - V_0 + s_3 hK\left.\frac{\partial V}{\partial x}\right|_0}{\frac{s_3^2 h^2}{2}} + \frac{\left(\frac{V_2}{s_2}+\frac{V_4}{s_4}\right) - V_0\left(\frac{1}{s_2}+\frac{1}{s_4}\right)}{\frac{h^2\left(s_2+s_4\right)}{2}} + \frac{\left(\frac{V_5}{s_5}+\frac{V_6}{s_6}\right) - V_0\left(\frac{1}{s_5}+\frac{1}{s_6}\right)}{\frac{h^2\left(s_5+s_6\right)}{2}} = 0 \qquad \ldots 14.39$$

Eliminating $\left.\frac{\partial V}{\partial x}\right|_0$ from eqns. (14.38) and (14.39),

$$V_0 = \frac{\frac{V_1}{s_1}+\frac{V_3}{s_3 K}+\frac{s_1 K + s_3}{K}\left[\frac{1}{\left(s_2+s_4\right)}\left(\frac{V_2}{s_2}+\frac{V_4}{s_4}\right)+\frac{1}{\left(s_5+s_6\right)}\left(\frac{V_5}{s_5}+\frac{V_6}{s_6}\right)\right]}{\frac{1}{s_1}+\frac{1}{s_3 K}+\frac{s_1 K + s_3}{K}\left[\frac{1}{s_2 s_4}+\frac{1}{s_5 s_6}\right]} \qquad \ldots 14.40$$

Eqn.(14.40) is the FDM equation for unknown potential of a node lying on the dielectric interface in three-dimensional system with unequal nodal distances.

For equal nodal distances in three-dimensional multi-dielectric system, i.e. when $s_1 = s_2 = s_3 = s_4 = s_5 = s_6 = 1$, eqn.(14.40) reduces to

$$V_0 = \frac{V_1\frac{2K}{K+1}+V_2+\frac{2V_3}{K+1}+V_4+V_5+V_6}{6} \qquad \ldots 14.41$$

For two-dimensional multi-dielectric system with unequal nodal distances, the FDM equation for unknown potential of a node lying on the dielectric interface will be as follows, where the dielectric interface is considered to be along the y-axis, as shown in Fig. 14.11.

$$V_0 = \frac{\frac{V_1}{s_1}+\frac{V_3}{s_3 K}+\frac{s_1 K + s_3}{K\left(s_2+s_4\right)}\left(\frac{V_2}{s_2}+\frac{V_4}{s_4}\right)}{\frac{1}{s_1}+\frac{1}{s_3 K}+\frac{s_1 K + s_3}{K s_2 s_4}} \qquad \ldots 14.42$$

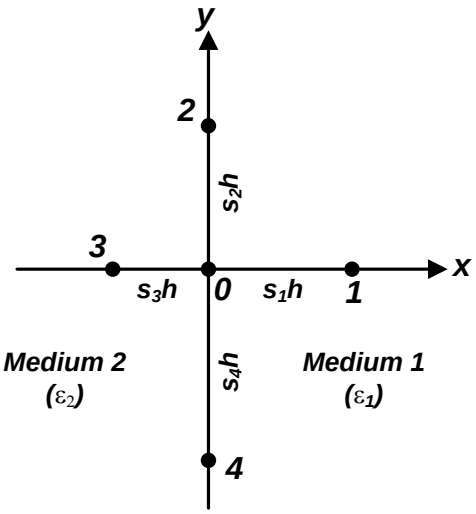

Fig. 14.11 Nodal arrangement for FDM equation development in 2-D system with multi-dielectric media

For equal nodal distances in two-dimensional multi-dielectric system, i.e. when $s_1 = s_2 = s_3 = s_4 = 1$, eqn.(14.42) reduces to

$$V_0 = \frac{V_1 \frac{2K}{K+1} + V_2 + \frac{2V_3}{K+1} + V_4}{4} \qquad \ldots 14.43$$

Problem 14.5

For the three-dimensional arrangement with two different dielectric media as shown in Fig. 14.12, write the FDM equations for the nodes *1*, *2* and *3*. The known node potentials are as follows: $V_{13}=V_{23}=V_{33}=100$V, $V_{14}=V_{24}=V_{34}=0$V, $V_{11}=V_{21}=V_{31}=50$V, $V_{12}=V_{22}=V_{32}=60$V and $V_{15}=V_{35}=55$V. Given that $\varepsilon_1=4$ and $\varepsilon_2=1$.

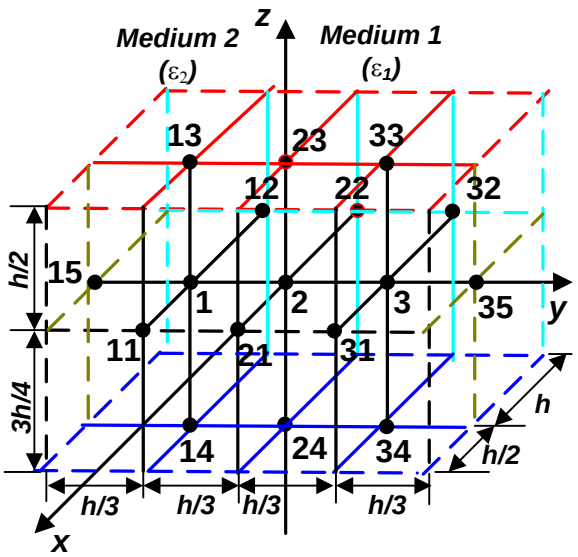

Fig. 14.12 Nodal arrangement pertaining to Problem 14.5

Solution:

In this problem, the largest nodal distance is *h*.

For *node-1*: $s_1=0.5$, $s_3=1$, $s_2= s_4=0.333$, $s_5=0.5$ and $s_6=0.75$. So as per eqn. 14.8

$$V_1 = \frac{\frac{1}{0.5+1}\left(\frac{50}{0.5}+\frac{60}{1}\right)+\frac{1}{0.333+0.333}\left(\frac{V_2}{0.333}+\frac{55}{0.333}\right)+\frac{1}{0.5+0.75}\left(\frac{100}{0.5}+\frac{0}{0.75}\right)}{\frac{1}{0.5\times1}+\frac{1}{0.333\times0.333}+\frac{1}{0.5\times0.75}}$$

Similarly for *node-3*: s_1=0.5, s_3=1, s_2= s_4=0.333, s_5=0.5 and s_6=0.75. So as per eqn. 14.8

$$V_3 = \frac{\frac{1}{0.5+1}\left(\frac{50}{0.5}+\frac{60}{1}\right)+\frac{1}{0.333+0.333}\left(\frac{55}{0.333}+\frac{V_2}{0.333}\right)+\frac{1}{0.5+0.75}\left(\frac{100}{0.5}+\frac{0}{0.75}\right)}{\frac{1}{0.5\times1}+\frac{1}{0.333\times0.333}+\frac{1}{0.5\times0.75}}$$

For *node-2*, as per eqn. 14.40, V_1=V_3, V_3=V_1, V_2=V_{23}=100V, V_4=V_{24}=0V, V_5=V_{21}=50V and V_6=V_{22}=60V and s_1= s_3=0.333, s_2=0.5, s_4=0.75, s_5=0.5, s_6=1 and K= ($\varepsilon_1/\varepsilon_2$)=4.

$$V_2 = \frac{\frac{V_3}{0.333}+\frac{V_1}{0.333\times4}+\frac{0.333\times4+0.333}{4}\left[\frac{1}{(0.5+0.75)}\left(\frac{100}{0.5}+\frac{0}{0.75}\right)+\frac{1}{(0.5+1)}\left(\frac{50}{0.5}+\frac{60}{1}\right)\right]}{\frac{1}{0.333}+\frac{1}{0.333\times4}+\frac{0.333\times4+0.333}{4}\left[\frac{1}{0.5\times0.75}+\frac{1}{0.5\times1}\right]}$$

Problem 14.6

For the 2-dimensional multi-dielectric configuration with series dielectric arrangement as shown in Fig. 14.13, write the FDM equations for the nodes having unknown potentials.

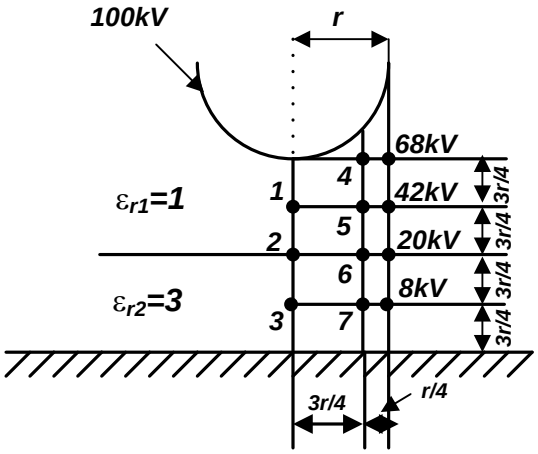

Fig. 14.13 Nodal arrangement pertaining to problem 14.6

Solution:

For the nodes *1, 2* and *3*, symmetry of the configuration has to be considered wrt the central plane. The nodal distances are equal for these three nodes.

For *node-1*:

$$V_1 = \frac{1}{4}\left(V_5 + 100 + V_5 + V_2\right)$$

For *node-2*: As per eqn. 14.43, V_1=V_1, V_2=V_6, V_3=V_3 and V_4=V_6 and K = (1/3).

$$V_2 = \frac{\frac{2\times0.333}{0.333+1}V_1 + V_6 + \frac{2V_3}{0.333+1} + V_6}{4}$$

For *node-3*:

$$V_3 = \frac{1}{4}\left(V_7 + V_2 + V_7 + 0\right)$$

For *node-4*: The nodal distances are unequal such that s_1=(1/3), s_2=0.882, s_3=s_4=1 because the largest nodal distance is (*3r/4*). Then as per eqn. 14.10

$$V_4 = \frac{\frac{1}{0.333+1}\left(\frac{68}{0.333}+\frac{100}{1}\right)+\frac{1}{0.882+1}\left(\frac{100}{0.882}+\frac{V_5}{1}\right)}{\frac{1}{0.333\times 1}+\frac{1}{0.882\times 1}}$$

For *node-5*: The nodal distances are unequal such that s_1=(1/3), s_2=1, s_3=s_4=1. Then as per eqn. 14.10

$$V_5 = \frac{\frac{1}{0.333+1}\left(\frac{42}{0.333}+\frac{V_1}{1}\right)+\frac{1}{1+1}\left(\frac{V_4}{1}+\frac{V_6}{1}\right)}{\frac{1}{0.333\times 1}+\frac{1}{1\times 1}}$$

For *node-6*: As per eqn. 14.42, V_1=V_5, V_2=V_2, V_3=V_7 and V_4=20 and K = (1/3). Nodal distance factors are s_1=s_2=s_3=1 and s_4=(1/3).

$$V_6 = \frac{\frac{V_5}{1}+\frac{V_7}{1\times 0.333}+\frac{1\times 0.333+1}{0.333(1+0.333)}\left(\frac{V_2}{1}+\frac{V_4}{0.333}\right)}{\frac{1}{1}+\frac{1}{1\times 0.333}+\frac{1\times 0.333+1}{0.333\times 1\times 0.333}}$$

For *node-7*: The nodal distances are unequal such that s_1=(1/3), s_2=s_3=s_4=1. Then as per eqn. 14.10

$$V_7 = \frac{\frac{1}{0.333+1}\left(\frac{8}{0.333}+\frac{V_3}{1}\right)+\frac{1}{1+1}\left(\frac{V_6}{1}+\frac{0}{1}\right)}{\frac{1}{0.333\times 1}+\frac{1}{1\times 1}}$$

Problem 14.7

For the 2-dimensional multi-dielectric configuration with parallel dielectric arrangement as shown in Fig. 14.14, write the FDM equations for the nodes having unknown potentials.

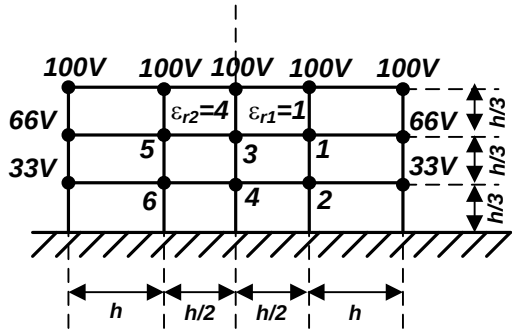

Fig. 14.14 Nodal arrangement pertaining to problem 14.7

Solution:

The largest nodal distance for this arrangement is *h*.

So, for *node-1*: s_1=1, s_2= s_4=0.333 and s_3=0.5. Then as per eqn. 14.10

$$V_1 = \frac{\frac{1}{1+0.5}\left(\frac{66}{1}+\frac{V_3}{0.5}\right)+\frac{1}{0.333+0.333}\left(\frac{100}{0.333}+\frac{V_2}{0.333}\right)}{\frac{1}{1\times 0.5}+\frac{1}{0.333\times 0.333}}$$

For *node-2*: s_1=1, s_2= s_4=0.333 and s_3=0.5. Then as per eqn. 14.10

$$V_2 = \frac{\frac{1}{1+0.5}\left(\frac{33}{1}+\frac{V_4}{0.5}\right)+\frac{1}{0.333+0.333}\left(\frac{V_1}{0.333}+\frac{0}{0.333}\right)}{\frac{1}{1\times 0.5}+\frac{1}{0.333\times 0.333}}$$

For *node-3*: As per eqn. 14.42, $V_1=V_1$, $V_2=100$, $V_3=V_5$ and $V_4= V_4$ and K = (1/4). Nodal distance factors are $s_1=s_3=0.5$ and $s_2= s_4= 0.333$.

$$V_3 = \frac{\frac{V_1}{0.5}+\frac{V_5}{0.5\times 0.25}+\frac{0.5\times 0.25+0.5}{0.25(0.333+0.333)}\left(\frac{100}{0.333}+\frac{V_4}{0.333}\right)}{\frac{1}{0.5}+\frac{1}{0.5\times 0.25}+\frac{0.5\times 0.25+0.5}{0.25\times 0.333\times 0.333}}$$

For *node-4*: As per eqn. 14.42, $V_1=V_2$, $V_2=V_3$, $V_3=V_6$ and $V_4=0$ and K = (1/4). Nodal distance factors are $s_1=s_3=0.5$ and $s_2= s_4= 0.333$.

$$V_4 = \frac{\frac{V_2}{0.5}+\frac{V_6}{0.5\times 0.25}+\frac{0.5\times 0.25+0.5}{0.25(0.333+0.333)}\left(\frac{V_3}{0.333}+\frac{0}{0.333}\right)}{\frac{1}{0.5}+\frac{1}{0.5\times 0.25}+\frac{0.5\times 0.25+0.5}{0.25\times 0.333\times 0.333}}$$

For *node-5*: $s_1=0.5$, $s_2= s_4=0.333$ and $s_3=1$. Then as per eqn. 14.10

$$V_5 = \frac{\frac{1}{0.5+1}\left(\frac{V_3}{0.5}+\frac{66}{1}\right)+\frac{1}{0.333+0.333}\left(\frac{100}{0.333}+\frac{V_6}{0.333}\right)}{\frac{1}{0.5\times 1}+\frac{1}{0.333\times 0.333}}$$

For *node-6*: $s_1=0.5$, $s_2= s_4=0.333$ and $s_3=1$. Then as per eqn. 14.10

$$V_6 = \frac{\frac{1}{0.5+1}\left(\frac{V_4}{0.5}+\frac{33}{1}\right)+\frac{1}{0.333+0.333}\left(\frac{V_5}{0.333}+\frac{0}{0.333}\right)}{\frac{1}{0.5\times 1}+\frac{1}{0.333\times 0.333}}$$

FDM Equations in Axi-symmetric System for Multi-Dielectric Media

For series dielectric media

In this case, the dielectric interface is considered to be normal to the axis of symmetry. The FDM equations need to be developed for a node lying on the dielectric interface. This node could be away from the axis of symmetry and could also be on the axis of symmetry.

For the node on the dielectric interface lying away from the axis of symmetry

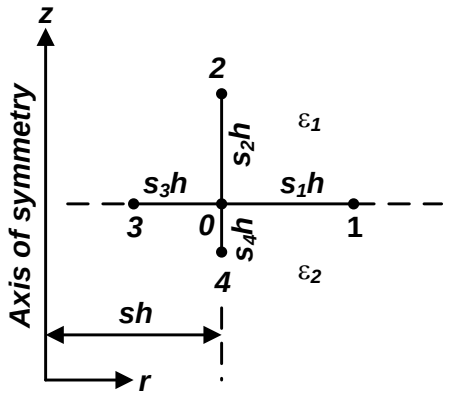

Fig. 14.15 Nodal arrangement for FDM equation development in axi-symmetric system with multi-dielectric media in series dielectric arrangement when the node is lying away from the axis of symmetry

For the nodal arrangement shown in Fig. 14.15, the *z*-component of electric flux density is the normal component on the dielectric interface that is parallel to the *r*-axis.

$$\vec{D}_z = \vec{D}'_z$$

$$or,\ \varepsilon_1 \vec{E}_z = \varepsilon_2 \vec{E}'_z$$

$$or,\ -\varepsilon_1 \frac{\partial V}{\partial z} = -\varepsilon_2 \frac{\partial V'}{\partial z} \qquad \ldots 14.44$$

$$or,\ \frac{\partial V'}{\partial z} = \frac{\varepsilon_1}{\varepsilon_2}\frac{\partial V}{\partial z} = K\frac{\partial V}{\partial z}$$

$$where\ K = \frac{\varepsilon_1}{\varepsilon_2}$$

Here, it is to be noted again the potential function V is valid for medium-*1* and V' is valid for medium-*2*.

Accordingly two Laplace's equation, one with V and the other with V', need to be satisfied in this case, as given in eqn. (14.45a) and (14.45b). Eqn. (14.45a) is valid for medium-*1*, while eqn. (14.45b) is valid for medium-*2*.

$$\frac{\partial^2 V}{\partial r^2} + \frac{1}{r}\frac{\partial V}{\partial r} + \frac{\partial^2 V}{\partial z^2} = 0 \qquad \ldots 14.45a$$

$$\frac{\partial^2 V'}{\partial r^2} + \frac{1}{r}\frac{\partial V'}{\partial r} + \frac{\partial^2 V'}{\partial z^2} = 0 \qquad \ldots 14.45b$$

Now, from Taylor series expansion between the pair of nodes, the following expressions are obtained

$$V_1 = V_0 + s_1 h\left.\frac{\partial V}{\partial r}\right|_0 + \frac{s_1^2 h^2}{2}\left.\frac{\partial^2 V}{\partial r^2}\right|_0 \quad \text{between the nodes } 1 \text{ and } 0 \qquad \ldots 14.46a$$

$$V_3 = V_0 - s_3 h\left.\frac{\partial V}{\partial r}\right|_0 + \frac{s_3^2 h^2}{2}\left.\frac{\partial^2 V}{\partial r^2}\right|_0 \quad \text{between the nodes } 0 \text{ and } 3 \qquad \ldots 14.46b$$

$$V_2 = V_0 + s_2 h\left.\frac{\partial V}{\partial z}\right|_0 + \frac{s_2^2 h^2}{2}\left.\frac{\partial^2 V}{\partial z^2}\right|_0 \quad \text{between the nodes } 2 \text{ and } 0 \qquad \ldots 14.46c$$

$$V_4 = V_0 - s_4 h \left.\frac{\partial V'}{\partial z}\right|_0 + \frac{s_4^2 h^2}{2} \left.\frac{\partial^2 V'}{\partial z^2}\right|_0 \quad \text{between the nodes } 0 \text{ and } 4 \qquad \ldots 14.46d$$

It is to be noted here that the nodes *1, 0* and *3* lie on the dielectric interface. According to the boundary conditions on dielectric-dielectric interface, electric potential and tangential component of electric field remain constant on the dielectric interface.

From eqns. (14.46a) and (14.46b) along the *r*-direction on the dielectric interface,

$$\left.\frac{\partial^2 V}{\partial r^2}\right|_0 = \frac{\left(\frac{V_1}{s_1} + \frac{V_3}{s_3}\right) - V_0\left(\frac{1}{s_1} + \frac{1}{s_3}\right)}{\frac{h^2(s_1 + s_3)}{2}} = \left.\frac{\partial^2 V'}{\partial r^2}\right|_0 \qquad \ldots 14.47$$

From eqns. (14.46a) and (14.46b) considering the radial distance of the *node-0* from the axis of symmetry to be *sh*, i.e. *r = sh*,

$$\frac{1}{r}\left.\frac{\partial V}{\partial r}\right|_0 = \frac{1}{sh}\left.\frac{\partial V}{\partial r}\right|_0 = \frac{\frac{V_1}{s_1^2} - \frac{V_3}{s_3^2} - V_o\left(\frac{1}{s_1^2} - \frac{1}{s_3^2}\right)}{sh^2\left(\frac{1}{s_1} + \frac{1}{s_3}\right)} = \frac{1}{r}\left.\frac{\partial V'}{\partial r}\right|_0 \qquad \ldots 14.48$$

From eqn. (14.46c) $$\left.\frac{\partial^2 V}{\partial z^2}\right|_0 = \frac{V_2 - V_0 - s_2 h \left.\frac{\partial V}{\partial z}\right|_0}{\frac{s_2^2 h^2}{2}} \qquad \ldots 14.49$$

and from eqn. (14.46d) $$\left.\frac{\partial^2 V'}{\partial z^2}\right|_0 = \frac{V_4 - V_0 + s_4 h \left.\frac{\partial V'}{\partial z}\right|_0}{\frac{s_4^2 h^2}{2}} = \frac{V_4 - V_0 + s_4 hK \left.\frac{\partial V}{\partial z}\right|_0}{\frac{s_4^2 h^2}{2}} \qquad \ldots 14.50$$

From eqns. 14.45a, 14.47, 14.48 and 14.49

$$\frac{\left(\frac{V_1}{s_1} + \frac{V_3}{s_3}\right) - V_0\left(\frac{1}{s_1} + \frac{1}{s_3}\right)}{\frac{h^2(s_1 + s_3)}{2}} + \frac{\frac{V_1}{s_1^2} - \frac{V_3}{s_3^2} - V_o\left(\frac{1}{s_1^2} - \frac{1}{s_3^2}\right)}{sh^2\left(\frac{1}{s_1} + \frac{1}{s_3}\right)} + \frac{V_2 - V_0 - s_2 h \left.\frac{\partial V}{\partial z}\right|_0}{\frac{s_2^2 h^2}{2}} = 0 \qquad \ldots 14.51$$

and from eqns. 14.45b, 14.47, 14.48 and 14.50

$$\frac{\left(\frac{V_1}{s_1} + \frac{V_3}{s_3}\right) - V_0\left(\frac{1}{s_1} + \frac{1}{s_3}\right)}{\frac{h^2(s_1 + s_3)}{2}} + \frac{\frac{V_1}{s_1^2} - \frac{V_3}{s_3^2} - V_o\left(\frac{1}{s_1^2} - \frac{1}{s_3^2}\right)}{sh^2\left(\frac{1}{s_1} + \frac{1}{s_3}\right)} + \frac{V_4 - V_0 + s_4 hK \left.\frac{\partial V}{\partial z}\right|_0}{\frac{s_4^2 h^2}{2}} = 0 \qquad \ldots 14.52$$

Eliminating $\left.\frac{\partial V}{\partial z}\right|_0$ from eqns. (14.51) and (14.52),

$$V_0 = \frac{\frac{(Ks_2 + s_4)\left(2 + \frac{s_3}{s}\right)}{s_1(s_1 + s_3)} V_1 + \frac{2K}{s_2} V_2 + \frac{(Ks_2 + s_4)\left(2 - \frac{s_1}{s}\right)}{s_3(s_1 + s_3)} V_3 + \frac{2}{s_4} V_4}{\frac{2(Ks_2 + s_4)}{s_1 s_3} + \frac{(s_3 - s_1)(Ks_2 + s_4)}{s s_1 s_3} + \frac{2K}{s_2} + \frac{2}{s_4}} \qquad \ldots 14.53$$

Eqn.(14.53) is the FDM equation for unknown potential of a node lying on the dielectric interface, where the node is away from the axis of symmetry, in axi-symmetric system with unequal nodal distances having series dielectric arrangement.
For equal nodal distances, i.e. for $s_1 = s_2 = s_3 = s_4 = 1$, eqn.(14.53) reduces to

$$V_0 = \frac{1}{4}\left(V_1 + \frac{2K}{K+1}V_2 + V_3 + \frac{2}{K+1}V_4\right) + \frac{V_1 - V_3}{8s} \quad \ldots 14.54$$

and for single dielectric system, i.e. for K=1, with equal nodal distances eqn.(14.54) reduces to

$$V_0 = \frac{1}{4}(V_1 + V_2 + V_3 + V_4) + \frac{V_1 - V_3}{8s} \quad \ldots 14.55$$

For the node on the dielectric interface lying on the axis of symmetry

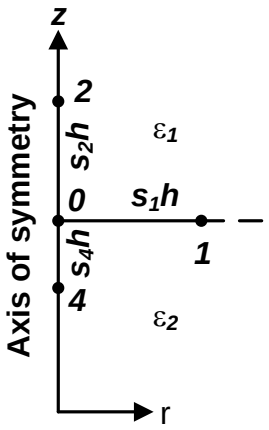

Fig. 14.16 Nodal arrangement for FDM equation development in axi-symmetric system with multi-dielectric media in series dielectric arrangement when the node is lying on the axis of symmetry

Laplace's equation in medium-*1*: $2\frac{\partial^2 V}{\partial r^2} + \frac{\partial^2 V}{\partial z^2} = 0$ … 14.56

Laplace's equation in medium-*2*: $2\frac{\partial^2 V'}{\partial r^2} + \frac{\partial^2 V'}{\partial z^2} = 0$ … 14.57

As per eqn. 14.44 $\frac{\partial V'}{\partial z} = K\frac{\partial V}{\partial z}, \text{where } K = \frac{\varepsilon_1}{\varepsilon_2}$

Now, from Taylor series expansion between the pair of nodes, the following expressions are obtained

$$V_1 = V_0 + s_1 h\left.\frac{\partial V}{\partial r}\right|_0 + \left.\frac{s_1^2 h^2}{2}\frac{\partial^2 V}{\partial r^2}\right|_0$$ between the nodes *1* and *0* … 14.58a

$$V_2 = V_0 + s_2 h\left.\frac{\partial V}{\partial z}\right|_0 + \left.\frac{s_2^2 h^2}{2}\frac{\partial^2 V}{\partial z^2}\right|_0$$ between the nodes *2* and *0* … 14.58b

$$V_4 = V_0 - s_4 h\left.\frac{\partial V'}{\partial z}\right|_0 + \left.\frac{s_4^2 h^2}{2}\frac{\partial^2 V'}{\partial z^2}\right|_0$$ between the nodes *0* and *4* … 14.58c

In eqn. 14.58a, $\left.\frac{\partial V}{\partial r}\right|_0 \to 0, \ as \ r \to 0$. Hence,

$$2\left.\frac{\partial^2 V}{\partial r^2}\right|_0 = \frac{4(V_1 - V_o)}{s_1^{\,2} h^2} \qquad \ldots 14.59$$

From eqn. 14.58b, $\left.\dfrac{\partial^2 V}{\partial z^2}\right|_0 = \dfrac{2(V_2 - V_0 - s_2 h \left.\dfrac{\partial V}{\partial z}\right|_0)}{s_2^{\,2} h^2}$

From eqn. 14.58c, $\left.\dfrac{\partial^2 V'}{\partial z^2}\right|_0 = \dfrac{2(V_4 - V_0 + s_4 hK \left.\dfrac{\partial V}{\partial z}\right|_0)}{s_4^{\,2} h^2}$

So, from Laplace's equation in medium-*1*, i.e. eqn.(14.56),

$$\frac{4(V_1 - V_o)}{s_1^{\,2} h^2} + \frac{2(V_2 - V_0 - s_2 h \left.\dfrac{\partial V}{\partial z}\right|_0)}{s_2^{\,2} h^2} = 0 \qquad \ldots 14.60$$

and from Laplace's equation in medium-*2*, i.e. eqn.(14.57),

$$\frac{4(V_1 - V_o)}{s_1^{\,2} h^2} + \frac{2(V_4 - V_0 + s_4 hK \left.\dfrac{\partial V}{\partial z}\right|_0)}{s_4^{\,2} h^2} = 0 \qquad \ldots 14.61$$

Eliminating $\left.\dfrac{\partial V}{\partial z}\right|_0$ from eqns. (14.60) and (14.61),

$$V_0 = \frac{\dfrac{2(Ks_2 + s_4)}{s_1^{\,2}} V_1 + \dfrac{K}{s_2} V_2 + \dfrac{1}{s_4} V_4}{\dfrac{2(Ks_2 + s_4)}{s_1^{\,2}} + \dfrac{K}{s_2} + \dfrac{1}{s_4}} \qquad \ldots 14.62$$

Eqn.(14.62) is the FDM equation for unknown potential of a node lying on the dielectric interface, where the node is on the axis of symmetry, in axi-symmetric system with unequal nodal distances having series dielectric arrangement.

For equal nodal distances, i.e. for $s_1 = s_2 = s_4 = 1$, eqn.(14.62) reduces to

$$V_0 = \frac{2(K+1)V_1 + KV_2 + V_4}{2(K+1) + K + 1} \qquad \ldots 14.63$$

and for single dielectric system, i.e. for K=1, with equal nodal distances eqn.(14.63) reduces to

$$V_0 = \frac{1}{6}(4V_1 + V_2 + V_4)$$

For parallel dielectric media

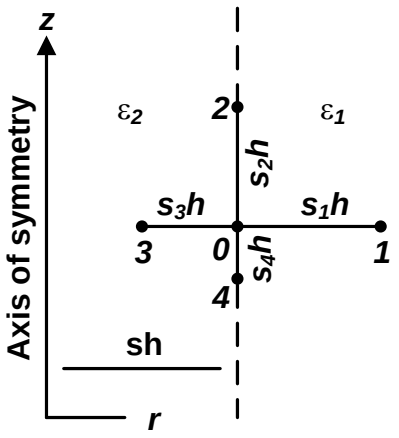

Fig. 14.17 Nodal arrangement for FDM equation development in axi-symmetric system with multi-dielectric media in parallel dielectric arrangement when the node is lying away from the axis of symmetry

In this case, the dielectric interface is considered to be parallel to the axis of symmetry. The FDM equations need to be developed for a node lying on the dielectric interface. This node is away from the axis of symmetry, as in this case the dielectric interface cannot be on the axis of symmetry.

For the nodal arrangement shown in Fig. 14.17, the *r*-component of electric flux density is the normal component on the dielectric interface that is parallel to the *z*-axis.

$$\vec{D}_r = \vec{D}'_r$$

$$or,\ \frac{\partial V'}{\partial r} = K\frac{\partial V}{\partial r}\ ,\ where\ K = \frac{\varepsilon_1}{\varepsilon_2} \qquad \ldots 14.64$$

Now, from Taylor series expansion between the pair of nodes, the expressions that may be obtained are as follows

$$V_1 = V_0 + s_1 h\frac{\partial V}{\partial r}\bigg|_0 + \frac{s_1^2 h^2}{2}\frac{\partial^2 V}{\partial r^2}\bigg|_0 \quad \text{between the nodes } 1 \text{ and } 0 \qquad \ldots 14.65a$$

$$V_3 = V_0 - s_3 h\frac{\partial V'}{\partial r}\bigg|_0 + \frac{s_3^2 h^2}{2}\frac{\partial^2 V'}{\partial r^2}\bigg|_0 \quad \text{between the nodes } 0 \text{ and } 3 \qquad \ldots 14.65b$$

$$V_2 = V_0 + s_2 h\frac{\partial V}{\partial z}\bigg|_0 + \frac{s_2^2 h^2}{2}\frac{\partial^2 V}{\partial z^2}\bigg|_0 \quad \text{between the nodes } 2 \text{ and } 0 \qquad \ldots 14.65c$$

$$V_4 = V_0 - s_4 h\frac{\partial V}{\partial z}\bigg|_0 + \frac{s_4^2 h^2}{2}\frac{\partial^2 V}{\partial z^2}\bigg|_0 \quad \text{between the nodes } 0 \text{ and } 4 \qquad \ldots 14.65d$$

From eqn. (14.65a)
$$\frac{\partial^2 V}{\partial r^2}\bigg|_0 = \frac{V_1 - V_0 - s_1 h\dfrac{\partial V}{\partial r}\bigg|_0}{\dfrac{s_1^2 h^2}{2}} \qquad \ldots 14.66$$

and from eqn. (14.65b)
$$\frac{\partial^2 V'}{\partial r^2}\bigg|_0 = \frac{V_3 - V_0 + s_3 h K\dfrac{\partial V}{\partial r}\bigg|_0}{\dfrac{s_3^2 h^2}{2}} \qquad \ldots 14.67$$

Again, from eqn. (14.65a) $$\frac{1}{r}\frac{\partial V}{\partial r}\bigg|_0 = \frac{V_1 - V_0}{ss_1h^2} - \frac{s_1h}{2sh}\frac{\partial^2 V}{\partial r^2}\bigg|_0 \quad \text{as } r=sh \qquad \ldots 14.68$$

and from eqn. (14.65b) $$\frac{1}{r}\frac{\partial V'}{\partial r}\bigg|_0 = \frac{V_0 - V_3}{ss_3h^2} + \frac{s_3h}{2sh}\frac{\partial^2 V'}{\partial r^2}\bigg|_0 \quad \text{as } r=sh \qquad \ldots 14.69$$

From eqns. (14.65c) and (14.65d) along the *z*-direction on the dielectric interface,

$$\frac{\partial^2 V}{\partial z^2}\bigg|_0 = \frac{\left(\frac{V_2}{s_2}+\frac{V_4}{s_4}\right) - V_0\left(\frac{1}{s_2}+\frac{1}{s_4}\right)}{\frac{h^2(s_2+s_4)}{2}} = \frac{\partial^2 V'}{\partial z^2}\bigg|_0 \qquad \ldots 14.70$$

Satisfying Laplace's equation in medium-*1*:

$$\frac{\partial^2 V}{\partial r^2}+\frac{1}{r}\frac{\partial V}{\partial r}+\frac{\partial^2 V}{\partial z^2}=0$$

$$\frac{V_1 - V_0 - s_1h\frac{\partial V}{\partial r}\Big|_0}{\frac{s_1^2h^2}{2}} + \frac{V_1 - V_0}{ss_1h^2} - \frac{s_1h}{2sh}\frac{V_1 - V_0 - s_1h\frac{\partial V}{\partial r}\Big|_0}{\frac{s_1^2h^2}{2}} + \frac{\left(\frac{V_2}{s_2}+\frac{V_4}{s_4}\right) - V_0\left(\frac{1}{s_2}+\frac{1}{s_4}\right)}{\frac{h^2(s_2+s_4)}{2}} = 0 \qquad \ldots 14.71$$

Similarly, satisfying Laplace's equation in medium-*2*:

$$\frac{\partial^2 V'}{\partial r^2}+\frac{1}{r}\frac{\partial V'}{\partial r}+\frac{\partial^2 V'}{\partial z^2}=0$$

$$\frac{V_3 - V_0 + s_3hK\frac{\partial V}{\partial r}\Big|_0}{\frac{s_3^2h^2}{2}} + \frac{V_0 - V_3}{ss_3h^2} + \frac{s_3h}{2sh}\frac{V_3 - V_0 + s_3hK\frac{\partial V}{\partial r}\Big|_0}{\frac{s_3^2h^2}{2}} + \frac{\left(\frac{V_2}{s_2}+\frac{V_4}{s_4}\right) - V_0\left(\frac{1}{s_2}+\frac{1}{s_4}\right)}{\frac{h^2(s_2+s_4)}{2}} = 0 \qquad \ldots 14.72$$

Eliminating $\frac{\partial V}{\partial r}\Big|_0$ from eqns. (14.71) and (14.72),

$$V_0 = \frac{\frac{K}{s_1(2s-s_1)}V_1 + \frac{1}{(2s+s_3)}V_3 + \frac{1}{(s_2+s_4)}\left[\left\{\frac{s_1K}{(2s-s_1)}+\frac{s_3}{(2s+s_3)}\right\}\left(\frac{V_2}{s_2}+\frac{V_4}{s_4}\right)\right]}{\frac{K}{s_1(2s-s_1)}+\frac{1}{(2s+s_3)}+\frac{1}{s_2s_4}\left\{\frac{s_1K}{(2s-s_1)}+\frac{s_3}{(2s+s_3)}\right\}} \qquad \ldots 14.73$$

Eqn.(14.73) is the FDM equation for unknown potential of a node lying on the dielectric interface, where the node is away from the axis of symmetry, in axi-symmetric system with unequal nodal distances having parallel dielectric arrangement.

For equal nodal distances, i.e. when $s_1 = s_2 = s_3 = s_4 = 1$, eqn.(14.73) reduces to

$$V_0 = \frac{\frac{K}{(2s-1)}V_1 + \frac{1}{(2s+1)}V_3 + \frac{1}{2}\left[\left\{\frac{K}{(2s-1)}+\frac{1}{(2s+1)}\right\}(V_2+V_4)\right]}{2\left\{\frac{K}{(2s-1)}+\frac{1}{(2s+1)}\right\}} \qquad \ldots 14.74$$

and for single dielectric system, i.e. K=1, with equal nodal distances eqn.(14.74) reduces to

$$V_0 = \frac{1}{4}(V_1+V_2+V_3+V_4)+\frac{V_1-V_3}{8s}$$

Problem 14.8

For the axi-symmetric multi-dielectric configuration with series dielectric arrangement as shown in Fig. 14.18, write the FDM equations for the nodes having unknown potentials.

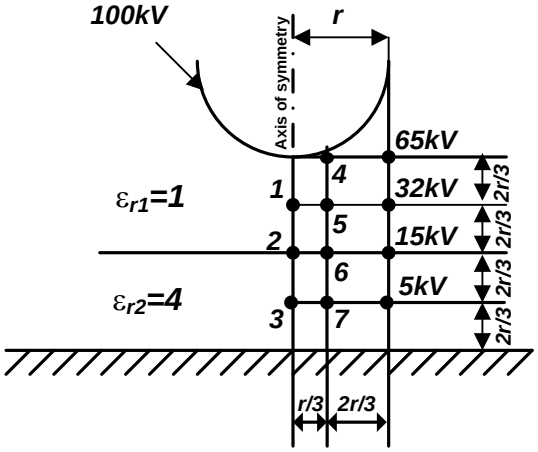

Fig. 14.18 Nodal arrangement pertaining to problem 14.8

Solution:

In this configuration the largest nodal distance is (*2r/3*). So the respective nodal distance factors are calculated based on this largest nodal distance.

For *node-1*: As per eqn. 14.29, $V_1 = V_5$, $V_2 = 100$, $V_4 = V_2$, $s_1 = 0.5$ and $s_2 = s_4 = 1$.

$$V_1 = \frac{\dfrac{2\times V_5}{0.5^2} + \dfrac{1}{1+1}\left(\dfrac{100}{1} + \dfrac{V_2}{1}\right)}{\dfrac{2}{0.5^2} + \dfrac{1}{1\times 1}}$$

For *node-2*: As per eqn. 14.62, $V_1 = V_6$, $V_2 = V_1$, $V_4 = V_3$, $s_1 = 0.5$, $s_2 = s_4 = 1$ and $K = (1/4)$.

$$V_2 = \frac{\dfrac{2(0.25\times 1+1)}{0.5^2}V_6 + \dfrac{0.25}{1}V_1 + \dfrac{1}{1}V_3}{\dfrac{2(0.25\times 1+1)}{0.5^2} + \dfrac{0.25}{1} + \dfrac{1}{1}}$$

For *node-3*: As per eqn. 14.29, $V_1 = V_7$, $V_2 = V_2$, $V_4 = 0$, $s_1 = 0.5$ and $s_2 = s_4 = 1$.

$$V_3 = \frac{\dfrac{2\times V_7}{0.5^2} + \dfrac{1}{1+1}\left(\dfrac{V_2}{1} + \dfrac{0}{1}\right)}{\dfrac{2}{0.5^2} + \dfrac{1}{1\times 1}}$$

For *node-4*: The nodal distances are unequal such that $s_1 = 1$, $s_2 = 0.086$, $s_3 = 0.5$, $s_4 = 1$, $s = 0.5$ and $V_1 = 65$, $V_2 = 100$, $V_3 = 100$ and $V_4 = V_5$. Then as per eqn. 14.23

$$V_4 = \frac{\dfrac{1}{1+0.5}\left\{\left(\dfrac{2\times 0.5+0.5}{1}\right)65 + \left(\dfrac{2\times 0.5-1}{0.5}\right)100\right\} + \dfrac{2\times 0.5}{0.086+1}\left(\dfrac{100}{0.086} + \dfrac{V_5}{1}\right)}{\dfrac{2\times 0.5+0.5-1}{1\times 0.5} + \dfrac{2\times 0.5}{0.086\times 1}}$$

For *node-5*: The nodal distances are unequal such that $s_1 = s_2 = s_4 = 1$, $s_3 = 0.5$, $s = 0.5$ and $V_1 = 32$, $V_2 = V_4$, $V_3 = V_1$ and $V_4 = V_6$. Then as per eqn. 14.23

$$V_5 = \frac{\dfrac{1}{1+0.5}\left\{\left(\dfrac{2\times 0.5+0.5}{1}\right)32 + \left(\dfrac{2\times 0.5-1}{0.5}\right)V_1\right\} + \dfrac{2\times 0.5}{1+1}\left(\dfrac{V_4}{1} + \dfrac{V_6}{1}\right)}{\dfrac{2\times 0.5+0.5-1}{1\times 0.5} + \dfrac{2\times 0.5}{1\times 1}}$$

For *node-6*: As per eqn. 14.53, V_1=15, V_2=V_5, V_3=V_2, V_4=V_7, s_1=s_2=s_4=1, s_3=0.5, s=0.5, and K = (1/4).

$$V_6=\frac{\frac{(0.25\times1+1)\left(2+\frac{0.5}{0.5}\right)}{1\times(1+0.5)}\times15+\frac{2\times0.25}{1}V_5+\frac{(0.25\times1+1)\left(2-\frac{1}{0.5}\right)}{0.5\times(1+0.5)}V_2+\frac{2}{1}V_7}{\frac{2(0.25\times1+1)}{1\times0.5}+\frac{(0.5-1)(0.25\times1+1)}{0.5\times1\times0.5}+\frac{2\times0.25}{1}+\frac{2}{1}}$$

For *node-7*: The nodal distances are unequal such that s_1=s_2= s_4=1, s_3=0.5, s=0.5 and V_1= 5, V_2= V_6, V_3= V_3 and V_4= 0. Then as per eqn. 14.23

$$V_7=\frac{\frac{1}{1+0.5}\left\{\left(\frac{2\times0.5+0.5}{1}\right)5+\left(\frac{2\times0.5-1}{0.5}\right)V_3\right\}+\frac{2\times0.5}{1+1}\left(\frac{V_6}{1}+\frac{0}{1}\right)}{\frac{2\times0.5+0.5-1}{1\times0.5}+\frac{2\times0.5}{1\times1}}$$

Problem 14.9

For the axi-symmetric multi-dielectric configuration with parallel dielectric arrangement as shown in Fig. 14.19, write the FDM equations for the nodes having unknown potentials.

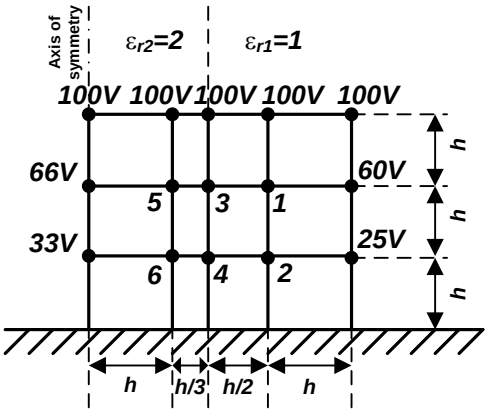

Fig. 14.19 Nodal arrangement pertaining to problem 14.9

Solution:

In this configuration the largest nodal distance is (h). So the respective nodal distance factors are calculated based on this largest nodal distance.

For *node-1*: The nodal distances are unequal such that s_1=s_2= s_4=1, s_3=0.5, s=1.833 and V_1= 60, V_2= 100, V_3= V_3, and V_4= V_2. Then as per eqn. 14.23

$$V_1=\frac{\frac{1}{1+0.5}\left\{\left(\frac{2\times1.833+0.5}{1}\right)60+\left(\frac{2\times1.833-1}{0.5}\right)V_3\right\}+\frac{2\times1.833}{1+1}\left(\frac{100}{1}+\frac{V_2}{1}\right)}{\frac{2\times1.833+0.5-1}{1\times0.5}+\frac{2\times1.833}{1\times1}}$$

For *node-2*: The nodal distances are unequal such that s_1=s_2= s_4=1, s_3=0.5, s=1.833 and V_1= 25, V_2= V_1, V_3= V_4, and V_4= 0. Then as per eqn. 14.23

$$V_2=\frac{\frac{1}{1+0.5}\left\{\left(\frac{2\times1.833+0.5}{1}\right)25+\left(\frac{2\times1.833-1}{0.5}\right)V_4\right\}+\frac{2\times1.833}{1+1}\left(\frac{V_1}{1}+\frac{0}{1}\right)}{\frac{2\times1.833+0.5-1}{1\times0.5}+\frac{2\times1.833}{1\times1}}$$

For *node-3*: The nodal distances are unequal such that s_1=0.5, s_2= s_4=1, s_3=0.333, s=1.333 and V_1= V_1, V_2= 100, V_3= V_5, V_4= V_4 and K=(1/2). Then as per eqn. 14.73

$$V_3 = \frac{\dfrac{0.5}{0.5(2\times1.333-0.5)}V_1 + \dfrac{1}{(2\times1.333+0.333)}V_5 + \dfrac{1}{(1+1)}\left[\left\{\dfrac{0.5\times0.5}{(2\times1.333-0.5)}+\dfrac{0.333}{(2\times1.333+0.333)}\right\}\left(\dfrac{100}{1}+\dfrac{V_4}{1}\right)\right]}{\dfrac{0.5}{0.5(2\times1.333-0.5)}+\dfrac{1}{(2\times1.333+0.333)}+\dfrac{1}{1\times1}\left\{\dfrac{0.5\times0.5}{(2\times1.333-0.5)}+\dfrac{0.333}{(2\times1.333+0.333)}\right\}}$$

For *node-4*: The nodal distances are unequal such that s_1=0.5, s_2= s_4=1, s_3=0.333, s=1.333 and V_1= V_2, V_2= V_3, V_3= V_6, V_4= 0 and K=(1/2). Then as per eqn. 14.73

$$V_4 = \frac{\dfrac{0.5}{0.5(2\times1.333-0.5)}V_2 + \dfrac{1}{(2\times1.333+0.333)}V_6 + \dfrac{1}{(1+1)}\left[\left\{\dfrac{0.5\times0.5}{(2\times1.333-0.5)}+\dfrac{0.333}{(2\times1.333+0.333)}\right\}\left(\dfrac{V_3}{1}+\dfrac{0}{1}\right)\right]}{\dfrac{0.5}{0.5(2\times1.333-0.5)}+\dfrac{1}{(2\times1.333+0.333)}+\dfrac{1}{1\times1}\left\{\dfrac{0.5\times0.5}{(2\times1.333-0.5)}+\dfrac{0.333}{(2\times1.333+0.333)}\right\}}$$

For *node-5*: The nodal distances are unequal such that s_2=s_3= s_4=1, s_1=0.333, s=1 and V_1= V_3, V_2= 100, V_3= 66, and V_4= V_6. Then as per eqn. 14.23

$$V_5 = \frac{\dfrac{1}{0.333+1}\left\{\left(\dfrac{2\times1+1}{0.333}\right)V_3+\left(\dfrac{2\times1-0.333}{1}\right)\times66\right\}+\dfrac{2\times1}{1+1}\left(\dfrac{100}{1}+\dfrac{V_6}{1}\right)}{\dfrac{2\times1+1-0.333}{0.333\times1}+\dfrac{2\times1}{1\times1}}$$

For *node-6*: The nodal distances are unequal such that s_2=s_3= s_4=1, s_1=0.333, s=1 and V_1= V_4, V_2= V_5, V_3= 33, and V_4= 0. Then as per eqn. 14.23

$$V_6 = \frac{\dfrac{1}{0.333+1}\left\{\left(\dfrac{2\times1+1}{0.333}\right)V_4+\left(\dfrac{2\times1-0.333}{1}\right)\times33\right\}+\dfrac{2\times1}{1+1}\left(\dfrac{V_5}{1}+\dfrac{0}{1}\right)}{\dfrac{2\times1+1-0.333}{0.333\times1}+\dfrac{2\times1}{1\times1}}$$

Simulation Details

Discretization

In Finite Difference Method, for two-dimensional system the entire region of interest, i.e. the region where the field distribution is required to be calculated, is discretized using either rectangles or squares. In three-dimensional system, discretization is done using either rectangular parallelepipeds or cubes. Since potential is commonly assumed to vary linearly between two successive nodes, hence the nodes need to be closely spaced where the field varies significantly in space. This is generally the case near the electrodes or dielectric boundaries, particularly in the cases of contours having sharp corners. On the other hand, in the region away from the electrodes or dielectric boundaries, where the field does not change rapidly in space, the nodes may be spaced relatively widely apart.

For multi-dielectric problems, care should be taken during discretization to make sure that only one dielectric is present between two consecutive nodes. This is achieved by arranging one layer of nodes along the dielectric-dielectric interface.

The finite difference model of a problem gives a point-wise approximation to the governing equations, e.g. Laplace's equation. This model is formed by writing difference equations for

an array of grid points called nodes, which is improved as more nodes are used in the simulation. With the help of finite difference method, one can treat some fairly difficult problems; but for problems having irregular geometries or an unusual specification of boundary conditions, the finite difference method become hard to use.
As an example of how finite difference method might be used to represent a complex geometrical shape, consider the high voltage insulator cross section shown in Fig. 14.20. A finite difference mesh would reasonably cover the insulator volume, but the boundaries must be approximated by a series of horizontal and vertical lines or "stair steps". This results in poor approximation of the curved insulator boundary.

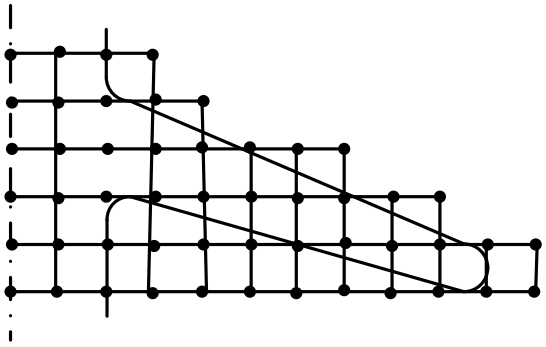

Fig. 14.20 Discretization of insulator geometry by FDM mesh

Simulation of Unbounded Field Region

FDM is well-suited for simulating bounded field regions, i.e. field regions having well defined boundaries. For unbounded field regions, a major difficulty in the implementation of FDM is the placement of nodes in the space which is far away from the components that affect the field distribution. This difficulty is surmounted by placing a fictitious boundary as shown in Fig. 14.21 at a location relatively distant from the components influencing the field. This fictitious boundary is placed with the assumption that the pair of nodes on both sides of this boundary has same potential, e.g. the potential of the nodes *1, 3, 5* & *7* are assumed to be same as that of the nodes *2, 4, 6* & *8*, respectively. If this fictitious boundary is placed in a region where the field does not vary rapidly in space, then the imposition of this fictitious boundary does not incorporate any significant error in the field computation.

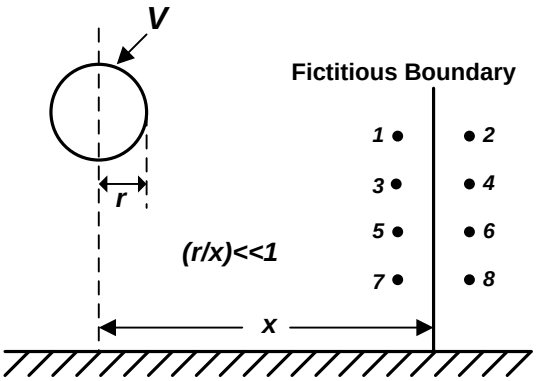

Fig. 14.21 Simulation of unbounded field region

Accuracy Criteria

The accuracy of simulation is dependent upon the nature of discretization of the field region and hence it is important to determine the simulation accuracy using certain well-accepted criteria as detailed below.

The “potential error” on the electrode boundaries can be determined at a number of checkpoints on the electrode surface between two consecutive nodes. Such check points are often called control points. This potential error is defined as the difference between the known potential of the electrode and the computed potential at the control point. From such calculations one can determine the average or the maximum or the mean squared value of the potential error.

The error in the electric field intensity is usually higher than the potential error. Hence, compared to the potential error the “deviation angle” on the electrode surface is a more sensitive indicator of the simulation accuracy. The deviation angle is defined as the angular deviation of the electric stress vector at the control point on the electrode surface from the direction of the normal to its surface.

In multi-dielectric systems, the discrepancy in the tangential electric stress at the control points on the dielectric interface can be computed. Another criterion for checking the simulation accuracy is to compute the discrepancy in the normal flux density at the control point on the dielectric interface. For a good simulation such discrepancies should be small.

System of FDM Equation

In FDM, the potential of any node is related to either four connected nodes in two-dimensional system or six connected nodes in three-dimensional system. Hence, if a field region is discretized using N ($N>>1$) number of nodes, then the system of FDM equation will be an $N\times N$ matrix. But in each row of this matrix, there will be non-zero value in only five or seven elements depending upon the dimension of the simulated system and all the other elements out of N elements of each row of the matrix will be zero. Hence, it is obvious that the system of FDM equations generates a highly sparse matrix.

Hence, it is advisable to solve the system of FDM equations by an iterative technique such as Gauss-Seidel method rather than using a direct method such as Gaussian Elimination. In the iterative techniques, suitable technique is to be employed to achieve accelerated convergence.

Numerical Computation of HV Field by Finite Element Method (FEM)

Introduction

The Finite Element Method (FEM) is a numerical analysis technique to obtain solutions to the differential equations that describe, or approximately describe a wide variety of physical problems ranging from solid, fluid and soil mechanics, to electromagnetism or dynamics. The underlying premise of the FEM is that a complicated region of interest can be sub-divided into a series of smaller sub-regions in which the differential equations are approximately solved. By assembling the set of equations for each sub-region, the behavior over the entire region of interest is determined.

It is difficult to state the exact origin of the FEM, because the basic concepts have evolved over a period of 100 or more years. The term finite element was first coined by Clough in 1960. In the early 1960s, FEM was used for approximate solution of problems in stress analysis, fluid flow, heat transfer, and some other areas. In the late 1960s and early 1970s, application of FEM was extended to much wider variety of engineering problems. Significant advances in mathematical treatments, including the development of new elements, and convergence studies were made in 1970s. Most of the commercial FEM software packages originated in the 1970s and 1980s. The FEM is one of the most important developments in computational methods to occur in the 20th century. The method has evolved from one with applications in structural engineering at the beginning to a widely utilized and richly varied computational approach for many scientific and technological areas at present.

Basics of Finite Element Method

Using the finite element method, the region of interest is discretized into smaller sub-regions called elements as shown in Fig. 15.1, and the solution is determined in terms of discrete values of some primary field variables, e.g. electric potential, at the nodes. The governing equation, e.g. Laplace's or Poisson's equation, is now applied to the domain of a single element. At the element level, the solution to the governing equation is replaced by a continuous function approximating the distribution of the field variable ϕ over the element domain, expressed in terms of the unknown nodal values ϕ_1, ϕ_2 and ϕ_3 of the solution ϕ. A system of equations in terms of ϕ_1, ϕ_2 and ϕ_3 can then be formulated for the element. Once the element equations have been determined, the elements are assembled to form the entire region of interest. Assembly is accomplished using the basic rule that the value of the field variable at a node must be the same for each element that shares that node. The solution ϕ to the problem becomes a piecewise approximation, expressed in terms of the nodal values of ϕ. The assembly procedure results in a system of linear algebraic equations.

Several approaches can be used to transform the physical formulation of the problem to its finite element discrete analogue. If the physical formulation of the problem is known as a differential equation, e.g. Laplace's or Poisson's equation, then the most popular method of its finite element formulation is the Galerkin method. If the physical problem can be formulated as minimization of a functional then variational formulation of the finite element equations is usually used. For problems in high voltage fields, the functional turns out to be the energy stored in the electric field.

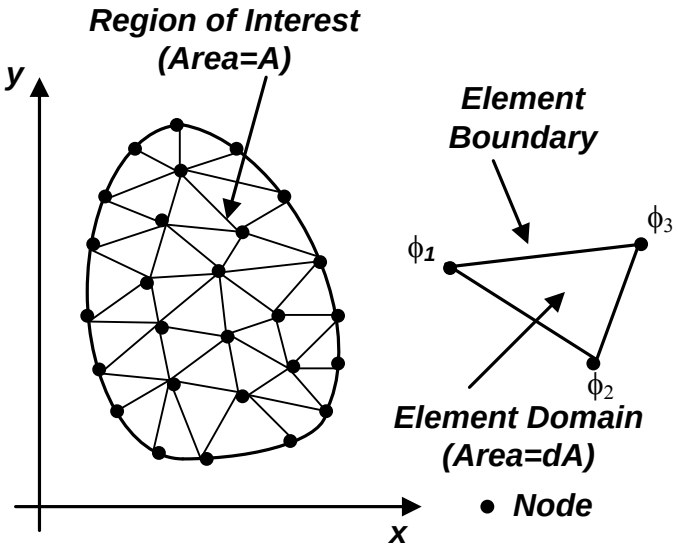

Fig. 15.1 Depiction of Region of interest, element and nodes for FEM formulation

A third and even more versatile approach to deriving element properties is known as the weighted residuals approach. The weighted residuals approach begins with the governing equations of the problem and proceeds without relying on a variational statement. This approach is advantageous because it makes it possible to extend the finite element method to problems where no functional is available.

Procedural Steps in FEM

In general terms, the main steps of the finite element solution procedure are as follows.

1. At the beginning the region of interest is discretized into finite elements.
2. Suitable functions are considered to interpolate the field variables over the element.
3. The matrix equation for the finite element is formed relating the nodal values of the unknown field variables to other physical parameters.
4. Global equation system is formed for the entire region of interest by assembling all the element equations. Element connectivities are used for the assembly process. Boundary conditions, which are not accounted in element equations, are imposed before the solution of equations.
5. The finite element global equation system is solved to get the nodal values of the sought field variables.
6. In many cases additional parameters need to be calculated after the solution of global equation system. For example, in high voltage field problems electric field intensity, electric flux density and charges are of interest in addition to electric potential, which are obtained after solution of the global equation system.

Variational Approach towards FEM Formulation

For high voltage field problems, the principle of minimum potential energy is used in this approach. The principle of minimum potential energy can be stated as: Out of all possible potential functions $\phi(x,y,z)$ the one which minimizes the total potential energy is the potential solution that will satisfy equilibrium, and will be the actual potential due to the applied field forces.

Thus, a potential function that will minimize the functional, i.e potential energy, is desired. Minimization of functionals falls within the field of variational calculus. In most cases an exact function is impossible to determine, necessitating the use of approximate numerical methods. The minimization of potential energy in a finite element formulation is carried out using the energy approach. The finite element method develops the equations from simple element shapes, in which the unknowns of the solution are the potentials at the nodes. The calculus of variations enables the energy equation to be reduced to a set of simultaneous equations with the nodal potentials as the unknown quantities.

FEM Formulation in 2-D System with Single Dielectric Medium

The potential energy in a two-dimensional electric field is given by

$$U_{Total} = \iint_A \frac{1}{2}\varepsilon_o \varepsilon_r \left|\vec{E}\right|^2 .l.dA \qquad \text{…. 15.1}$$

or, $$U_{Total} = \iint_A \frac{1}{2}\varepsilon_o \varepsilon_r \left|-\vec{\nabla}\phi\right|^2 .l.dA \qquad \text{…. 15.2}$$

where, E = electric field intensity, ϕ = electric potential, l = length normal to the area A (usually considered as unity for 2-D field), ε_o = permittivity of free space and ε_r = relative permittivity of dielectric.

The integration of eqn. 15.1 must be carried out over the area A, which is identical to the field region under consideration as shown in Fig. 15.1. Since, this area must be finite, FEM cannot be applied to the problems with "open fields" without modifications.

To apply FEM, the region of interest is to be discretized by so-called finite elements as shown in Fig. 15.1. If a region of interest is divided into elements such that continuity of electric potential between elements is enforced, then the total potential energy is equal to the sum of the individual energies of each element. For N number of elements, the total potential energy can then be stated as:

$$U_{Total} = \sum_{e=1}^{N} U(e) \qquad \text{…. 15.3}$$

To minimize the total potential energy, U, of the entire region of interest, $U(e)$ must be minimized for each element. Seeking a set of nodal potentials for each element will minimize $U(e)$. Observe that the functional, $U(e)$ is a function only of the nodal potentials. Using calculus of variations, an extremization of $U(e)$ occurs when the vector of the first partial derivatives with respect to ϕ is zero.

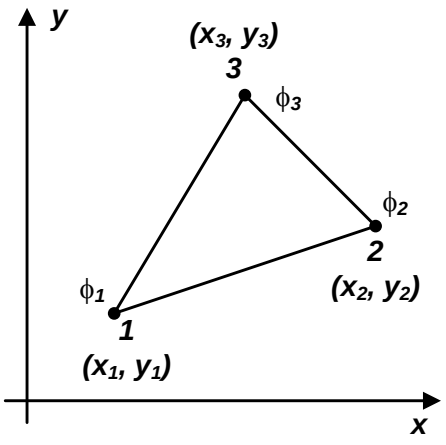

Fig. 15.2 Linear Triangular Element

The simplest 2-D element is the linear triangular element as shown in Fig. 15.2. For this element there are three nodes at the vertices of the triangle, which are numbered around the element in anti-clockwise direction. Electric potential ϕ is assumed to be varying linearly within the element such that

$$\phi = \alpha_1 + \alpha_2 x + \alpha_3 y \quad \text{…. 15.4}$$

Hence, $\vec{E}_x = -\frac{\partial V}{\partial x} = -\alpha_2$ and $\vec{E}_y = -\frac{\partial V}{\partial y} = -\alpha_3$ …. 15.5

Thus, for this element electric field intensity components are constant throughout the element. As a result, this type of element is also known constant stress element (CST).

Now, considering a triangular element as shown in Fig. 15.2

$$\begin{aligned} \phi_1 &= \alpha_1 + \alpha_2 x_1 + \alpha_3 y_1 \\ \phi_2 &= \alpha_1 + \alpha_2 x_2 + \alpha_3 y_2 \\ \phi_3 &= \alpha_1 + \alpha_2 x_3 + \alpha_3 y_3 \end{aligned} \quad \text{…. 15.6}$$

So, from eqn.3.6

$$\alpha_2 = \frac{\begin{vmatrix} 1 & \phi_1 & y_1 \\ 1 & \phi_2 & y_2 \\ 1 & \phi_3 & y_3 \end{vmatrix}}{\begin{vmatrix} 1 & x_1 & y_1 \\ 1 & x_2 & y_2 \\ 1 & x_3 & y_3 \end{vmatrix}}$$

or, $\alpha_2 = \frac{1}{D}\left[\phi_1(y_2 - y_3) + \phi_2(y_3 - y_1) + \phi_3(y_1 - y_2)\right]$ …. 15.7

where, $D = (x_2 y_3 - x_3 y_2) + (x_3 y_1 - x_1 y_3) + (x_1 y_2 - x_2 y_1)$ …. 15.8

= 2 times the area of the triangle

Similarly, $\alpha_3 = \frac{1}{D}\left[\phi_1(x_3 - x_2) + \phi_2(x_1 - x_3) + \phi_3(x_2 - x_1)\right]$ …. 15.9

The magnitude of the electric field intensity within an element *T*,

$$\left|\vec{E}_T\right| = \sqrt{\left|E_x^2\right| + \left|E_y^2\right|} = \sqrt{\alpha_2^2 + \alpha_3^2} \quad \text{…. 15.10}$$

Hence, the electric potential energy in an element *T*

$$U_T = \frac{1}{2}\varepsilon_o \varepsilon_r \left|\vec{E}_T\right|^2 A.l = \frac{1}{2}\varepsilon_o \varepsilon_r A.l.\left(\alpha_2^2 + \alpha_3^2\right) \quad \text{…. 15.11}$$

For electric potential energy in an element to be minimum,

$$\frac{\partial U_T}{\partial \phi_1} = \frac{1}{2}\varepsilon_o \varepsilon_r A.l.2\left(\alpha_2 \frac{\partial \alpha_2}{\partial \phi_1} + \alpha_3 \frac{\partial \alpha_3}{\partial \phi_1}\right) = 0 \quad \text{…. 15.12}$$

Eqn. 15.12 is to be applied to every node where the unknown potential is to be determined. It may be noted here that the node under consideration may belong to more than one element. Then Eqn. 15.12 is to be applied for all such elements considering the node under consideration as *node-1* and the other two nodes of the element being *node-2* and *node-3* taken in anti-clockwise direction.

Now, $\frac{\partial \alpha_2}{\partial \phi_1} = \frac{y_2 - y_3}{D}$, $\frac{\partial \alpha_3}{\partial \phi_1} = \frac{x_3 - x_2}{D}$ and *A=D/2*

So, from eqn. 15.12

$$\frac{1}{2}\varepsilon_o\varepsilon_r\frac{D}{2}.l.2\left[\alpha_2\frac{y_2-y_3}{D}+\alpha_3\frac{x_3-x_2}{D}\right]=0$$

$$or,\quad \frac{1}{2}\varepsilon_o\varepsilon_r.l.\left[\alpha_2(y_2-y_3)+\alpha_3(x_3-x_2)\right]=0 \qquad \text{…. 15.13}$$

Hence, from eqns. 15.7, 15.9 and 15.13

$$\frac{\varepsilon_o\varepsilon_r l}{2D}\left[\{\phi_1(y_2-y_3)+\phi_2(y_3-y_1)+\phi_3(y_1-y_2)\}(y_2-y_3)\right.$$
$$\left.+\{\phi_1(x_3-x_2)+\phi_2(x_1-x_3)+\phi_3(x_2-x_1)\}(x_3-x_2)\right]=0 \qquad \text{…. 15.14a}$$

or,
$$\frac{\varepsilon_r}{D}\left[\phi_1\left\{(x_3-x_2)^2+(y_2-y_3)^2\right\}+\phi_2\{(x_3-x_2)(x_1-x_3)+(y_2-y_3)(y_3-y_1)\}\right.$$
$$\left.+\phi_3\{(x_3-x_2)(x_2-x_1)+(y_2-y_3)(y_1-y_2)\}\right]=0 \qquad \text{…. 15.14b}$$

or,
$$K_{1T}\phi_1+K_{2T}\phi_2+K_{3T}\phi_3=0 \qquad \text{…. 15.15}$$

where,
$$K_{1T}=\frac{\varepsilon_{rT}}{D_T}\left[(x_{3T}-x_{2T})^2+(y_{2T}-y_{3T})^2\right]$$

$$K_{2T}=\frac{\varepsilon_{rT}}{D_T}\left[(x_{3T}-x_{2T})(x_{1T}-x_{3T})+(y_{2T}-y_{3T})(y_{3T}-y_{1T})\right] \qquad \text{…. 15.16}$$

$$K_{3T}=\frac{\varepsilon_{rT}}{D_T}\left[(x_{3T}-x_{2T})(x_{2T}-x_{1T})+(y_{2T}-y_{3T})(y_{1T}-y_{2T})\right]$$

In eqn. 15.16, subscript T denotes the element number, D_T is twice the area of the element as given by eqn. 15.8 and ε_{rT} is the permittivity of the dielectric within the element.

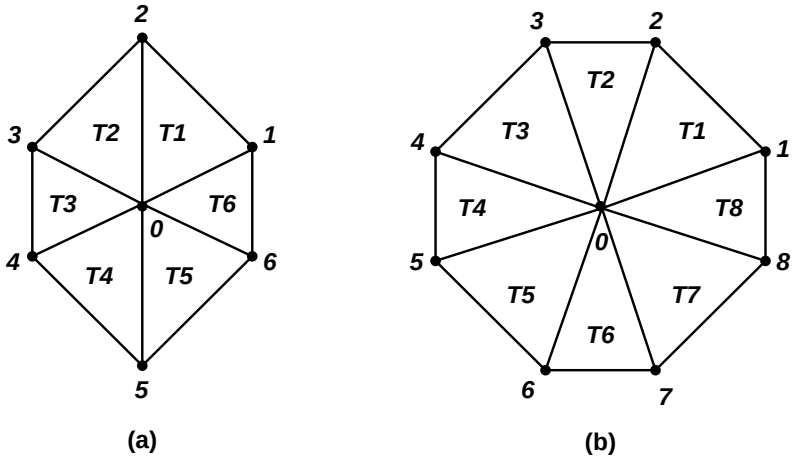

Fig. 15.3 Nodal connectivity – a) 6-element (Hexagonal), b) 8-element (Octagonal)

Discretization using triangular elements is usually done is such a way that one particular node is connected to either 6 other nodes in hexagonal connectivity as shown in Fig. 15.3(a) or to 8 other nodes in octagonal connectivity as shown in Fig. 15.3(b). For hexagonal connectivity, an equation may be formed involving potentials of all the six nodes surrounding the node "*0*" applying eqn. 15.15. In such case, for every element, *node-0* of Fig. 15.3 is considered to be *node-1* of eqn. 15.15 and the other two nodes are considered to be *node-2* and *node-3* in anti-clockwise direction. Application of eqn. 15.15 thus results in six simultaneous linear equations, the summation of which may be represented as follows.

$$F_1\phi_1 + F_2\phi_2 + F_3\phi_3 + F_4\phi_4 + F_5\phi_5 + F_6\phi_6 + F_0\phi_0 = 0 \quad \text{…. 15.17}$$

where,

$$F_1 = K_{2(T1)} + K_{3(T6)}$$
$$F_2 = K_{2(T2)} + K_{3(T1)}$$
$$F_3 = K_{2(T3)} + K_{3(T2)}$$
$$F_4 = K_{2(T4)} + K_{3(T3)} \quad \text{…. 15.18}$$
$$F_5 = K_{2(T5)} + K_{3(T4)}$$
$$F_6 = K_{2(T6)} + K_{3(T5)}$$
$$\text{and } F_0 = \sum_{T=1}^{6} K_{1T}$$

Application of eqn. 15.17 to all the nodes having unknown potential will generate the FEM system of simultaneous linear equations, which needs to be solved for determining the node potentials. Eqns. 15.17 and 15.18 could be suitably modified for octagonal nodal connectivity. Here, it may also be noted that FEM formulation as described above automatically takes into account the unequal elemental sizes as the coefficients as in eqn. 15.18 are all computed in terms of nodal coordinates that may have any numerical values.

FEM Formulation in 2-D System with Multi-Dielectric Media

For computing electric field in a multi-dielectric media, triangular elements are so positioned that any given triangular element comprises only one dielectric medium. In other words, a set of nodal points are to be placed on the interface between two dielectrics as shown in Fig. 15.4. Hence, the coefficients K_{1T}, K_{2T} and K_{3T} for any node are to be calculated depending on its nodal position (i.e. *1*, *2* or *3*) in an element considering the proper value of ε_r.

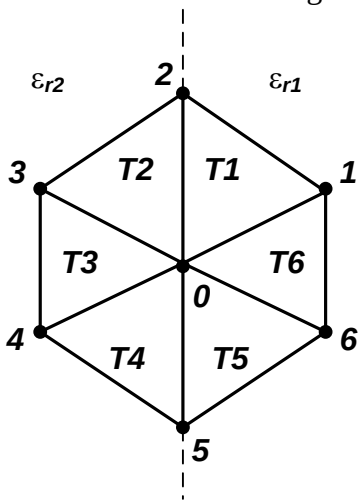

Fig. 15.4 Elemental discretization for multi-dielectric media

While applying eqn. 15.17 for the nodal connectivity shown in Fig. 15.4, the following modifications need to be made for F_2, F_5 and F_0 keeping the others unchanged.

$$F_2 = K_{2(T2)} + K_{3(T1)} \;,\; F_5 = K_{2(T5)} + K_{3(T4)} \text{ and } F_0 = \sum_{T=1}^{6} K_{1T}$$

where,

$$K_{2(T2)} = \frac{\varepsilon_{r2}}{D_{T2}}\left[(x_3 - x_2)(x_0 - x_3) + (y_2 - y_3)(y_3 - y_0)\right]$$

$$K_{3(T1)} = \frac{\varepsilon_{r1}}{D_{T1}}\left[(x_2 - x_1)(x_1 - x_0) + (y_1 - y_2)(y_0 - y_1)\right]$$

$$K_{2(T5)} = \frac{\varepsilon_{r1}}{D_{T5}}\left[(x_6 - x_5)(x_0 - x_6) + (y_5 - y_6)(y_6 - y_0)\right]$$

$$K_{3(T4)} = \frac{\varepsilon_{r2}}{D_{T4}}\left[(x_5 - x_4)(x_4 - x_0) + (y_4 - y_5)(y_0 - y_4)\right]$$

For the computation of F_0, K_{1T} is to be calculated considering ε_{r1} for the elements *1, 5* and *6* and considering ε_{r2} for the elements *2, 3* and *4*, using eqn. 15.16. For example, for elements *T3* and *T6*, respectively, the expressions for K_{1T} will be as follows.

$$K_{1(T3)} = \frac{\varepsilon_{r2}}{D_{T3}}\left[(x_4 - x_3)^2 + (y_3 - y_4)^2\right]$$

and $$K_{1(T6)} = \frac{\varepsilon_{r1}}{D_{T6}}\left[(x_1 - x_6)^2 + (y_6 - y_1)^2\right]$$

Here, it may be noted that no separate formulation is required for multi-dielectric media in FEM in contrast to FDM.

FEM Formulation in Axi-symmetric System

As already discussed, electric potential energy in a triangular element is

$$U_e = \frac{1}{2}\varepsilon_o\varepsilon_r\left|\vec{E}\right|^2.A.l \qquad \text{…. 15.19}$$

where, (*A.l*) is the volume of the element.

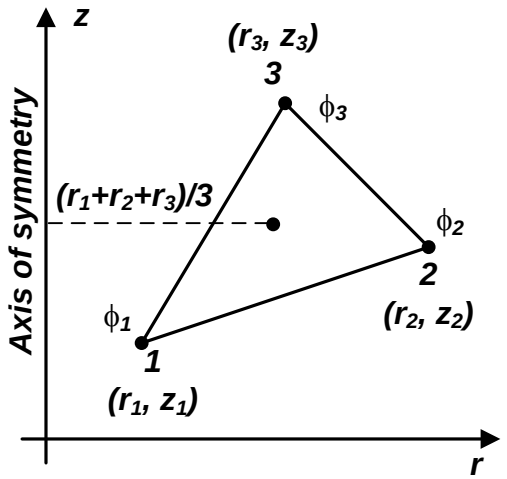

Fig. 15.5 Triangular element for axi-symmetric formulation

For axi-symmetric system, this volume is created due to the rotation of a triangular element around the axis of symmetry. The area of the triangle being *A*, *l* should then be the mean length of rotation, i.e. 2π times the radial distance of the centroid of the triangle.

So, $$l = 2\pi\frac{(r_1 + r_2 + r_3)}{3} \qquad \text{…. 15.20}$$

Putting this expression for *l* in eqn. 15.14b

$$\frac{\varepsilon_o\varepsilon_r}{2D}.\frac{2\pi(r_1+r_2+r_3)}{3}\Big[\phi_1\{(r_3-r_2)^2+(z_2-z_3)^2\}+\phi_2\{(r_3-r_2)(r_1-r_3)+(z_2-z_3)(z_3-z_1)\}$$
$$+\phi_3\{(r_3-r_2)(r_2-r_1)+(z_2-z_3)(z_1-z_2)\}\Big]=0 \quad \ldots\ 15.21$$

So, from eqn. 15.21 in axi-symmetric system

$$K_{1T}\phi_1+K_{2T}\phi_2+K_{3T}\phi_3=0$$

$$K_{1T}=\frac{R\varepsilon_{rT}}{D_T}\left[(r_{3T}-r_{2T})^2+(z_{2T}-z_{3T})^2\right]$$

where, $$K_{2T}=\frac{R\varepsilon_{rT}}{D_T}\left[(r_{3T}-r_{2T})(r_{1T}-r_{3T})+(z_{2T}-z_{3T})(z_{3T}-z_{1T})\right] \quad \ldots.\ 15.22$$

$$K_{3T}=\frac{R\varepsilon_{rT}}{D_T}\left[(r_{3T}-r_{2T})(r_{2T}-r_{1T})+(z_{2T}-z_{3T})(z_{1T}-z_{2T})\right]$$

and $$R=(r_1+r_2+r_3)$$

For axi-symmetric system with multi-dielectric media, the modifications to be brought in are the same as those described for two-dimensional formulation discussed in section 15.4.2.

FEM Formulation in 3-D System

The potential energy in a two-dimensional electric field is given by

$$U_{Total}=\iiint_V\frac{1}{2}\varepsilon_o\varepsilon_r\left|\vec{E}\right|^2dV \quad \ldots.\ 15.41$$

or, $$U_{Total}=\iiint_V\frac{1}{2}\varepsilon_o\varepsilon_r\left|-\nabla\phi\right|^2dV \quad \ldots.\ 15.42$$

To apply FEM, the region of interest is to be discretized by solid finite elements. For *N* number of solid elements, the total potential energy can then be stated as:

$$U_{Total}=\sum_{e=1}^{N}U(e)$$

To minimize the total potential energy, *U*, of the entire region of interest, *U(e)* must be minimized for each solid element.

The simplest 3-D solid element is the linear tetrahedron element as shown in Fig. 15.13. For this element there are four nodes at the four corners of the tetrahedron, which are numbered in such a way that first three nodes are arranged in anti-clockwise direction when viewed from the fourth node, e.g. *1*, *2* and *3* nodes of Fig. 15.13 are arranged in anti-clockwise direction when viewed from node-*4*.

Electric potential ϕ is assumed to be varying linearly within the element such that

$$\phi=\alpha_1+\alpha_2x+\alpha_3y+\alpha_4z \quad \ldots.\ 15.43$$

Hence, $\vec{E}_x=-\frac{\partial V}{\partial x}=-\alpha_2$, $\vec{E}_y=-\frac{\partial V}{\partial y}=-\alpha_3$ and $\vec{E}_z=-\frac{\partial V}{\partial z}=-\alpha_4$ $\ldots.\ 15.44$

Electric field intensity components are constant within a linear tetrahedral element. Hence, it is called a constant stress element in HV field computation.

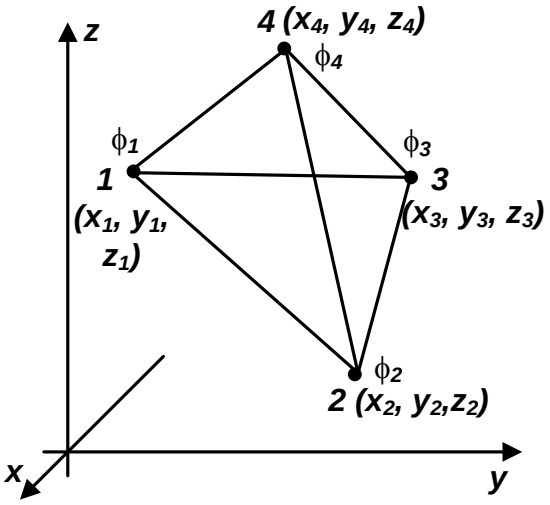

Fig. 15.13 Linear Tetrahedral Element

Again, the potentials at the four corners of the element are given by

$$\begin{aligned}\phi_1 &= \alpha_1 + \alpha_2 x_1 + \alpha_3 y_1 + \alpha_4 z_1 \\ \phi_2 &= \alpha_1 + \alpha_2 x_2 + \alpha_3 y_2 + \alpha_4 z_2 \\ \phi_3 &= \alpha_1 + \alpha_2 x_3 + \alpha_3 y_3 + \alpha_4 z_3 \\ \phi_4 &= \alpha_1 + \alpha_2 x_4 + \alpha_3 y_4 + \alpha_4 z_4\end{aligned} \qquad \text{…. 15.45}$$

Hence,

$$\alpha_2 = \frac{\begin{vmatrix} 1 & \phi_1 & y_1 & z_1 \\ 1 & \phi_2 & y_2 & z_2 \\ 1 & \phi_3 & y_3 & z_3 \\ 1 & \phi_4 & y_4 & z_4 \end{vmatrix}}{\begin{vmatrix} 1 & x_1 & y_1 & z_1 \\ 1 & x_2 & y_2 & z_2 \\ 1 & x_3 & y_3 & z_3 \\ 1 & x_4 & y_4 & z_4 \end{vmatrix}} = \frac{\Delta_2}{\Delta} \qquad \text{…. 15.46}$$

where, Δ = 6 times the volume of the element and

$$\begin{aligned}\Delta_2 &= -\phi_1 \begin{vmatrix} 1 & y_2 & z_2 \\ 1 & y_3 & z_3 \\ 1 & y_4 & z_4 \end{vmatrix} + \phi_2 \begin{vmatrix} 1 & y_1 & z_1 \\ 1 & y_3 & z_3 \\ 1 & y_4 & z_4 \end{vmatrix} - \phi_3 \begin{vmatrix} 1 & y_1 & z_1 \\ 1 & y_2 & z_2 \\ 1 & y_4 & z_4 \end{vmatrix} + \phi_4 \begin{vmatrix} 1 & y_1 & z_1 \\ 1 & y_2 & z_2 \\ 1 & y_3 & z_3 \end{vmatrix} \\ &= -\phi_1 \Delta_{1yz} + \phi_2 \Delta_{2yz} - \phi_3 \Delta_{3yz} + \phi_4 \Delta_{4yz}\end{aligned} \qquad \text{…. 15.47}$$

where, Δ_{1yz}, Δ_{2yz}, Δ_{3yz}, Δ_{4yz} are 2 times the area of triangles opposite to the nodes *1*, *2*, *3*, *4*, respectively, when these triangles are projected to the *y*-*z* plane.

Therefore,

$$\alpha_2 = \frac{-\phi_1 \Delta_{1yz} + \phi_2 \Delta_{2yz} - \phi_3 \Delta_{3yz} + \phi_4 \Delta_{4yz}}{\Delta} \qquad \text{…. 15.48}$$

Similarly, $\alpha_3 = \dfrac{\phi_1\Delta_{1zx} - \phi_2\Delta_{2zx} + \phi_3\Delta_{3zx} - \phi_4\Delta_{4zx}}{\Delta}$ *and*

$$\alpha_4 = \frac{-\phi_1\Delta_{1xy} + \phi_2\Delta_{2xy} - \phi_3\Delta_{3xy} + \phi_4\Delta_{4xy}}{\Delta} \qquad \text{…. 15.49}$$

where, Δ_{1zx}, Δ_{2zx}, Δ_{3zx}, Δ_{4zx} are 2 times the area of triangles opposite to the nodes *1*, *2*, *3*, *4*, respectively, when these triangles are projected to the *z-x* plane and Δ_{1xy}, Δ_{2xy}, Δ_{3xy}, Δ_{4xy} are 2 times the area of triangles opposite to the nodes *1*, *2*, *3*, *4*, respectively, when these triangles are projected to the *x-y* plane.

Now, electric potential energy in a tetrahedral element is given by

$$U_e = \frac{1}{2}\varepsilon_0\varepsilon_r\left|\vec{E}\right|^2 V = \frac{1}{2}\varepsilon_0\varepsilon_r V\,(E_x^2 + E_y^2 + E_z^2)$$

$$= \frac{1}{2}\varepsilon_0\varepsilon_r V\,(\alpha_2^2 + \alpha_3^2 + \alpha_4^2) \qquad \text{…. 15.50}$$

For electric potential energy in an element to be minimum,

$$\frac{\partial U_e}{\partial \phi_1} = \frac{1}{2}\varepsilon_0\varepsilon_r V \times 2\left(\alpha_2\frac{\partial \alpha_2}{\partial \phi_1} + \alpha_3\frac{\partial \alpha_3}{\partial \phi_1} + \alpha_4\frac{\partial \alpha_4}{\partial \phi_1}\right) = 0 \qquad \text{…. 15.51}$$

or, $$\varepsilon_0\varepsilon_r V\left(\alpha_2\frac{\partial \alpha_2}{\partial \phi_1} + \alpha_3\frac{\partial \alpha_3}{\partial \phi_1} + \alpha_4\frac{\partial \alpha_4}{\partial \phi_1}\right) = 0 \qquad \text{…. 15.52}$$

In eqn. 15.52

$$\frac{\partial \alpha_2}{\partial \phi_1} = -\frac{\Delta_{1yz}}{\Delta}, \quad \frac{\partial \alpha_3}{\partial \phi_1} = \frac{\Delta_{1zx}}{\Delta} \quad \text{and} \quad \frac{\partial \alpha_4}{\partial \phi_1} = -\frac{\Delta_{1xy}}{\Delta} \qquad \text{…. 15.53}$$

So, from eqns. 15.48, 15.49, 15.52 and 15.53

$$\varepsilon_0\varepsilon_r\frac{\Delta}{6}\left[-\frac{\Delta_{1yz}}{\Delta}\left(\frac{-\Delta_{1yz}\phi_1 + \Delta_{2yz}\phi_2 - \Delta_{3yz}\phi_3 + \Delta_{4yz}\phi_4}{\Delta}\right)\right.$$

$$+\frac{\Delta_{1zx}}{\Delta}\left(\frac{\Delta_{1zx}\phi_1 - \Delta_{2zx}\phi_2 + \Delta_{3zx}\phi_3 - \Delta_{4zx}\phi_4}{\Delta}\right) \qquad \text{…. 15.54}$$

$$\left.-\frac{\Delta_{1xy}}{\Delta}\left(\frac{-\Delta_{1xy}\phi_1 + \Delta_{2xy}\phi_2 - \Delta_{3xy}\phi_3 + \Delta_{4xy}\phi_4}{\Delta}\right)\right] = 0$$

$$\frac{\varepsilon_r}{6\,\Delta}[\,\phi_1\{\,(\,\Delta_{1yz})^2+(\,\Delta_{1zx})^2+(\,\Delta_{1xy})^2\}$$

or, $$-\phi_2\{\,\Delta_{1yz}\Delta_{2yz}+\Delta_{1zx}\Delta_{2zx}+\Delta_{1xy}\Delta_{2xy}\} \quad \text{…. 15.55}$$

$$+\phi_3\{\,\Delta_{1yz}\Delta_{3yz}+\Delta_{1zx}\Delta_{3zx}+\Delta_{1xy}\Delta_{3xy}\}$$

$$-\phi_4\{\,\Delta_{1yz}\Delta_{4yz}+\Delta_{1zx}\Delta_{4zx}+\Delta_{1xy}\Delta_{4xy}\}\,]=0$$

Eqn. 15.55 can be represented as

$$k_{1e}\phi_1+k_{2e}\phi_2+k_{3e}\phi_3+k_{4e}\phi_4=0 \quad \text{…. 15.56}$$

where, subscript *e* denotes the element number and

$$k_{1e}=\frac{\varepsilon_{re}}{6\,\Delta_e}[\,(\,\Delta_{(1yz)e})^2+(\,\Delta_{(1zx)e})^2+(\,\Delta_{(1xy)e})^2\,]$$

$$k_{2e}=-\frac{\varepsilon_{re}}{6\,\Delta_e}[\,\Delta_{(1yz)e}\Delta_{(2yz)e}+\Delta_{(1zx)e}\Delta_{(2zx)e}+\Delta_{(1xy)e}\Delta_{(2xy)e}\,]$$

$$k_{3e}=\frac{\varepsilon_{re}}{6\,\Delta_e}[\,\Delta_{(1yz)e}\Delta_{(3yz)e}+\Delta_{(1zx)e}\Delta_{(3zx)e}+\Delta_{(1xy)e}\Delta_{(3xy)e}\,]$$

$$k_{4e}=-\frac{\varepsilon_{re}}{6\,\Delta_e}[\,\Delta_{(1yz)e}\Delta_{(4yz)e}+\Delta_{(1zx)e}\Delta_{(4zx)e}+\Delta_{(1xy)e}\Delta_{(4xy)e}\,]$$

…. 15.57

Features of Discretization in FEM

In FEM the continuous domain is replaced by a series of simple, interconnected elements whose field variable characteristics are comparatively easy to compute. In true sense, these elements are connected to each other along their boundaries but the assumption that the elements are connected only at their nodes is made in order to perform a theoretical approximation. A wide variety of elements types in one, two, and three dimensions are now available. It is a duty of the person doing the analysis to determine not only the appropriate type of elements for the problem at hand, but also the density required to sufficiently approximate the solution. It is essential to apply engineering judgment.

Refinement of FEM Mesh

In FEM mesh, every element has a size (*h*) and an order (*p*). Either reducing the element size (*h*) or increasing the element order (*p*) reduces the error in FEM. Consequently, there are three basic approaches towards mesh refinement in FEM: the *h*, *p*, and the *h*-*p* methods.

i) In the *h* method, the element order (*p*) is kept constant and the mesh is refined by making the size (*h*) smaller.

ii) On the other hand, in the *p* method, the element size (h) is kept constant and the element order *p* is increased for mesh refinement.

iii) In the *h*-*p* method, simultaneously the size (*h*) is made smaller and the order (*p*) is increased to create higher order smaller sized elements in the mesh refinement process.

It is often claimed that higher order elements, which require more nodes per element, results in less computational time using a smaller number of larger sized elements. But in real-life, geometries defining the practical objects are complex, which anyway require a fine mesh to accurately discretize the geometry. In such cases, the mesh size is usually small and hence the error does not exceed what is required for engineering accuracy. Therefore, use of higher

order *h* elements offers no benefit over the use of lower order *h* elements in most of the cases. Thus, the *h* method accompanied by a robust quadrilateral or hex generator is most often the best solution for practical design jobs.

Acceptability of Element after Discretization

Traditionally discretization of irregular shaped regions has been performed manually. Now-a-days, state-of-the-art software packages automate the mesh generation process. However, with any mesh-generation package, the user's judgment and experience are still very important. Once a finite element mesh has been created, it must be checked to ensure that each element satisfies certain criteria for acceptability, for example distortion, which may produce spurious results. For all types of elements in FEM, the best results are obtained if the elements have reasonable shape. Distorted elements lead to major inaccuracies, as in the case of isoparametric elements distortions very often lead to non-unique mapping between the global and natural coordinates. Experience shows that good results are normally obtained if the internal angles of the elements are within 30^0 and 150^0. Another criterion is the ratio between the longest and shortest sides of the element. Preferably this ratio should be smaller than 5:1.
Fig. 15.21 shows a few elements having very bad shape that need to be avoided in FEM mesh.

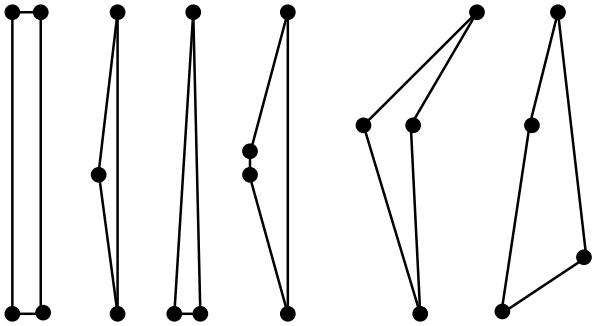

Fig. 15.21 Elements having distorted shape

Solution of System of Equations in FEM

Applications of the finite element method to practical systems lead to large systems of simultaneous linear algebraic equations, which are symmetric, positive definite and sparse. Many solution methods make use of these properties to provide fast and efficient computation algorithms, which are now implemented in nearly all finite element packages. Only half of the matrix including diagonal entries needs to be stored because of the symmetry. Positive definite matrices are characterized by large positive entries on the main diagonal. As a result, solution can be carried out without pivoting. Storage and computations could be economized using sparsity. Solution methods for simultaneous linear equation systems can be broadly divided into two groups: direct methods and iterative methods. Direct solution methods are usually used for problems of moderate size. For large problems iterative methods are preferable as they require less computing time. The choice of solution method is very much dependent on the size of the problem as well as the type of analysis

Sources of Error in FEM

There are three main sources of error in a typical FEM solution, viz. discretization error, formulation error and numerical error.

Discretization error results from transforming the continuous physical region of interest into a finite element model, and can be related to modeling the boundary shape, the boundary conditions, etc. In many problems, poor geometry representation causes serious discretization error. Discretization error can be effectively reduced by refinement of FEM mesh.
Formulation error results from the use of elements that don't precisely describe the behavior of the physical problem. For example a particular finite element might be formulated on the assumption that electric potential varies in a linear manner over the domain. Such an element will produce no formulation error when it is used to model a linearly varying electric potential, but would create a significant formulation error if it used to represent a quadratic or cubic varying electric potential. The magnitude of this error depends on the size of the elements relative to nature of variation of field variables. Formulation error in most physical problems reduces as the element size decreases.
Numerical error occurs as a result of numerical calculation procedures, and includes truncation errors and round off errors. This is a function of the computer accuracy, the computer algorithm, the number of equations, and the element subdivision. Both truncation and round off errors sources are reduced with good modeling practices.

Advantages of FEM

Early work on numerical solution of boundary-valued problems can be traced to the use of finite difference method. Use of such method was reported by Southwell in his book published long back in the mid 1940's. The FDM is generally restricted to simple geometries in which an orthogonal grid is possible to construct. For irregular geometries, a global transformation of the governing equations (e.g., Poisson's equation in HV fields) must be made to create an orthogonal computational domain. Moreover, implementation of boundary conditions in FDM is often cumbersome.
The beginning of the finite element method actually stem from the difficulties associated with using finite difference method for solving difficult, geometrically irregular problems. Unlike the finite difference method, which envisions the solution region as an array of grid points, the finite element method envisions the solution region as made up of many small, interconnected sub-regions or elements. A finite element model of a problem gives a piecewise approximation to the governing equations. The basic premise of the finite element method is that a solution region can be analytically modeled or approximated by replacing it with an assemblage of discrete elements. Since these elements can be put together in a variety of ways, they can be used to represent exceedingly complex shapes.
For the high voltage insulator problem, the finite element model gives a good approximation of the region of interest using the simplest two-dimensional element, i.e. the linear triangular element, as shown in the Fig. 15.22. In FEM a better approximation of the boundary shape is obtained because the curved boundary is represented by straight lines of any inclination. However, it is not intended here to suggest that finite element models are decidedly better for all problems. The only purpose of the example is to demonstrate that the finite element method is particularly well suited for problems with complex geometries.

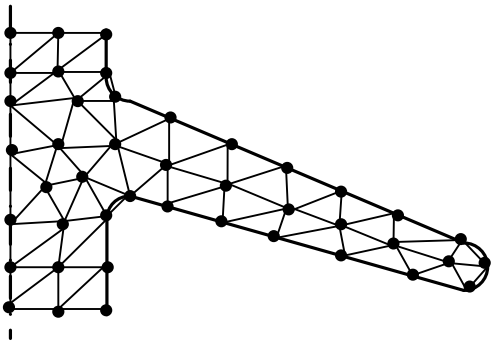

Fig. 15.22 Modelling of HV insulator using triangular element

Using FEM in the Design Cycle

Using FEM analysis in the design cycle of a product is advantageous. FEM can be used to determine the real life behavior of a new design concept under various practical conditions, and therefore to make possible refinement prior to the creation of drawings in CAD, when changes are inexpensive. Once a detailed CAD model has been developed, FEM can be used to analyze the design in detail, which saves time and money by reducing the number of prototypes required. Further an existing product, which is experiencing a field problem or is being improved, can be analyzed to speed up the change in engineering design and reduce its cost. In addition, FEM analysis can now be performed on increasingly affordable personal computers. However, FEM analysis can reduce product testing, but cannot totally replace it. It is important to note here that an inexperienced user of FEM can deliver incorrect answers, upon which significant and expensive decisions will be based. FEM is a demanding tool, in that the analyst must be proficient not only in subject being solved, but also in mathematics, computer applications, and especially the finite element method itself.

Numerical Computation of HV Field by Charge Simulation Method (CSM)

Introduction

The principle of FDM and FEM is to provide the entire region of interest into a large number of sub-regions, and solve for unknown potentials a set of coupled simultaneous linear equations which approximate Laplace's or Poisson's equation. Compared to these two methods, only boundary surfaces, i.e. electrode surfaces and dielectric interfaces, are subdivided and charges are taken as unknowns in CSM. It follows, firstly, that the amount of human time and effort needed for subdivision is greatly reduced in CSM. Secondly, the electric field strength can be given explicitly in CSM without any numerical differentiation of the potential, which results in significant reduction in error. The second characteristic is very important because the field strength is usually more important for the design of an insulating system than electric potential.
The earlier attempts for numerical field solutions employing CSM were reported by Loeb et a1 in 1950 and then by Abou-Seada and Nasser (IEEE-PAS, 1969, pp1802-1814). Subsequently, in a comprehensive paper Singer, Steinbigler and Weiss presented the details of CSM (IEEE-PAS, 1974, pp1660-1668). Since then many refinements to the original method have been proposed and CSM has evolved into a very powerful and efficient tool for computing electric fields in HV equipments. CSM is very simple and applicable to systems having more than one dielectric medium. This method is also suitable for 3-D fields with or without symmetry.

CSM Formulation for Single Dielectric Medium

The basic principle of conventional CSM is very simple. For the calculation of electric fields, the distributed charges on the surface of the electrode are replaced by N number of fictitious charges placed inside the electrode as shown in Fig.16.1. The fictitious charges are placed inside the electrode to avoid singularity problem. In general, the fictitious charges are to be always placed outside the region of interest (ROI), as the field is ideally required to be determined at all the points within the ROI. If the fictitious charges are placed within the ROI, then at the location of the fictitious charges singularity arises because at these points the distance between the charge and the point at which the field solution is required becomes zero.

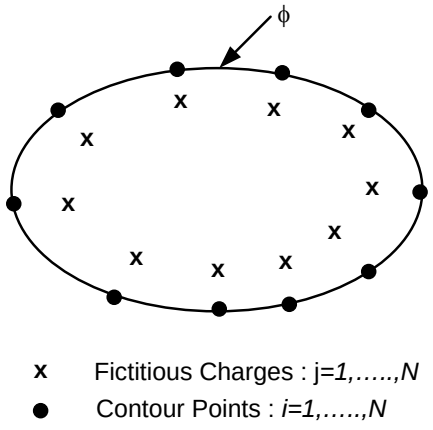

Fig. 16.1 Fictitious charges and contour points for CSM formulation in single dielectric medium

The types and positions of these fictitious charges are predetermined, i.e. user-defined, but their magnitudes are unknown. In order to determine their magnitude some collocation points, which are called contour points, are selected on the surface of electrode. In the conventional CSM the number of contour points is chosen to be equal to the number of fictitious charges. Then it is required that at any one of these contour points the potential resulting from superposition of effects all the fictitious charges is equal to the known electrode potential. Let, Q_j be the *jth* fictitious charge and ϕ be the known potential of the electrode. Then according to the superposition principle

$$\sum_{j=1}^{N} P_{ij} Q_j = \phi \qquad \text{…. 16.1}$$

where, P_{ij} is the potential coefficient, i.e. the potential at the point *i* due to a unit charge at the location *j*, which can be evaluated analytically for different types of fictitious charges by solving Laplace's equation. When Eqn. 16.1 is applied to *N* no. of contour points, it leads to the following system of *N* linear equations for N unknown fictitious charges

$$\begin{aligned}
&P_{11}Q_1 + P_{12}Q_2 + ... + P_{1j}Q_j + ... + P_{1N}Q_N = \phi \\
&P_{21}Q_1 + P_{22}Q_2 + ... + P_{2j}Q_j + ... + P_{2N}Q_N = \phi \\
&. \\
&P_{i1}Q_1 + P_{i2}Q_2 + ... + P_{ij}Q_j + ... + P_{iN}Q_N = \phi \\
&. \\
&P_{N1}Q_1 + P_{N2}Q_2 + ... + P_{Nj}Q_j + ... + P_{NN}Q_N = \phi
\end{aligned} \qquad \text{…. 16.2}$$

In matrix form, Eqn 16.2 can be written as

$$\begin{bmatrix}
P_{11} & P_{12} ..... P_{1j} ..... P_{1N} \\
P_{21} & P_{22} ..... P_{2j} ..... P_{2N} \\
. & \\
P_{i1} & P_{i2} ..... P_{ij} ..... P_{iN} \\
. & \\
P_{N1} & P_{N2} ..... P_{Nj} ..... P_{NN}
\end{bmatrix}_{N\times N}
\begin{bmatrix} Q_1 \\ Q_2 \\ . \\ Q_i \\ . \\ Q_N \end{bmatrix}_{N\times 1}
= [\phi]_{N\times 1} \qquad \text{…. 16.3}$$

where, $[P]$ = potential coefficient matrix, $[\phi]$ = column vector of known potential of contour points.

Eqn. 16.3 is solved for the unknown fictitious charges. As soon as the required fictitious charge system is determined, the potential and the field intensity at any point within the ROI can be calculated. While the potential is found by Eqn. 16.1, the electric field intensities are calculated by superposition of all the stress vector components. For example, in Cartesian co-ordinate system, the three superimposed field components at any point *i* are given as follows.

$$E_{x,i} = -\sum_{j=1}^{N} \frac{\partial P_{ij}}{\partial x} Q_j = -\sum_{j=1}^{N} F_{x,ij} Q_j \qquad \text{…. 16.4}$$

$$E_{y,i} = -\sum_{j=1}^{N} \frac{\partial P_{ij}}{\partial y} Q_j = -\sum_{j=1}^{N} F_{y,ij} Q_j \qquad \text{…. 16.5}$$

and $$E_{z,i} = -\sum_{j=1}^{N} \frac{\partial P_{ij}}{\partial z} Q_j = -\sum_{j=1}^{N} F_{z,ij} Q_j \qquad \text{…. 16.6}$$

where, $F_{x,ij}$, $F_{y,ij}$ and $F_{z,ij}$ are the electric field intensity coefficients in the *x*, *y* and *z* directions, respectively, i.e. the components in the *x*, *y* and *z* directions, respectively, of electric field intensity at the point *i* for a unit charge at the location *j*.
In many cases the effect of the ground plane is to be considered for electric field calculation. This plane can be taken into account by the introduction of image charge.

Formulation for Floating Potential Electrodes

Floating potential conductors are often present in high voltage system, the most common example being condenser bushings. If floating electrodes are present, whose potentials are constant but unknown, then the boundary condition that is imposed for field computation is given below.

$$\phi_{i+1} - \phi_i = 0, \quad for \;\; i = 1,....,N-1 \qquad \ldots. 16.7$$

Moreover, a supplementary condition is included such that the sum of fictitious charges for each floating electrode is zero.
Then the system of equation that is obtained will be as follows

$$\begin{bmatrix} 1 & 1 & ..... & 1 & ..... & 1 \\ (P_{21}-P_{11}) & (P_{22}-P_{12}) & ..... & (P_{2j}-P_{1j}) & ..... & (P_{2N}-P_{1N}) \\ (P_{31}-P_{21}) & (P_{32}-P_{22}) & ..... & (P_{3j}-P_{2j}) & ..... & (P_{3N}-P_{2N}) \\ . & & & & & \\ (P_{(i+1)1}-P_{i1}) & (P_{(i+1)2}-P_{i2}) & ..... & (P_{(i+1)j}-P_{ij}) & ..... & (P_{(i+1)N}-P_{iN}) \\ . & & & & & \\ (P_{N1}-P_{(N-1)1}) & (P_{N2}-P_{(N-1)2}) & ..... & (P_{Nj}-P_{(N-1)j}) & ..... & (P_{NN}-P_{(N-1)N}) \end{bmatrix}_{N\times N} \begin{bmatrix} Q_1 \\ Q_2 \\ . \\ Q_i \\ . \\ Q_N \end{bmatrix}_{N\times 1} = [0]_{N\times 1} \quad \ldots 16.8$$

If the floating electrode has a net charge, then the supplementary condition is included such that the sum of its fictitious charges is equal to the known net charge value (Q_E). In Eqn. 16.8 the first row is then modified as follows

$$Q_1 + Q_2 + ... + Q_j + ... + Q_N = Q_E \qquad \ldots. 16.9$$

CSM Formulation for Multi-Dielectric Media

The field computation for a multi-dielectric system is somewhat complicated due to the fact that the dipoles are realigned in dielectric media under the influence of the applied voltage. Such realignment of dipoles produces a net surface charge on the dielectric interface. Thus in addition to the electrodes, each dielectric interface needs to be simulated by fictitious charges. Here, it is important to note that the dielectric boundary does not correspond to an equipotential surface. Moreover, it must be possible to calculate the electric field on both sides of the dielectric boundary.
It has been mentioned earlier that the fictitious charges should be outside the ROI. In the case of electrodes this has been achieved by placing the charges within the electrodes. But, for dielectric-dielectric interface, both the sides are within the ROI. Hence, any fictitious charge placed on either side of the interface would cause singularity problem. This issue is solved by placing two charges for every contour point on the dielectric –dielectric interface. For solving the field within the dielectric-A, the set of charges placed within dielectric-B are considered and vice-versa.

In the simple example shown in Fig. 16.2, there are N_1 number of charges and contour points to simulate the electrode, of which N_A are on the side of dielectric-*A* and (N_1-N_A) are on the side of dielectric-*B*. These N_1 charges are valid for field calculation in both the dielectrics. At the dielectric interface there are N_2 contour points sequentially numbered from $(N_1+1,\ldots,N_1+N_2)$, with N_2 charges $(N_1+1,\ldots,N_1+N_2)$ in dielectric-*A* valid for dielectric-*B* and N_2 charges $(N_1+N_2+1,\ldots, N_1+2N_2)$ in dielectric-*B* valid for dielectric-*A*. Altogether there are (N_1+N_2) number of contour points and (N_1+2N_2) number of fictitious charges.

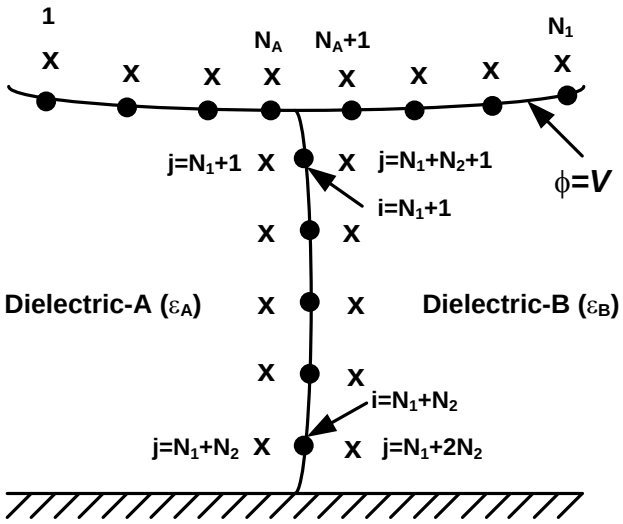

Fig. 16.2 Arrangement of fictitious charges for multi-dielectric media

In order to determine the fictitious charges, a system of equations is formulated by imposing the following boundary conditions.

i) At each contour point on the electrode surface the potential must be equal to the known electrode potential. This condition is also known as Dirichlet's condition on the electrode surface.

ii) At each contour point on the dielectric interface, the potential and the normal component of flux density must be same when computed from either side of the boundary.

Thus the application of the first boundary condition to contour points *1* to N_1 yields the following equations.

$$\sum_{j=1}^{N_1} P_{ij}Q_j + \sum_{j=N_1+N_2+1}^{N_1+2N_2} P_{ij}Q_j = V \qquad .....i = 1, N_A \qquad \text{…. 16.10}$$

and

$$\sum_{j=1}^{N_1} P_{ij}Q_j + \sum_{j=N_1+1}^{N_1+N_2} P_{ij}Q_j = V \qquad .....i = N_A+1, N_1 \qquad \text{…. 16.11}$$

Again the application of the second boundary condition for potential and normal flux density to contour points N_1+1 to N_1+N_2 on the dielectric interface results into the following equations.

From potential continuity condition:

$$\sum_{j=N_1+1}^{N_1+N_2} P_{ij}Q_j - \sum_{j=N_1+N_2+1}^{N_1+N_2} P_{ij}Q_j = 0 \qquad .....i = N_1+1, N_1+N_2 \qquad \text{…. 16.12}$$

From continuity condition of normal flux density D_n :

$$D_{nA}(i) - D_{nB}(i) = 0 \qquad .....i = N_1+1, N_1+N_2 \qquad \text{…. 16.13}$$

Eqn. 16.13 can be expanded as follows.

$$(\varepsilon_A - \varepsilon_B)\sum_{j=1}^{N_1} F_{n,ij}Q_j - \varepsilon_B \sum_{j=N_1+1}^{N_1+N_2} F_{n,ij}Q_j + \varepsilon_A \sum_{j=N_1+N_2+1}^{N_1+2N_2} F_{n,ij}Q_j = 0 \ldots\ldots i = N_1+1, N_1+N_2 \quad \ldots. 16.14$$

where, $F_{n,ij}$ is the field coefficient in the normal direction to the dielectric boundary at the respective contour point and ε_A & ε_B are the permittivities of dielectric *A* and *B*, respectively. Eqns. 16.10 to 16.14 are solved to determine the unknown fictitious charges. These equations can be presented in matrix form as detailed below.

	1	N_1	N_1+N_2	N_1+2N_2		1		1
1	P_{ij}	0	P_{ij}		Q_j	=	V	
N_A	P_{ij}	P_{ij}	0					N_1
N_1	0	P_{ij}	$-P_{ij}$				0	
N_1+N_2	$(\varepsilon_A-\varepsilon_B)$ $F_{n,ij}$	$-\varepsilon_B$ $F_{n,ij}$	ε_A $F_{n,ij}$					
N_1+2N_2					N_1+2N_2		N_1+2N_2	

Types of Fictitious Charges

The successful application of the CSM requires a proper choice of the types of fictitious charges. Point and line charges of infinite and semi-infinite lengths were used in the initial works on this method. Steinbigler et al introduced ring charges and finite length line charges. Subsequently, a large variety of different charge configurations have been proposed. These other types of charge configurations include elliptic cylindrical charge, axi-spheroidal charge, plane sheet charge, disk charge, ring segment charge, volume charges, shell and annular plate charges as well as variable density line charge.

In general, the choice of type of fictitious charge to be used depends upon the complexity of the physical system and the available computational facilities. The potential and field coefficients for point and line charges are given by simple expressions and require very small computation time. For complex charge configuration, such coefficients may have to be computed numerically. On the other hand, a smaller number of charges may be used if complex charge configurations are employed, which reduces the overall memory requirement and computation time. In practice, most of the HV systems can be successfully simulated by using point, line and ring charges or a suitable combination of these charges.

Point Charge

Point charge is the simplest of all types of fictitious charges. It can be used in 2-D as well as 3-D configurations. Fig. 16.3 shows the point charge Q_j along with its image wrt to the *x-y* plane in 3-D system.

Then, the potential at the point *i* due to the point charge Q_j and its image is given by

$$\phi_{ij} = \frac{Q_j}{4\pi\varepsilon}\left[\frac{1}{r_1} - \frac{1}{r_2}\right] \quad \ldots. 16.15$$

where, $r_1 = \left[(x_i - x_j)^2 + (y_i - y_j)^2 + (z_i - z_j)^2\right]^{1/2}$ and $r_2 = \left[(x_i - x_j)^2 + (y_i - y_j)^2 + (z_i + z_j)^2\right]^{1/2}$

Putting Q_j =1 in Eqn. 16.15, the expression for potential coefficient is given by

$$P_{ij} = \frac{1}{4\pi\varepsilon}\left[\frac{1}{r_1} - \frac{1}{r_2}\right] \quad \ldots. 16.16$$

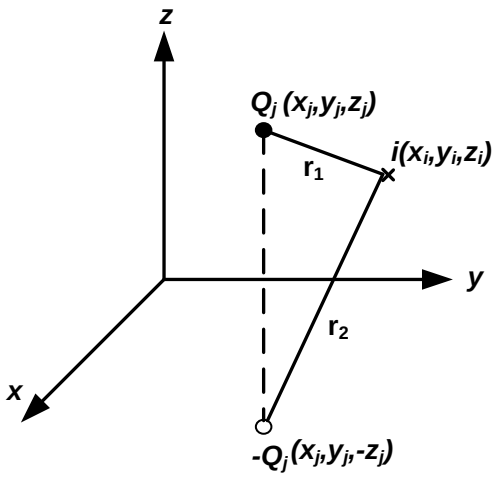

Fig. 16.3 Point Charge configuration along with its image

Expressions for the electric field intensity coefficients are as follows:

$$F_{x,ij} = -\frac{\partial P_{ij}}{\partial x} = \frac{1}{4\pi\varepsilon}\left[\frac{x_i - x_j}{r_1^{3/2}} - \frac{x_i - x_j}{r_2^{3/2}}\right] \quad \text{…. 16.17}$$

$$F_{y,ij} = -\frac{\partial P_{ij}}{\partial y} = \frac{1}{4\pi\varepsilon}\left[\frac{y_i - y_j}{r_1^{3/2}} - \frac{y_i - y_j}{r_2^{3/2}}\right] \quad \text{…. 16.18}$$

$$F_{z,ij} = -\frac{\partial P_{ij}}{\partial z} = \frac{1}{4\pi\varepsilon}\left[\frac{z_i - z_j}{r_1^{3/2}} - \frac{z_i + z_j}{r_2^{3/2}}\right] \quad \text{…. 16.19}$$

Infinite Length Line Charge

Infinite length line charges are used in 2-D configurations, particularly for simulating long conductors in the case of transmission lines, cables etc. Fig. 16.4 shows the infinite length line charge Q_j along with its image wrt to the *x*-*z* plane. In this configuration, electric field is considered to be independent of *z*-axis, i.e. the length of the long conductors, while the field varies in the *x*-*y* plane, which is normal to the length of the long conductors.

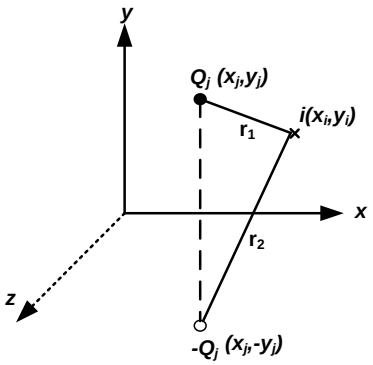

Fig. 16.4 Infinite length line charge configuration along with its image

In 2-D system, all computations are performed for unit length of the system under consideration. Hence, Q_j is the charge per unit length for the infinite length line charge.

The expression for potential coefficient is then given by

$$P_{ij} = \frac{1}{2\pi\varepsilon} \ln \frac{r_2}{r_1} \qquad \text{…. 16.20}$$

where, $r_1 = \left[(x_i - x_j)^2 + (y_i - y_j)^2 \right]^{1/2}$ and $r_2 = \left[(x_i - x_j)^2 + (y_i + y_j)^2 \right]^{1/2}$

Expressions for the electric field intensity coefficients are as follows:

$$F_{x,ij} = \frac{1}{2\pi\varepsilon} \left[\frac{(x_i - x_j)}{r_1^{\,2}} - \frac{(x_i - x_j)}{r_2^{\,2}} \right] \qquad \text{…. 16.21}$$

$$F_{y,ij} = \frac{1}{2\pi\varepsilon} \left[\frac{(y_i - y_j)}{r_1^{\,2}} - \frac{(y_i + y_j)}{r_2^{\,2}} \right] \qquad \text{…. 16.22}$$

Finite Length Line Charge

Finite length line charges of uniform charge density are used in axi-symmetric configurations, particularly for simulating cylindrical geometries in the case of bushings, circuit breakers etc. Fig. 16.5 shows the finite length line charge along with its image. Finite length line charges of uniform charge density are commonly placed on the *z*-axis, i.e. the axis of symmetry. Let, the magnitude of the finite length line charge be Q_j and the length of the charge be (z_{j2}-z_{j1}) as shown in Fig. 16.5. Then considering uniform charge density, charge per unit length is [Q_j/(z_{j2}-z_{j1})]. The expressions for potential and electric field intensity coefficients were first developed by Steinbigler et al [IEEE-PAS, 1974, pp 1660-1668] and are given below.

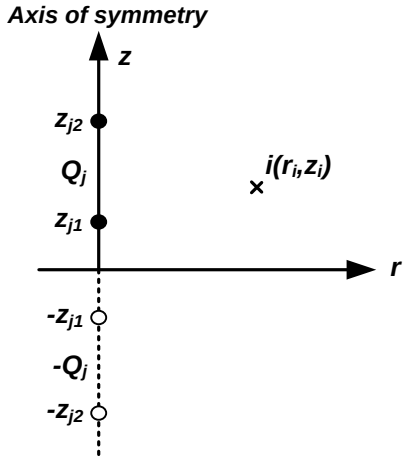

Fig. 16.5 Finite length line charge along with its image

The expression for potential coefficient is given by

$$P_{ij} = \frac{1}{4\pi\varepsilon(z_{j2} - z_{j1})} \left[\ln \frac{(z_{j2} - z_i + \gamma_1)(z_{j1} + z_i + \gamma_2)}{(z_{j1} - z_i + \delta_1)(z_{j2} + z_i + \delta_2)} \right] \qquad \text{…. 16.23}$$

where, $\gamma_1 = \sqrt{r_i^{\,2} + (z_{j2} - z_i)^2}$; $\delta_1 = \sqrt{r_i^{\,2} + (z_{j1} - z_i)^2}$

$\gamma_2 = \sqrt{r_i^{\,2} + (z_{j1} + z_i)^2}$ and $\delta_2 = \sqrt{r_i^{\,2} + (z_{j2} + z_i)^2}$

The expressions for the electric field intensity coefficients are as follows:

$$F_{r,ij} = \frac{1}{4\pi\varepsilon\left(z_{j2}-z_{j1}\right)}\left[\frac{z_{j2}-z_i}{r_i\gamma_1}-\frac{z_{j1}-z_i}{r_i\delta_1}+\frac{z_{j1}+z_i}{r_i\gamma_2}-\frac{z_{j2}+z_i}{r_i\delta_2}\right] \quad \text{…. 16.24}$$

$$F_{z,ij} = \frac{1}{4\pi\varepsilon\left(z_{j2}-z_{j1}\right)}\left[\frac{1}{\gamma_1}-\frac{1}{\delta_1}-\frac{1}{\gamma_2}+\frac{1}{\delta_2}\right] \quad \text{…. 16.25}$$

Ring Charge

Ring charges of uniform charge density are used in axi-symmetric configurations, particularly for simulating spherical and cylindrical shaped geometries etc. Fig. 16.6 shows the ring charge along with its image. Ring charges of uniform charge density are commonly placed with their axes on the *z*-axis, i.e. the axis of symmetry. Let, the magnitude of the ring charge be Q_j and the radius of the ring charge be r_j as shown in Fig. 16.6. Then considering uniform charge density, charge per unit length is $[Q_j /(2\pi r_j)]$. The expressions for potential and electric field intensity coefficients were first developed by Steinbigler et al [IEEE-PAS, 1974, pp 1660-1668] and are given below.

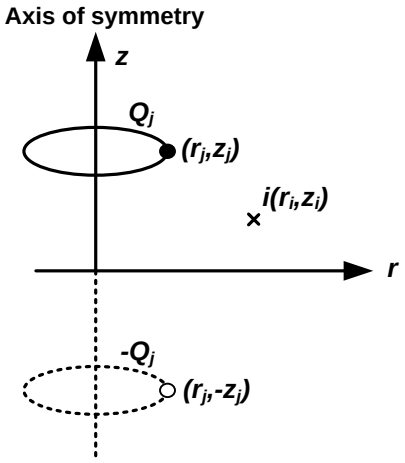

Fig. 16.6 Ring charge of uniform charge density along with its image

The expression for potential coefficient is given by

$$P_{ij} = \frac{1}{2\pi^2\varepsilon}\left[\frac{K(k_1)}{\alpha_1}-\frac{K(k_2)}{\alpha_2}\right] \quad \text{…. 16.26}$$

where, $\alpha_1 = \sqrt{\left(r_j+r_i\right)^2+\left(z_j-z_i\right)^2}$ and $\alpha_2 = \sqrt{\left(r_j+r_i\right)^2+\left(z_j+z_i\right)^2}$

$K(k_1)$ and $K(k_2)$ are elliptic integrals of first kind such that

$$K(k_1) = \int_o^{\pi/2}\frac{d\theta}{\sqrt{1-k_1^2\sin^2\theta}} \quad \text{and} \quad K(k_2) = \int_o^{\pi/2}\frac{d\theta}{\sqrt{1-k_2^2\sin^2\theta}}$$

$$k_1 = \frac{2\sqrt{r_i r_j}}{\alpha_1} \quad \text{and} \quad k_2 = \frac{2\sqrt{r_i r_j}}{\alpha_2}$$

The expressions for the electric field intensity coefficients are as follows:

$$F_{r,ij} = \frac{1}{4\pi^2 \varepsilon r_i}\left[\left\{\frac{\{(r_j^2 - r_i^2)+(z_j + z_i)^2\}E(k_2) - \beta_2^2 K(k_2)}{\alpha_2 \beta_2^2}\right\} - \left\{\frac{\{(r_j^2 - r_i^2)+(z_j - z_i)^2\}E(k_1) - \beta_1^2 K(k_1)}{\alpha_1 \beta_1^2}\right\}\right]$$

…. 16.27

$$F_{z,ij} = \frac{1}{2\pi^2 \varepsilon}\left[\frac{(z_j - z_i)E(k_1)}{\alpha_1 \beta_1^2} - \frac{(z_j + z_i)E(k_2)}{\alpha_2 \beta_2^2}\right] \qquad \text{…. 16.28}$$

where, $E(k_1)$ and $E(k_2)$ are elliptic integrals of second kind such that

$$E(k_1) = \int_o^{\pi/2} \sqrt{1 - k_1^2 \sin^2\theta}\; d\theta \quad \text{and} \quad E(k_2) = \int_o^{\pi/2} \sqrt{1 - k_2^2 \sin^2\theta}\; d\theta$$

$$\beta_1 = \{(r_j - r_i)^2 + (z_j - z_i)^2\}^{1/2} \quad \text{and} \quad \beta_2 = \{(r_j - r_i)^2 + (z_j + z_i)^2\}^{1/2}$$

Accuracy Criteria

If the fictitious charges completely satisfy the boundary conditions, then these charges give the correct field distribution not only on the boundary but also everywhere outside it. But in the CSM, the fictitious charges are required to satisfy the boundary conditions only at a selected number of contour points. Again the number of contour points is kept small in order to reduce the computer memory and computation time. Hence, it is essential to ensure that the simulation is accurate. To determine the simulation accuracy, the following criteria can be used.

i) The "potential error" on the electrode can be computed at a number of control points on the electrode surface between two contour points. The potential error is defined as the difference between the known potential of the electrode and the computed potential at the control point.

ii) Compared to the potential error the "deviation angle" on the electrode surface is a more sensitive indicator of the simulation accuracy. The deviation angle is defined as the angular deviation of the electric field intensity vector at the control point on the electrode surface from the direction of the normal to its surface.
Another very severe accuracy criterion is to check that the derivative of the potential gradient perpendicular to the electrode surface at the control point divided by the gradient itself is equal to the curvature at this point or not. This is especially applicable for simulation of areas of the electrode with a small radius of curvature.

iii) In multi-dielectric systems the "potential discrepancy" can be computed at a number of control points for each dielectric interface. The potential discrepancy is defined as the difference in the value of potential at the control point when computed from both the sides of the dielectric interface. Alternatively, the discrepancy in the tangential electric stress at the control points on the dielectric interface can also be computed. Another criterion for checking the simulation accuracy is to compute the discrepancy in the normal flux density at the control point on the dielectric interface.

For a good simulation all the above discrepancies should be small.

Factors Affecting Simulation Accuracy

The simulation accuracy in the CSM depends upon the types and number of fictitious charges as well as locations of fictitious charges and contour points. In general, the simulation error can be reduced by increasing the number of charges. However, it has been found that increasing the number of fictitious charges beyond a certain limit does not necessarily improve the simulation accuracy. Generally, the "assignment factor" (λ) defined as the ratio of the distance between a contour point and the corresponding charge (*a2*) to the distance between two successive contour points (*a1*), as shown in Fig. 16.14, considerably affects the simulation accuracy. Steinbigler et al (IEEE-PAS, 1974) suggested that this factor should be between 1.0 and 2.0. Several others suggest a range of $0.7<\lambda<1.5$.
In a good simulation, potential error values as low as 0.001% are possible. However, for sharp corners and thin electrodes, such low values are difficult to achieve. Since the electric field intensity error is an order of magnitude higher than the potential error, potential error values of about 0.1% are considered reasonable. For multi-dielectric systems, if the dielectric boundary has a complex shape, comparatively large potential discrepancy values of the order of 1% are usually acceptable.

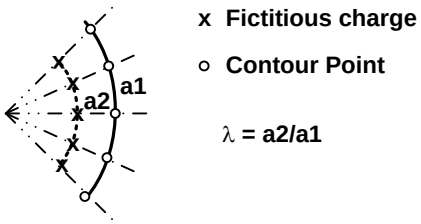

Fig. 16.14 Definition of assignment factor

Manufacturing tolerances of the conductors define the practical limit for the accuracy of the simulation of electrodes. In the same way, the accuracy of the determination of dielectric constants of the involved media puts the practical limit on the accuracy of the simulation of dielectrics.

Solution of System of Equations in CSM

The application of CSM for numerical field calculation involves solutions of linear systems of equations as explained in earlier sections. In the conventional CSM, for a single dielectric case, the matrix of the linear system of equations to be solved is in general asymmetrical without a zero term as detailed in section 16.2. In such cases, the equations could be solved using the Gaussian elimination technique with or without partial or complete pivoting.
In multi-dielectric systems, the matrix of systems of equations to be solved is rather heterogeneous and is not symmetrical as detailed in section 16.3. Due to bad conditioning of the matrix, it is preferable to solve it by using a direct method, e.g. Gaussian elimination technique, to avoid non-convergence problem, which may arise in the case of iterative methods. However, for complicated problems the size of the matrix becomes too large. In such cases, iterative methods such as Gauss-Seidel method or the successive over relaxation method with varying values of acceleration factor have also been found to be successful.

Other Development in CSM

Least Square Error CSM (LSECSM)

In this method, compared to conventional CSM, boundary conditions are satisfied at a larger number of contour points than the number of charges as shown in Fig. 16.15.

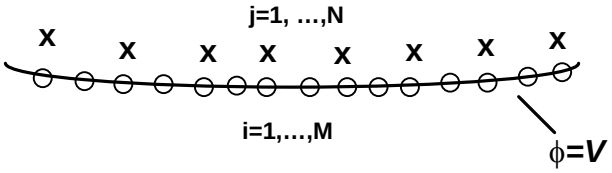

Fig. 16.15 Fictitious charges and contour points LSECSM

Hence, in the case of LSECSM the matrix of system of equation is a rectangular one having *M* rows and *N* columns.

$$[P]_{M\times N}\ [Q]_N = [V]_M \qquad \text{…. 16.84}$$

This equation is solved in the following way

$$[P^t]_{N\times M}\ [P]_{M\times N}\ [Q]_N = [P^t]_{N\times M}\ [V]_M$$

or,
$$[D]_{N\times N}\ [Q]_N = [F]_N \qquad \text{…. 16.85}$$

Eqn. 16.85 can be solved to find out the unknown fictitious charges. Anis et al (IEEE-PAS, 1977, pp1721-1730) most comprehensively presented this method. This method is expected to be more accurate than conventional CSM, but at the expense of more computation time. Again the accuracy depends upon the fitting ratio, i.e., the ratio of number of contour points to the number of charges. This ratio should be kept between 1 and 2. This method is applicable to multi-dielectric system, too.

Optimized CSM (OCSM)

In conventional CSM and also in LSECSM, the positions of the charges are specified and their magnitudes are solved. In OCSM, both magnitudes and locations of charges are determined by minimizing certain objective functions. Various versions of OCSM discussed in literature differ in the choice of objective function and the optimization algorithm. Most authors have used the least squared potential error as the objective function. Regarding the optimization techniques, constrained as well as unconstrained optimization has been used. Different algorithms such as Fletcher method, Rosenbrock method and Pattern Search method can be used. OCSM are applicable to multi-dielectric system also. Yializis et al (IEEE-PAS, 1978, pp2434-2440) proposed OCSM in details.

For a fixed number of simulation charges, the optimized methods will produce more accurate results. However, such an increased accuracy will be obtained at the expense of more computation time as well as computer memory and will require more complex programming. Hence, it is recommended to be used in those problems where conventional CSM or LSECSM methods fail to produce adequate accuracy.

Region Oriented CSM (ROCSM)

Conventional CSM is also called surface oriented CSM as discrete charges are used to simulate the electrode and dielectric surfaces. Conventional CSM suffers from difficulties associated with positioning the charges for complex geometries and thin electrodes. Region

oriented CSM aims at removing these drawbacks and making CSM applicable for a wide variety of 2D and 3D problems in HV engineering. Blaszczyk et al (IEEE-Magnetics, 1994, pp2924-2927) proposed the ROCSM originally.

The basic concept of region-oriented CSM is shown in Fig. 16.16. A two-dielectric arrangement is divided into four regions. Each region is homogeneous with regard to its material properties, and consists of one linear dielectric (*R1*, *R2* and *R3* contain ε_1 and *R4* contains ε_2). As shown in Fig. 16.16, a set of charges encloses each region separately and the field and the potential inside each region are calculated from the superposition of the surrounding charges. Interestingly, only a relatively small number of charges are necessary to calculate the fields in each region. Charges assigned to a region are not placed inside the region, but always at a certain distance away from its boundary. In this way singularity problem can be avoided. Passing through an interface requires changing the set of charges used for field calculation.

An important advantage of the region-oriented CSM is its ability to solve problems with thin conducting foils and thin dielectric layers. The conventional CSM requires that charges be placed within thin electrodes or dielectrics (R4 of Fig. 16.16), which results in a large number of charges or is even impossible when the thickness of the electrode is very small.

In region oriented CSM, charges can be placed far away from surfaces of such electrodes and dielectrics provided that different regions have been defined on their two sides. In Fig. 16.16, the large region between the two electrodes has been divided in some smaller parts by introducing fictitious boundaries. In this way four regions have been created, although there are only two dielectric media in this example. Charges can then be placed easily for even smaller regions, as shown for *Region-4* in Fig. 16.16(e).

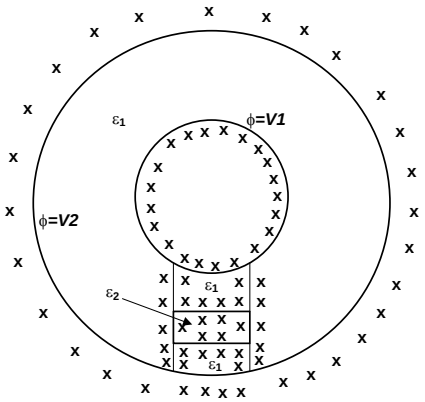

(a) Complete charge arrangement for ROCSM

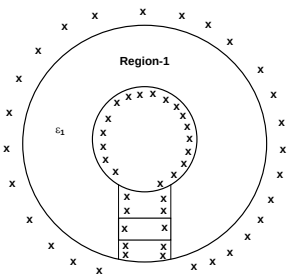

(b) Charge placement for Region-1

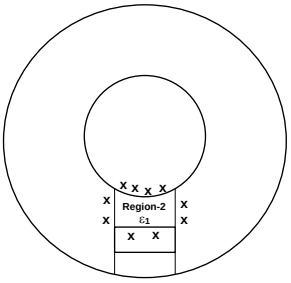

(c) Charge placement for Region-2

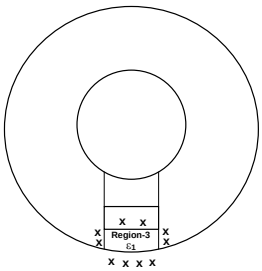

(d) Charge placement for Region-3

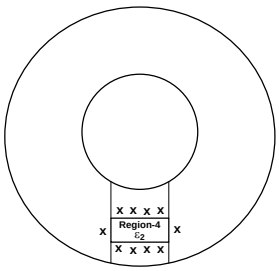

(e) Charge placement for Region-4

Fig. 16.16 Concept of arrangement of charges in Region Oriented CSM

Comparison of CSM with FEM

Both the FEM and CSM are extensively used for numerical calculation of electric field in high voltage engineering.

In FEM, the entire region of interest is subdivided into a large number of sub-regions and a set of coupled simultaneous linear equations, which minimize the electrostatic energy in the field region, are solved for unknown node potentials. On the other hand, in CSM only boundary surface, i.e. electrode surface and dielectric interfaces, are subdivided with fictitious charges which are taken as unknowns. Therefore, it follows that the amount of time and effort needed for subdivision is greatly reduced in CSM. Moreover, the system of equations thus obtained by discretization is of smaller dimension in CSM.

FEM is useful for two-dimensional and also three-dimensional systems with or without symmetry and is advantageous for the calculation of fields where the boundaries have complicated shapes. However, for computing field distribution at a large distance from the HV electrodes by FEM, a large number of nodes and hence excessive computation time and computer memory space are required. Thus, FEM is more suited for problems where the space is bounded. On the contrary, application of CSM is easy with high precision for field problems having infinity extended unbounded region and for relatively simple boundary geometries but not so for fields with complex electrode configurations.

In FEM exact field intensity at any point cannot be obtained. Instead average field intensity between two nodes is to be calculated from the known values of node potentials or numerical differentiation of the potential has to be done. But, in CSM the electric field intensity can be obtained explicitly with the fictitious charges without resorting to numerical differentiation of the potential, which results in significant reduction in error. With proper positioning of the fictitious charges and the contour points and with the optimum number of fictitious charges, the potential and stress errors can be made less than 0.01% and 0.1%, respectively, in CSM. Though FEM is more suited for multiple dielectric problems, CSM can also be effectively employed for fields with many dielectrics.

A major disadvantage of CSM was that the electric field is difficult to calculate in systems having very thin electrodes because fictitious charges have to be placed within the electrodes. However, this disadvantage is obviated by the application of Region Oriented CSM in recent years. Further, CSM is usually, more accurate and less trouble-some in computing Laplacian fields than FEM, but is difficult to use for non-Laplacian fields, e.g. Poissonian fields. However, CSM with complex fictitious charges has been developed for calculating Poissonian field including volume and surface resistance providing very accurate results. Again, CSM is not suited for specific fields containing space charges where FEM can be employed very effectively. But, now-a-days suitable boundary conditions have been postulated for use in connection with CSM for computing spacer surface fields in compact GIS as modified by the charges accumulated on the spacer surface.

Hybrid Method involving CSM and FEM

The most promising of the hybrid methods involving FEM and CSM is the so called combination method, which has been independently proposed by Steinbigler (3rd ISH, Milan, paper no. 11.11, 1979) and Okubo et al (3rd ISH, Milan, paper no. 11.13, 1979). In general, it may be observed that CSM has more or less the opposite properties of FEM. Thus attempts have been made to combine these two methods in a general purpose higher precision method that takes the superior properties and excludes the inferior properties of these two methods. Higher precision in numerical field computation can be obtained if the field region of interest is divided into parts to be analyzed by suitable methods. A field problem that could hardly be analyzed or that was analyzed approximately by only one method, may be analyzed with very good accuracy by applying an appropriate combination of different methods, e.g. FEM and CSM.

In the FEM-CSM hybrid method, the entire space is divided into regions, which are to be analyzed separately by the CSM (C-Domain) and by the FEM (F-Domain). The boundary between the two regions is called the combined surface. Due to the properties of each method, the CSM is mainly used for open areas with infinite boundary and the FEM is used for finite enclosed space usually containing dielectric interfaces, conductive dielectrics, space charges etc. It is to be noted that though CSM and FEM are two different methods, they result into similar linear system of equations. The coupling between C-Domain and F-Domain is based on the fact that the potential and the normal flux density must be continuous at the combined surface. Figs. 16.17(a) and 16.17(b) show how the entire field region is divided into CSM-region and FEM-region in the application of hybrid method in two-dielectric media and in space charge modified field computation, respectively.

Studies on combination method indicate that it offers advantages over the conventional CSM in 2D and 3D fields with axial symmetry for situation where space charges or conductive regions are present. Also, for the computation of 3D fields without axial symmetry, the advantages of combination method are significant.

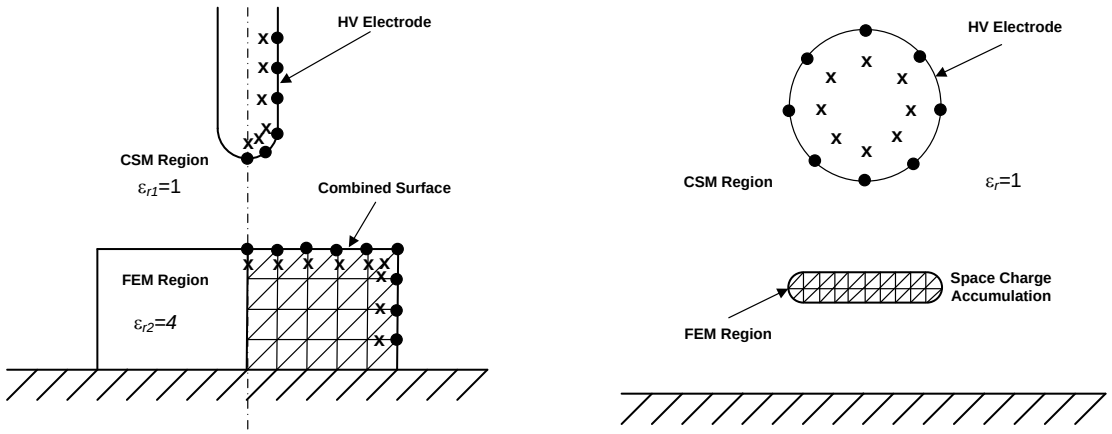

(a) Application in two-dielectric media (b) Application in space charge modified field

Fig. 16.17 Separation of field region into CSM-Region and FEM-Region in Hybrid Method

Numerical Computation of Capacitive-Resistive Field by Charge Simulation Method (CSM)

CSM with Complex Fictitious Charges

In order to calculate the field for a sinusoidal applied voltage, the calculations can be performed as a d.c. field in so far as the applied voltage does not change so fast that electromagnetic treatment is required. Then the instantaneous field strength is merely dependent on the applied voltage at that time instant. Thus the conventional CSM with real fictitious charges can be used to compute a.c. fields for three phase systems. It has been shown that the field distribution for sinusoidal applied voltage can be calculated in an efficient way by the use of complex fictitious charges. This is permitted because the fictitious charges also change sinusoidally with an angular frequency same as that of the applied voltage. Hence, by the use of complex fictitious charges, eqn. 16.1 is modified as follows.

$$\sum_{j=1}^{N} P_{ij}\overline{Q}_j = \overline{\phi} \qquad \text{…. 16.34}$$

where, a bar on a variable represents a complex quantity. Application of eqn. 16.34 to N number of contour points consists of a set of simultaneous linear equations for complex unknown charges $\overline{Q}_j$ with real coefficients as given below in matrix form.

$$[P]_{N\times N}\left[\overline{Q}\right]_N = \left[\overline{\phi}\right]_N \qquad \text{…. 16.35}$$

Eqn. 16.35 is solved to find complex solutions for the fictitious charges.

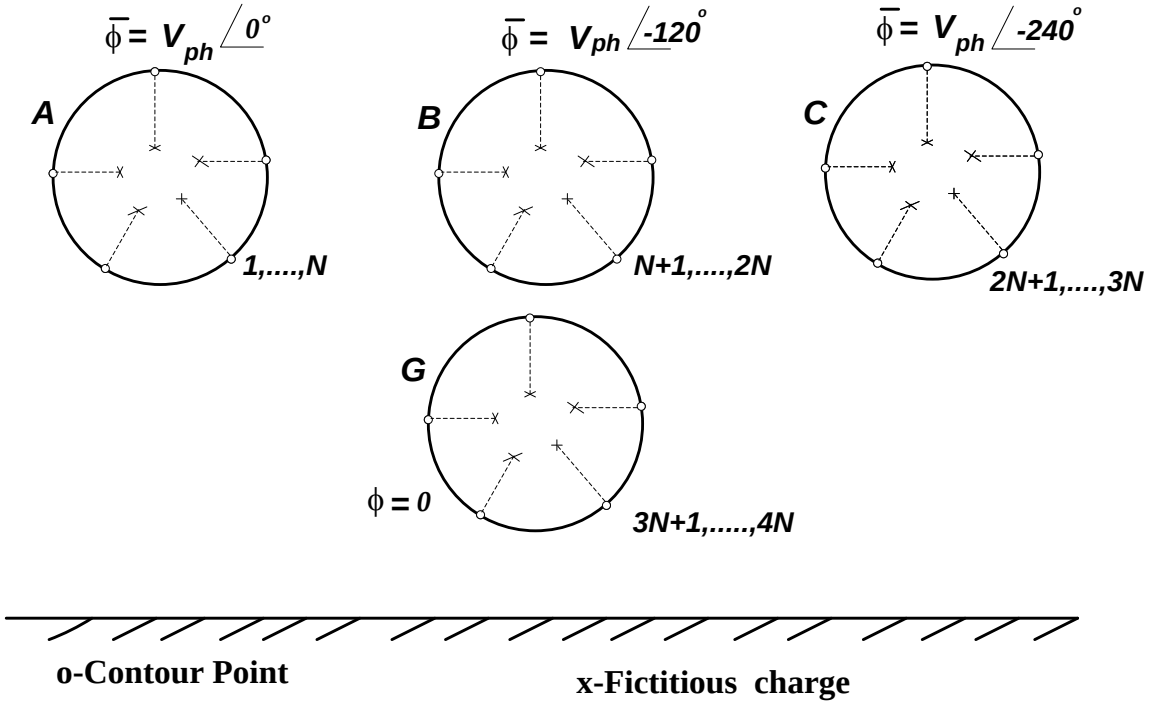

Fig. 16.9 Application of CSM with complex fictitious charge for a.c. field calculation

To explain the above technique in a detailed manner, consider the case of Fig. 16.9, which shows four conductors of which three are energized from a three-phase a.c. source, while the fourth one is grounded. Let, V_{ph} be the phase voltage of three phase source. Again, let there be N number of complex fictitious charges and contour points, respectively, for each

conductor. The charges and the contour points are numbered as follows, *1,……,N* for conductor *A*, *N+1,…..,2N* for conductor *B*, *2N+1,…..,3N* for conductor *C* and *3N+1,…..,4N* for conductor *G*. Then the application of eqn. 16.34 to all these contour points gives the following equations.

For conductor A: $$\sum_{j=1}^{4N} P_{ij}\overline{Q}_j = V_{ph}\angle 0^0, \quad for \quad i = 1,.....,N \qquad \text{…. 16.36}$$

For conductor B: $$\sum_{j=1}^{4N} P_{ij}\overline{Q}_j = V_{ph}\angle -120^0, \quad for\ i = N+1,.....,2N \qquad \text{…. 16.37}$$

For conductor C: $$\sum_{j=1}^{4N} P_{ij}\overline{Q}_j = V_{ph}\angle -240^0, \quad for\ i = 2N+1,.....,3N \qquad \text{…. 16.38}$$

For conductor G: $$\sum_{j=1}^{4N} P_{ij}\overline{Q}_j = 0, \quad for\ i = 3N+1,.....,4N \qquad \text{…. 16.39}$$

Eqns. 16.36 through 16.39 can be expressed in matrix form as follows:

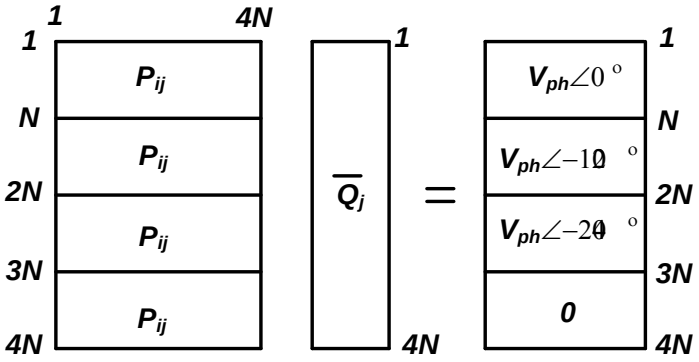

These equations are solved for the unknown complex fictitious charges $\overline{Q}_j$.

Capacitive-Resistive Field Computation by CSM

Normally high voltage equipment is insulated with materials of such a high resistivity that it can be treated as infinite for field calculation. In such cases, the field distribution is purely capacitive. But for lower values of volume or surface resistivity, the field distribution is capacitive-resistive or even resistive depending upon the value of resistivity. In the case of capacitive field distribution, the instantaneous field is independent of waveform of applied voltage. But a very distinctive feature of capacitive-resistive fields is their time dependency and dependency on the waveform of applied voltage. Hence, capacitive-resistive field calculation including volume or surface resistivity is very important in studying d.c. and low frequency fields, impulse fields, contaminated insulators, voltage dividers, cables etc.

Bachmann [3rd ISH, Milan, 1979, Paper No. 12.05] first proposed a technique based on CSM for capacitive-resistive field calculation. In his method, as the first step, the capacitive field distribution is calculated by CSM assuming resistivity to be infinite. Then the electrode-electrode and dielectric interface-electrode capacitances are calculated from this capacitive field distribution. After this as the second step, an equivalent *R-C* network is constructed which comprises of these capacitances and surface resistances. Finally, the voltage distribution for the capacitive-resistive field is calculated from the *R-C* network. This method has two major drawbacks. Firstly, the capacitances between the dielectric interface and electrode are dependent upon the field distribution and hence, are not identical in capacitive

and capacitive-resistive fields. Secondly, the calculation of field intensities from the *R-C* network is very laborious and results in significant errors.
Takuma et a1 [IEEE-PAS, 1981, pp 4665-4672] first proposed a method for direct simulation of the instantaneous capacitive-resistive field distribution with fictitious charges. Their method based on CSM and employing complex fictitious charges is generally extended so that any capacitive-resistive field including volume resistance or surface resistance can be calculated, when the field distribution is Laplacian in the region except on the boundaries. Use of complex fictitious charges as well as appropriate boundary conditions permits the simulation of non-linear and transient problems also. Singer [4th ISH, Athens, Paper No. 11.02, 1983] has used complex charges and Fourier integrals to calculate the impulse stresses of conductive dielectrics. Use of discrete as well as area complex charges have been reported for capacitive-resistive field calculation.

Capacitive-Resistive Field Computation including Volume Resistance

For capacitive-resistive field calculation including volume resistance, the principle of the method is that the field effect of the true charges produced by volume resistance is incorporated by means of complex fictitious charges in the CSM.
If the volume charge density is σ_v, then

$$\vec{\nabla}.\left(\varepsilon\overline{E}\right)=\sigma_v \qquad \text{…. 16.40}$$

where, $\overline{E}$ is the electric field intensity.
Again, if the current density through the volume of the dielectric is $\overline{J}$, then

$$\vec{\nabla}.\overline{J}=\vec{\nabla}.\left(\frac{\overline{E}}{\rho_v}\right)=-\frac{\partial\sigma_v}{\partial t} \qquad \text{…. 16.41}$$

where, ρ_v is the volume resistivity and is constant, i.e. independent of $\overline{E}$.
Now, if ε is independent of time *t* and *E*, then Eqn. 16.40 can be modified as follows

$$\vec{\nabla}.\left(\varepsilon\frac{\partial\overline{E}}{\partial t}\right)=\frac{\partial\sigma_v}{\partial t} \qquad \text{…. 16.42}$$

Eqns. 16.41 and 16.42 lead to

$$\vec{\nabla}.\left(\frac{\overline{E}}{\rho_v}+\varepsilon\frac{\partial\overline{E}}{\partial t}\right)=0 \qquad \text{…. 16.43}$$

For, a.c. fields of angular frequency ω, $\overline{E} = E_m sin\omega t$. Hence,

$$\frac{\partial\overline{E}}{\partial t}=j\omega\overline{E}$$

Thus, eqn. 16.43 can be rewritten as

$$\vec{\nabla}.\left(\frac{\overline{E}}{\rho_v}+j\omega\varepsilon\overline{E}\right)=0$$

or,

$$\vec{\nabla}.\left\{\left(\frac{1}{\rho_v}+j\omega\varepsilon\right)\overline{E}\right\}=0 \qquad \text{…. 16.44}$$

Eqn. 16.44 shows that the fields including volume resistivity ρ_v can be computed by replacing the permittivity ε in purely capacitive field with the complex permittivity $\bar{\varepsilon}$ such that,

$$\vec{\nabla}.\left(\bar{\varepsilon}.\overline{E}\right)=0 \qquad \text{…. 16.45}$$

where, $\left(\bar{\varepsilon} = \varepsilon + \frac{1}{j\omega\rho_v} \right)$

Again, if $\bar{\varepsilon}$ is constant in the region of field calculation, then eqn. 16.45 becomes the Laplace's equation as given below.

$$\vec{\nabla}.\bar{E} = 0$$

Eqn. 16.45 permits the use of CSM for capacitive-resistive field calculation including volume resistance. However, from the above discussion, it becomes clear that in fields containing volume resistance, CSM cannot be applied to problems where ε or ρ_v is dependent on the electric field. This is because in such cases the field distribution cannot be expressed by superposing solutions of Laplace's equation.

The above method can be explained explicitly as described below. Consider a two-dielectric arrangement as shown in Fig. 16.10. In Fig. 16.10 the two dielectric media are assumed to have volume resistivities of ρ_{vA} and ρ_{vB}, respectively. The charges and the contour points are numbered in the same way as that given in earlier section. However, in earlier section only real fictitious charges were taken for capacitive field calculation. But, for capacitive-resistive field calculation including volume resistance, complex fictitious charges are employed in place of real fictitious charges. The system of equations to be solved for unknown charges is derived by imposing the boundary conditions on the electrode surfaces and on the dielectric interfaces. The resulting equations with complex treatment are as follows.

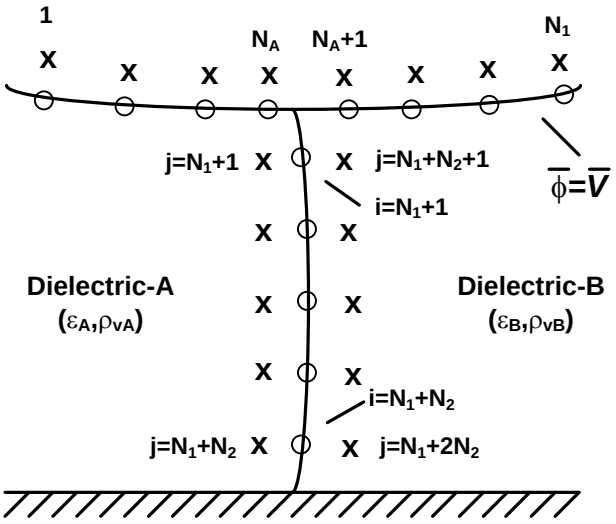

Fig. 16.10 Multi-dielectric arrangement with volume resistivities

i) Dirichlet's condition on the electrode surface:

$$\bar{\phi}(i) = \bar{V} \qquad \text{…. 16.46}$$

Eqn. 16.46 can be expanded for all the contour points on the electrode surface in the following way.

$$\sum_{j=1}^{N_1} P_{ij}\bar{Q}_j + \sum_{j=N_1+N_2+1}^{N_1+2N_2} P_{ij}\bar{Q}_j = \bar{V} \qquad \text{..... } i = 1,..., N_A \qquad \text{…. 16.47}$$

and

$$\sum_{j=1}^{N_1} P_{ij}\bar{Q}_j + \sum_{j=N_1+1}^{N_1+N_2} P_{ij}\bar{Q}_j = \bar{V} \qquad \text{..... } i = N_A+1,..., N_1 \qquad \text{…. 16.48}$$

ii) Potential continuity condition on the dielectric interface:

$$\bar{\phi}_A(i) = \bar{\phi}_B(i) \qquad \text{…. 16.49}$$

where, the subscripts *A* and *B* denote dielectric *A* and *B*, respectively. Eqn. 16.49 can be detailed explicitly as follows.

$$\sum_{j=N_1+1}^{N_1+N_2} P_{ij}\overline{Q}_j - \sum_{j=N_1+N_2+1}^{N_1+N_2} P_{ij}\overline{Q}_j = 0 \qquad \text{..... } i = N_1+1,...,N_1+N_2 \qquad \text{…. 16.50}$$

iii) Continuity condition of D_n on the dielectric interface:

$$\overline{D}_{nA}(i) - \overline{D}_{nB}(i) = \overline{\sigma}(i) \qquad \text{…. 16.51}$$

where, D_n and σ represent normal component of electric flux density and surface charge density, respectively.

Eqn. 16.51 can also be written as

$$\varepsilon_A \overline{E}_{nA}(i) - \varepsilon_B \overline{E}_{nB}(i) = \overline{\sigma}(i) \qquad \text{…. 16.52}$$

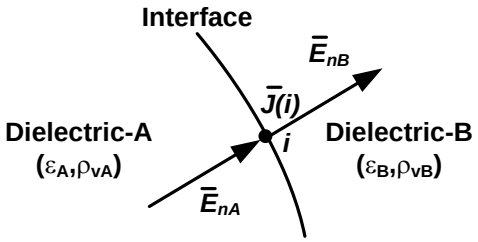

Fig. 16.11 Determination of surface current density due to volume resistivities

Now, the surface current density $\bar{J}(i)$ at any point *i* on the dielectric interface due to volume resistance can be obtained as follows from Eqn. 16.53. For the case shown in Fig. 16.11, $\bar{J}(i)$ is given by

$$\overline{J}(i) = \frac{\overline{E}_{nB}(i)}{\rho_{vB}} - \frac{\overline{E}_{nA}(i)}{\rho_{vA}} \qquad \text{…. 16.53}$$

The surface charge density $\bar{\sigma}(i)$ at any point *i* on the dielectric interface is given by

$$\overline{\sigma}(i) = \int \bar{J}(i)dt$$

Hence,

$$\overline{\sigma}(i) = \int \left[\frac{\overline{E}_{nB}(i)}{\rho_{vB}} - \frac{\overline{E}_{nA}(i)}{\rho_{vA}} \right] dt \qquad \text{…. 16.54}$$

Now, for a.c. fields of angular frequency ω, $\int \frac{\overline{E}_{nB}(i)}{\rho_{vB}} dt = \frac{\overline{E}_{nB}(i)}{j\omega\rho_{vB}}$

So, Eqn. 16.54 can be rewritten as

$$\overline{\sigma}(i) = \frac{\overline{E}_{nB}(i)}{j\omega\rho_{vB}} - \frac{\overline{E}_{nA}(i)}{j\omega\rho_{vA}} \qquad \text{…. 16.55}$$

Thus, Eqns. 16.52 and 16.55 lead to

$$\left(\varepsilon_A + \frac{1}{j\omega\rho_{vA}} \right) \overline{E}_{nA}(i) = \left(\varepsilon_B + \frac{1}{j\omega\rho_{vB}} \right) \overline{E}_{nB}(i) \qquad \text{…. 16.56}$$

or,

$$\bar{\varepsilon}_A \overline{E}_{nA}(i) - \bar{\varepsilon}_B \overline{E}_{nB}(i) = 0 \qquad \text{…. 16.57}$$

where,

$$\bar{\varepsilon}_A = \left(\varepsilon_A + \frac{1}{j\omega\rho_{vA}} \right) \text{ and } \bar{\varepsilon}_B = \left(\varepsilon_B + \frac{1}{j\omega\rho_{vB}} \right)$$

Eqn. 16.57 is given below in details

$$\bar{\varepsilon}_A\left[\sum_{j=1}^{N_1} F_{n,ij}\bar{Q}_j + \sum_{j=N_1+N_2+1}^{N_1+2N_2} F_{n,ij}\bar{Q}_j\right] - \bar{\varepsilon}_B\left[\sum_{j=1}^{N_1} F_{n,ij}\bar{Q}_j + \sum_{j=N_1+1}^{N_1+N_2} F_{n,ij}\bar{Q}_j\right] = 0 \qquad \ldots. 16.58$$

Eqns. 16.47, 16.48, 16.50 and 16.58 can be represented in matrix form as given below.

	1	N_1	N_1+N_2	N_1+2N_2		1		1
1	P_{ij}	0	P_{ij}					
N_A	P_{ij}	P_{ij}	0					
N_1	0	P_{ij}	$-P_{ij}$		$\bar{Q}_j$	=	$\bar{V}$	N_1
N_1+N_2	$(\bar{\varepsilon}_A-\bar{\varepsilon}_B)$ $F_{n,ij}$	$-\bar{\varepsilon}_B$ $F_{n,ij}$	$\bar{\varepsilon}_A$ $F_{n,ij}$				0	
N_1+2N_2					N_1+2N_2		N_1+2N_2	

$\ldots.$ 16.59

It follows from Eqn. 16.59 that these are same as those for capacitive field, if the real values of the fictitious charges, permittivity, potential and field strength are replaced by their complex values.

Capacitive-Resistive Field Computation including Surface Resistance

In fields including only surface resistance, true charges exist only on the boundary, i.e. electrode and dielectric surfaces, and not inside the dielectric medium. As a result, the field distribution is always Laplacian inside each medium. This permits the application of CSM to capacitive-resistive field calculation including surface resistance. The field distribution is obtained by superposing the effects of complex fictitious charges properly arranged inside the electrode and on both sides of the dielectric interface. The effect of true surface charges has to be incorporated into that of the complex fictitious charges.

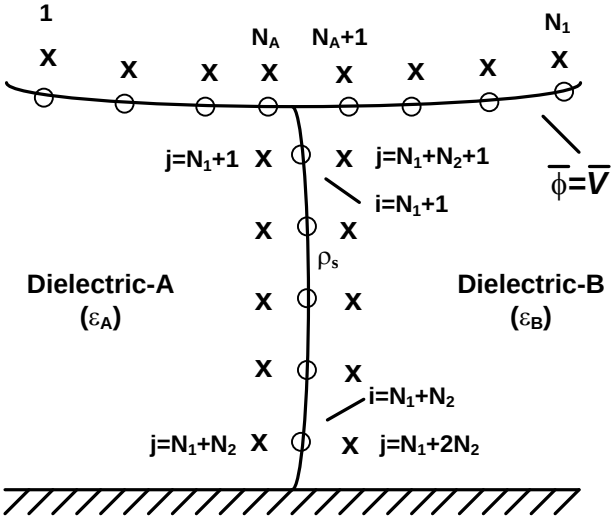

Fig. 16.12 Multi-dielectric arrangement with surface resistivity

The method can be better explained by considering the two-dielectric arrangement shown in Fig. 16.12. The difference is that, in this case, the volume resistivities of the two dielectrics are considered to be infinite and a uniform surface resistivities ρ_s is considered along the dielectric interface. The boundary conditions (i) and (ii) as given by eqns. 16.46 and 16.49, respectively, as well as the eqns. 16.47, 16.48 and 16.50, in the case of volume resistance as given in sub-section 16.6.1, are also valid in the case of surface resistance. However, the

expression of surface charge density σ in continuity condition of $\overline{D}_n$, as given by eqn. 16.51 in sub-section 16.6.1, has to be modified as follows.

In fields including surface resistance, the true surface charge density $\sigma(i)$ is expressed as given below.

$$\sigma(i) = \frac{1}{S(i)} \int_o^t I(i)\, dt \qquad \text{…. 16.60}$$

where, *I(i)* is the net surface current flowing into the *ith* contour point and *S(i)* is a small surface area corresponding to that contour point. For two-dimensional or axi–symmetric cases, where the surface current *I(i)* flows in a predetermined direction, $\sigma(i)$ can be expressed in terms of neighboring potentials and resistances as shown in Fig. 16.13.

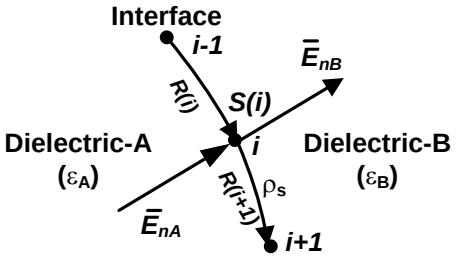

Fig. 16.13 Determination of surface current density due to surface resistivity

$$\sigma(i) = \frac{1}{S(i)} \int_o^t \left[\frac{\phi(i-1) - \phi(i)}{R(i)} - \frac{\phi(i) - \phi(i+1)}{R(i+1)} \right] \qquad \text{…. 16.61}$$

where, *R(i)* and *R(i+1)* are surface resistances corresponding to *ith* and *(i+1)th* contour points, respectively, as shown in Fig. 16.13. The expressions for *R(i)* and *S(i)* are detailed below.

i) For two–dimensional system (per unit length)

$$R(i) = \int_{i-1}^{i} \rho_s\, dl \qquad \text{…. 16.62}$$

$$S(i) = \int_{i-1}^{i+1} dl / 2 \qquad \text{…. 16.63}$$

ii) For axi-symmetric system

$$R(i) = \int_{i-1}^{i} \frac{\rho_s(i)}{2\pi r'} dl \qquad \text{…. 16.64}$$

$$S(i) = \int_{i-1}^{i+1} \pi r' dl \qquad \text{…. 16.65}$$

where, r' is the *r*-coordinate of *d1* and *d1* is a small length along the dielectric interface.

For a.c. fields of angular frequency ω, eqn. 16.61 is modified as follows.

$$\overline{\sigma}(i) = \frac{1}{j\omega S(i)} \left[\frac{\overline{\phi}(i-1) - \overline{\phi}(i)}{R(i)} - \frac{\overline{\phi}(i) - \overline{\phi}(i+1)}{R(i+1)} \right] \qquad \text{…. 16.66}$$

Hence, from eqns. 16.52 and 16.66, it follows that

$$\varepsilon_A \overline{E}_{nA}(i) - \varepsilon_B \overline{E}_{nB}(i) = \frac{1}{j\omega S(i)} \left[\frac{\overline{\phi}(i-1) - \overline{\phi}(i)}{R(i)} - \frac{\overline{\phi}(i) - \overline{\phi}(i+1)}{R(i+1)} \right] \qquad \text{…. 16.67}$$

Eqn. 16.67 can be expressed explicitly as follows for the system of Fig. 16.12.

$$\varepsilon_A\left[\sum_{j=1}^{N_1}F_{n,ij}\overline{Q}_j+\sum_{j=N_1+N_2+1}^{N_1+2N_2}F_{n,ij}\overline{Q}_j\right]-\varepsilon_B\left[\sum_{j=1}^{N_1}F_{n,ij}\overline{Q}_j+\sum_{j=N_1+1}^{N_1+N_2}F_{n,ij}\overline{Q}_j\right]$$
$$-\frac{1}{j\omega S(i)R(i)}\left[\sum_{j=1}^{N_1}P_{i-1,j}\overline{Q}_j+\sum_{j=N_1+1}^{N_1+N_2}P_{i-1,j}\overline{Q}_j\right]-\frac{1}{j\omega S(i)R(i+1)}\left[\sum_{j=1}^{N_1}P_{i+1,j}\overline{Q}_j+\sum_{j=N_1+1}^{N_1+N_2}P_{i+1,j}\overline{Q}_j\right]$$
$$+\frac{1}{j\omega S(i)}\left(\frac{1}{R(i)}+\frac{1}{R(i+1)}\right)\left[\sum_{j=1}^{N_1}P_{i,j}\overline{Q}_j+\sum_{j=N_1+1}^{N_1+N_2}P_{i,j}\overline{Q}_j\right]=0 \quad \textit{for } i=N_1+1,\ldots,N_1+N_2$$

…. 16.68

Now, the system of equations to be solved for unknown complex charges $\overline{Q}_j$ as given by Eqns. 16.47, 16.48, 16.50 and 16.68 can be expressed in matrix form as given below.

	1	N_1	N_1+N_2	N_1+2N_2		1		1
1	P_{ij}	0	P_{ij}					
N_A	P_{ij}	P_{ij}	0		$\overline{Q}_j$	=	$\overline{V}$	N_1
N_1	0	P_{ij}	$-P_{ij}$				0	
N_1+N_2	$\overline{C}_1$	$\overline{C}_2$	$\varepsilon_A F_{n,ij}$					
	N_1+2N_2					N_1+2N_2		N_1+2N_2

…. 16.69

where, $\overline{C}_1$ and $\overline{C}_2$ are two complex coefficients as given below.

$$\overline{C}_1=(\varepsilon_A-\varepsilon_B)F_{n,ij}-\frac{P_{i-1,j}}{j\omega S(i)R(i)}-\frac{P_{i+1,j}}{j\omega S(i)R(i+1)}+\frac{P_{ij}}{j\omega S(i)}\left(\frac{1}{R(i)}+\frac{1}{R(i+1)}\right) \quad \text{…. 16.70}$$

$$\overline{C}_2=-\varepsilon_B F_{n,ij}-\frac{P_{i-1,j}}{j\omega S(i)R(i)}-\frac{P_{i+1,j}}{j\omega S(i)R(i+1)}+\frac{P_{ij}}{j\omega S(i)}\left(\frac{1}{R(i)}+\frac{1}{R(i+1)}\right) \quad \text{…. 16.71}$$

From the matrix given in the sub-section 16.6.2 as well as the matrix given in sub-section 16.6.1, it is important to note that the equations contain not only complex charges but also complex coefficients.

Field Computation by CSM under Transient Voltage

Transient problems, where the applied voltage has an arbitrary waveform, are difficult to solve directly by CSM. For computing transient fields, there are two techniques. In the technique proposed by Singer (4th ISH, Athens, paper no. 11.02, 1983), the transient voltages are decomposed into sinusoidal components by means of Fourier analysis or Fourier transformation. Field distribution due to individual sinusoidal components is calculated by CSM using complex fictitious charges. The complex a.c. responses for the needed frequencies are then weighted and summed up in order to get the time-dependent capacitive-resistive field distribution. In general, it is not necessary to calculate the field distribution for all the frequencies and it is sufficient to calculate the field distribution for some fixed reference frequencies. The results for the intermediate frequencies are then interpolated from the results for the reference frequencies.

In the other technique proposed by Takuma et al (IEEE-PAS, 1981, pp4665-4672) for transient field calculation, the integral of eqn. 16.54 or 16.61 are approximated with a

summation over a succession of sufficiently short time intervals to obtain the field distribution in relation to time discretely by CSM. Only real fictitious charges are used in this case for computation of transient capacitive-resistive field. This technique can be better explained in the following way.

In transient fields, where the voltage applied is $\phi=V(t)$, the field distribution is calculated by dividing the entire time-span into short intervals Δt and by converting the integral form of eqns. 16.54 or 16.61 to the iterative summation. In this case, since the real fictitious charges are used, the eqns. 16.47, 16.48 and 16.50 are also valid without the complex treatment, for the arrangement shown in Fig. 16.10. However, the continuity condition of $\overline{D}_n$ has to be modified. The necessary modifications and the resulting equations for the transient field calculation including volume resistance or surface resistance are discussed below.

Transient Field Computation including Volume Resistance

At the time instant $t1=\Delta t1$, eqn. 16.52 without the complex treatment can be written as

$$\varepsilon_A E_{nA}(i)_1 - \varepsilon_B E_{nB}(i)_1 = \sigma(i)_1 \qquad \text{…. 16.72}$$

where, the integral form of surface charge density, as given by eqn. 16.54, is modified as follows.

$$\sigma(i)_1 = \Delta t_1 \left[\frac{E_{nB}(i)_1}{\rho_B} - \frac{E_{nA}(i)_1}{\rho_A} \right] \qquad \text{…. 16.73}$$

where, the subscript *1* denotes time instant $t1 = \Delta t1$.

Hence, eqn. 16.72 can be written as follows

$$\varepsilon_A E_{nA}(i)_1 - \varepsilon_B E_{nB}(i)_1 = \Delta t_1 \left[\frac{E_{nB}(i)_1}{\rho_B} - \frac{E_{nA}(i)_1}{\rho_A} \right] \qquad \text{…. 16.74}$$

Then the real fictitious charges can be determined for the time instant $t1 = \Delta t1$ by solving a set of simultaneous linear equations constructed from eqn. 16.74 along with eqns. 16.47, 16.48 and 16.50 without the complex treatment.

Then at the time instant $t2 = \Delta t1 + \Delta t2$

$$\varepsilon_A E_{nA}(i)_2 - \varepsilon_B E_{nB}(i)_2 = \sigma(i)_2 \qquad \text{…. 16.75}$$

where, $$\sigma(i)_2 = \sigma(i)_1 + \Delta t_2 \left[\frac{E_{nB}(i)_2}{\rho_B} - \frac{E_{nA}(i)_2}{\rho_A} \right] \qquad \text{…. 16.76}$$

Since $\sigma(i)_1$ is known for the time instant $t1 = \Delta t1$, the real fictitious charges and hence, the field distribution for the time instant $t2 = \Delta t1 + \Delta t2$ can be obtained from eqns. 16.75 and 16.76 along with eqns. 16.47, 16.48 and 16.50 without the complex treatment. Thus, this iterative sequence gives the field distribution for $\phi=V(t)$ at any time instant.

The equations to be solved for real fictitious charges at the *nth* time instant, $t_n = \Delta t_1 + \Delta t_2 + \text{---} + \Delta t_n$ can be given in matrix form as follows.

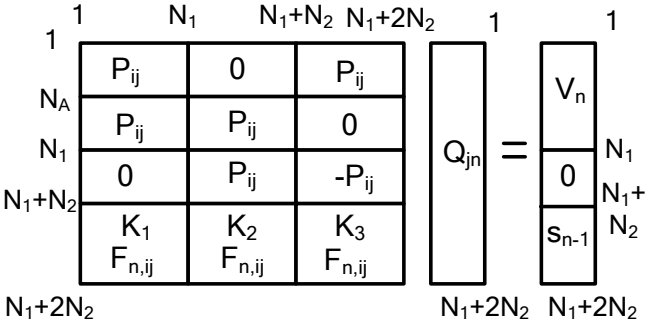

…. 16.77

where, the subscripts *n* and *n-1* denote *nth* and *(n-1)th* time instants respectively, and *K1*, *K2* and *K3* are three real constants as detailed below.

$$K_1 = \left(\varepsilon_A + \frac{\Delta t_n}{\rho_A}\right) - \left(\varepsilon_B + \frac{\Delta t_n}{\rho_B}\right),\ K_2 = -\left(\varepsilon_B + \frac{\Delta t_n}{\rho_B}\right) \text{and } K_3 = \left(\varepsilon_A + \frac{\Delta t_n}{\rho_A}\right)$$

Transient Field Computation including Surface Resistance

At the time instant $t1 = \Delta t1$, in the continuity condition of $\overline{D}_n$ the expression for the surface charge density $\sigma(i)_1$ can be written as follows.

$$\sigma(i)_1 = \frac{\Delta t_1}{S(i)}\left[\frac{\phi(i-1)_1 - \phi(i)_1}{R(i)} - \frac{\phi(i)_1 - \phi(i+1)_1}{R(i+1)}\right] \quad \text{…. 16.78}$$

Eqn. 16.78 is a modified equation derived from the integral form, as given by eqn. 16.61. Thus, the continuity condition of D_n can be written as follows

$$\varepsilon_A E_{nA}(i)_1 - \varepsilon_B E_{nB}(i)_1 = \frac{\Delta t_1}{S(i)}\left[\frac{\phi(i-1)_1 - \phi(i)_1}{R(i)} - \frac{\phi(i)_1 - \phi(i+1)_1}{R(i+1)}\right] \quad \text{…. 16.79}$$

Hence, the real fictitious charges can be determined for the time instant $t1 = \Delta t1$ from eqn. 16.79 along with eqns. 16.47, 16.48 and 16.50 without the complex treatment.

Then at the time instant $t2 = \Delta t1 + \Delta t2$

$$\varepsilon_A E_{nA}(i)_2 - \varepsilon_B E_{nB}(i)_2 = \sigma(i)_2$$

where,
$$\sigma(i)_2 = \sigma(i)_1 + \frac{\Delta t_2}{S(i)}\left[\frac{\phi(i-1)_2 - \phi(i)_2}{R(i)} - \frac{\phi(i)_2 - \phi(i+1)_2}{R(i+1)}\right] \quad \text{…. 16.80}$$

By using $\sigma(i)_1$ as obtained for the time instant $t1 = \Delta t1$ the real fictitious charges for the time instant $t2 = \Delta t1 + \Delta t2$ can be obtained from eqn. 16.80 along with eqns. 16.47, 16.48 and 16.50 without the complex treatment. Hence, this iterative sequence gives the field distribution for $\phi = V(t)$ at any time instant.

The equations to be solved for real fictitious charges at the *nth* time instant, $t_n = \Delta t_1 + \Delta t_2 + \text{---} + \Delta t_n$ can be given in matrix form as follows.

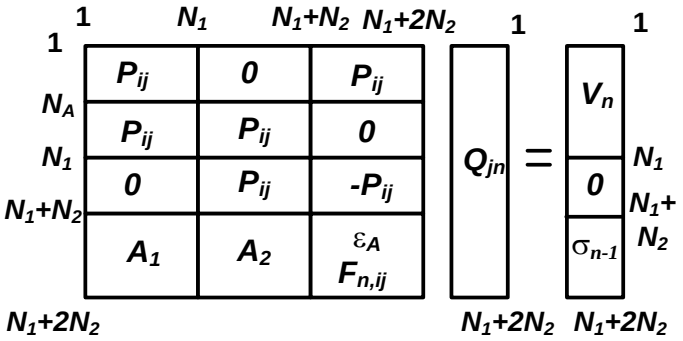

…. 16.81

where, *A1* and *A2* are two real coefficients as detailed below.

$$A_1 = (\varepsilon_A - \varepsilon_B)F_{n,ij} - \frac{\Delta t_n P_{i-1,j}}{S(i)R(i)} - \frac{\Delta t_n P_{i+1,j}}{S(i)R(i+1)} + \frac{\Delta t_n P_{ij}}{S(i)}\left(\frac{1}{R(i)} + \frac{1}{R(i+1)}\right) \quad \text{…. 16.82}$$

and $$A_2 = (-\varepsilon_B)F_{n,ij} - \frac{\Delta t_n P_{i-1,j}}{S(i)R(i)} - \frac{\Delta t_n P_{i+1,j}}{S(i)R(i+1)} + \frac{\Delta t_n P_{ij}}{S(i)}\left(\frac{1}{R(i)} + \frac{1}{R(i+1)}\right) \quad \text{…. 16.83}$$

In general, the time interval Δt for various time steps can have different values. However, they may be made equal for all the time steps for simplicity.

Sphere or Cylinder in Uniform External Field

Introduction

Conducting and dielectric components are integral parts of any electrical equipment. If the size of the conducting or dielectric object is very small compared to dimensions of the field region where the object is located, then the object contributes to the field only in the domain near the object. In many cases, such objects are present as stray bodies in high voltage insulation arrangement. As practical examples one may cite a small piece of conductor or dielectric floating in liquid insulation of large volume in transformers, metallic dust particles floating in gaseous insulation within gas insulated system etc. It is important to understand how the presence of a conducting or dielectric object modifies the external field in the vicinity of the object, because any enhancement of electric field intensity due to the conducting or dielectric object may lead to unwanted discharge or in the worst case failure of the insulation system.

If it is assumed that the source charges (in practical arrangement, the electrodes or conductors with specific potentials) that produce the external field is located far away from the object under consideration, then they are unaffected by the presence of the object. Consequently, the field due to the source charges may be considered to be uniform at the location of the object. If the object is such that its shape is defined by well known mathematical functions, e.g. cylinders or spheres, then the complete solution for electric field due to the source charges located at far away positions and the induced charges on the surface of the object could be obtained by solving Laplace's equation considering the field region to be free from any volume charge. However, in order to get the complete solution appropriate boundary conditions on the surface of the object, whether it is conducting or dielectric, need to be satisfied. One of the common methods of getting the analytical solution for cylinder or sphere in uniform external field is the method of separation of variables as described in this chapter.

Sphere in Uniform External Field

Consider a spherical object of radius *a* within a uniform external field as shown in Fig.10.1. Since the boundary is a sphere of *r=constant,* hence the system is best described in spherical coordinates as shown in Fig.10.1. The uniform external field is given by $\vec{E}_0 = -E_0\hat{u}_z$ and the potential at any point due to the external field is given by $E_0 r\cos\theta = E_0 z$ with respect to the center of the sphere. In order to get the complete solution for electric field in this system, Laplace's equation in spherical coordinates as given in eqn.(10.1) needs to be solved.

$$\frac{1}{r^2}\frac{\partial}{\partial r}\left(r^2\frac{\partial V}{\partial r}\right)+\frac{1}{r^2\sin\theta}\frac{\partial}{\partial\theta}\left(\sin\theta\frac{\partial V}{\partial\theta}\right)+\frac{1}{r^2\sin^2\theta}\frac{\partial^2 V}{\partial\phi^2}=0 \qquad \text{…. 10.1}$$

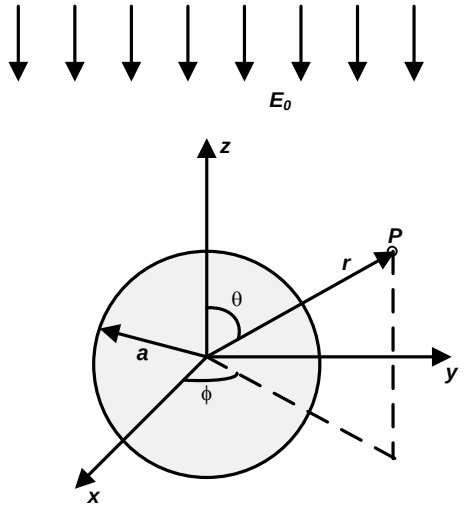

Fig.10.1 Sphere in uniform external field

The field system has azimuthal symmetry wrt the *z*-axis, i.e. the field system does not change with the rotation around the *z*-axis. So *z*-axis is made the polar axis in the spherical coordinate system. Then the field is independent of coordinate ϕ and the Laplace's equation reduces to

$$\frac{1}{r^2}\frac{\partial}{\partial r}\left(r^2\frac{\partial V}{\partial r}\right)+\frac{1}{r^2\sin\theta}\frac{\partial}{\partial\theta}\left(\sin\theta\frac{\partial V}{\partial\theta}\right)=0 \qquad \text{…. 10.2}$$

In order to separate the terms of the LHS of eqn.(10.2) into functions of only one variable, eqn.(10.2) may be rewritten by multiplying r^2 as

$$\frac{\partial}{\partial r}\left(r^2\frac{\partial V}{\partial r}\right)+\frac{1}{\sin\theta}\frac{\partial}{\partial\theta}\left(\sin\theta\frac{\partial V}{\partial\theta}\right)=0 \qquad \text{…. 10.3}$$

Then LHS of eqn.(10.3) is the sum of two terms which are functions of only one variable each, i.e. the first term is function of *r* only while the second term is function of θ only. The solution to eqn.(10.3) can be obtained as the product of two functions of which one is dependent only on *r* while the other is dependent only on θ.

Let the assumed solution be $V(r,\theta)=M(r)\,N(\theta)$ …. 10.4

The assumed solution is convenient as the boundary lies at *r=constant*.

Combining eqn.(10.3) and (10.4)

$$\frac{\partial}{\partial r}\left(r^2\frac{\partial M(r)\,N(\theta)}{\partial r}\right)+\frac{1}{\sin\theta}\frac{\partial}{\partial\theta}\left(\sin\theta\frac{\partial M(r)\,N(\theta)}{\partial\theta}\right)=0$$

$$\text{or, } N(\theta)\frac{\partial}{\partial r}\left(r^2\frac{\partial M(r)}{\partial r}\right)+M(r)\frac{1}{\sin\theta}\frac{\partial}{\partial\theta}\left(\sin\theta\frac{\partial N(\theta)}{\partial\theta}\right)=0$$

Dividing by $M(r)N(\theta)$,

$$\frac{1}{M(r)}\frac{d}{dr}\left(r^2\frac{d\,M(r)}{dr}\right)+\frac{1}{N(\theta)}\frac{1}{\sin\theta}\frac{d}{d\theta}\left(\sin\theta\frac{dN(\theta)}{d\theta}\right)=0 \qquad \text{…. 10.5}$$

The partial derivatives become total derivatives in eqn.(10.5) as each term is dependent on only one coordinate.

The sum of two terms of the LHS of eqn.(10.5) could be zero only when the two terms are separately equal to opposite and equal constant terms as given in eqn.(10.6).

Equal and opposite separation constant solution:

$$\frac{1}{M(r)}\frac{d}{dr}\left(r^2\frac{dM(r)}{dr}\right)=+p \text{ and } \frac{1}{N(\theta)}\frac{1}{\sin\theta}\frac{d}{d\theta}\left(\sin\theta\frac{dN(\theta)}{d\theta}\right)=-p \qquad \text{…. 10.6}$$

where, p is a positive constant.
Another solution is obtained when the separation constant is zero. Hence,
Zero separation constant solution:

$$\frac{1}{M(r)}\frac{d}{dr}\left(r^2\frac{dM(r)}{dr}\right)=0 \quad \text{and} \quad \frac{1}{N(\theta)}\frac{1}{\sin\theta}\frac{d}{d\theta}\left(\sin\theta\frac{dN(\theta)}{d\theta}\right)=0 \qquad \ldots. 10.7$$

Each of the above-mentioned two solutions is to be obtained separately.
Determination of the zero separation constant solution:
The first term of eqn.(10.7) is $\frac{1}{M(r)}\frac{d}{dr}\left(r^2\frac{dM(r)}{dr}\right)=0$, where $M(r)$ is non-zero. So

$$\frac{d}{dr}\left(r^2\frac{dM(r)}{dr}\right)=0, \text{ or, } r^2\frac{dM(r)}{dr}=C_0, \text{ or, } \frac{dM(r)}{dr}=\frac{C_0}{r^2}$$

Integrating and incorporating constants of integration

$$M(r)=\frac{C_{10}}{r}+C_{20} \qquad \ldots. 10.8$$

Next the second term of eqn.(10.7) is $\frac{1}{N(\theta)}\frac{1}{\sin\theta}\frac{d}{d\theta}\left(\sin\theta\frac{dN(\theta)}{d\theta}\right)=0$, where $N(\theta)$ is non-zero. So

$$\frac{1}{\sin\theta}\frac{d}{d\theta}\left(\sin\theta\frac{dN(\theta)}{d\theta}\right)=0, \text{ or, } \frac{d}{d\theta}\left(\sin\theta\frac{dN(\theta)}{d\theta}\right)=0, \text{ or, } \sin\theta\frac{dN(\theta)}{d\theta}=A_0$$

Integrating and incorporating constant of integration

$$N(\theta)=A_{10}\ln\left(\tan\frac{\theta}{2}\right)+A_{20} \qquad \ldots. 10.9$$

Eqn.(10.9) becomes undefined for $\theta=\pi$. But this is not feasible in the given system as potential must be a continuous function. So, A_{10} should be zero in eqn.(10.9). Therefore,

$$N(\theta)=A_{20} \qquad \ldots. 10.10$$

Then from eqns.(10.4), (10.8) and (10.10), the zero separation constant solution can be obtained as

$$V(r,\theta)=\frac{C_1}{r}+C_2 \qquad \ldots. 10.11$$

where, $C_1=A_{20}C_{10}$ and $C_2=A_{20}C_{20}$.
Determination of the equal and opposite separation constant solution:
The first term of eqn.(10.6) is $\frac{1}{M(r)}\frac{d}{dr}\left(r^2\frac{dM(r)}{dr}\right)=+p$,

$$\text{or, } \frac{d}{dr}\left(r^2\frac{dM(r)}{dr}\right)=+pM(r) \qquad \ldots. 10.12$$

Putting $M(r)=Cr^n$ in eqn.(10.12)

$$\frac{d}{dr}\left(r^2 Cnr^{n-1}\right)=+pCr^n, \text{ or, } Cn(n+1)r^n=pCr^n, \text{ or, } n^2+n-p=0$$

$$\text{Hence, } n=\frac{1}{2}\left(-1\pm\sqrt{1+4p}\right) \qquad \ldots. 10.13$$

The second term of eqn.(10.6) is $\frac{1}{N(\theta)}\frac{1}{\sin\theta}\frac{d}{d\theta}\left(\sin\theta\frac{dN(\theta)}{d\theta}\right)=-p$,

$$\text{or, } \frac{1}{\sin\theta}\frac{d}{d\theta}\left(\sin\theta\frac{dN(\theta)}{d\theta}\right)=-pN(\theta) \qquad \ldots. 10.14$$

Putting $N(\theta)=B\cos\theta$ in eqn.(10.14), $\frac{d}{d\theta}\left(-B\sin^2\theta\right)=-pB\cos\theta\sin\theta$, or, p = 2.

Hence, from eqn.(10.13) n = +1, -2.

Therefore, $M(r)=C'r+\frac{C''}{r^{-2}}$ and $N(\theta)=B\cos\theta$ …. 10.15

From eqns.(10.4) and (10.15),

$$V(r,\theta)=\left(C_3r+\frac{C_4}{r^2}\right)\cos\theta \quad \text{…. 10.16}$$

where, $C_3=C'B$ and $C_4=C''B$.

The complete solution for potential function is uniquely given as a linear combination of the two solutions given by eqns.(10.11) and (10.16).

$$V(r,\theta)=\frac{C_1}{r}+C_2+\left(C_3r+\frac{C_4}{r^2}\right)\cos\theta \quad \text{…. 10.17}$$

where, the constants are determined by satisfying the boundary conditions.

It is evident from eqn.(10.17) that the first term corresponds to a net charge on the sphere and the second term to a finite potential.

Conducting Sphere in Uniform Field

Consider that the sphere is a conducting one and is isolated and uncharged. Further, consider that the potential at the location of the center of the sphere due to the external field is V_0.

Since the perturbing action of the sphere is negligible at a large distance from the sphere, the potential at a large distance from the sphere ($r>>a$) is given by

$$V(r,\theta)=V_0+E_0r\cos\theta \quad \text{…. 10.18}$$

If the sphere is charged with a finite amount of charge Q, then

$$V(r,\theta)=\frac{Q}{4\pi\varepsilon_0 r}+V_0+E_0r\cos\theta \quad \text{…. 10.19}$$

In practical systems, floating metallic particles are usually not charged and hence eqn.(10.18) is taken here for further discussion.

Comparing eqns.(10.17) and (10.18) for r$\to\infty$, $C_2=V_0$, $C_3=E_0$. C_1 will be zero for uncharged sphere.

So, eqn.(10.17) can be rewritten as $V(r,\theta)=V_0+\left(E_0r+\frac{C_4}{r^2}\right)\cos\theta$ …. 10.20

On the conductor surface, i.e. for $r=a$, $V(a,\theta)=V_0+\left(E_0a+\frac{C_4}{a^2}\right)\cos\theta$ …. 10.21

But conducting sphere surface is an equipotential and hence electric potential is independent of θ on the conductor surface.

So, from eqn.(10.21), $C_4=-E_0a^3$

Hence, the complete solution for electric potential in the domain $r>a$ is given by

$$V(r,\theta)=V_0+E_0\left(r-\frac{a^3}{r^2}\right)\cos\theta \quad \text{…. 10.22}$$

The r and θ components of electric field intensity could be obtained as follows

$$E_r=-\frac{\partial V}{\partial r}=-E_0\left(1+\frac{2a^3}{r^3}\right)\cos\theta \quad \text{…. 10.23}$$

$$E_\theta = -\frac{1}{r}\frac{\partial V}{\partial \theta} = E_0\left(1-\frac{a^3}{r^3}\right)\sin\theta \quad \text{…. 10.24}$$

On the conducting sphere surface, tangential component of electric field intensity must be zero as it is an equipotential surface. Eqn.(10.24) shows that for $r=a$, E_θ is zero, which in turn validates the solution obtained.

Again, on the conducting sphere surface, E_r is the normal component of electric field intensity, which is given by $E_r\big|_{r=a} = -3E_0\cos\theta$. Thus the maximum value of electric field intensity on the surface of the conducting sphere is $3E_0$, i.e. three times the strength of uniform external field.

This is the reason why metallic dust particles should be avoided at all costs for gas insulated systems. Because presence of metallic dust particles will increase the local electric field intensity three times, which will result into partial discharge within the GIS that is very detrimental for GIS operation.

Induced surface charge density on the surface of the conducting sphere may be obtained as follows

$$\frac{\sigma_s}{\varepsilon_0} = E_r\Big|_{r=a} = -3E_0\cos\theta, \text{ or, } \sigma_s = -3\varepsilon_0 E_0\cos\theta \quad \text{…. 10.25}$$

As stated earlier, the sphere may be charged with an additional charge Q, which is distributed uniformly on the sphere surface and its effect on the field could be found by superposition.

Dielectric Sphere in Uniform Field

In the case of dielectric sphere present in a uniform external field, there will be two solutions to potential function, V_i valid for the region within the sphere having dielectric of permittivity ε_i and V_e valid for the region outside the sphere having dielectric of permittivity ε_e. So from eqn.(10.17)

$$V_i(r,\theta) = \frac{C_{1i}}{r} + C_{2i} + \left(C_{3i}r + \frac{C_{4i}}{r^2}\right)\cos\theta \quad \text{…. 10.26}$$

and $$V_e(r,\theta) = \frac{C_{1e}}{r} + C_{2e} + \left(C_{3e}r + \frac{C_{4e}}{r^2}\right)\cos\theta \quad \text{…. 10.27}$$

The potential at large distance r ($r>>a$) from the sphere

$$V(r,\theta) = V_0 + E_0 r\cos\theta \quad \text{…. 10.28}$$

where, V_0 is the potential at the location of the center of the sphere due to the external field.

Comparing eqns.(10.27) and (10.28) for $r\to\infty$, $C_{2e}=V_0, C_{3e}=E_0$. C_{1e} will be zero as a dielectric sphere is not considered to have any free charge.

Hence, eqn.(10.27) can be rewritten as $$V_e(r,\theta) = V_0 + \left(E_0 r + \frac{C_{4e}}{r^2}\right)\cos\theta \quad \text{…. 10.29}$$

Inside the dielectric sphere electric potential must be finite at all the points. Hence, from eqn.(10.26) $C_{1i}=C_{4i}=0$, $C_{2i}=V_0$. Hence, eqn.(10.26) can be rewritten as

$$V_i(r,\theta) = V_0 + C_{3i}r\cos\theta \quad \text{…. 10.30}$$

At $r=a$, both eqns.(10.29) and (10.30) should yield the same electric potential. Therefore,

$$V_0 + \left(E_0 a + \frac{C_{4e}}{a^2}\right)\cos\theta = V_0 + C_{3i}a\cos\theta$$

or, $$E_0 a + \frac{C_{4e}}{a^2} = C_{3i}a \quad \text{…. 10.31}$$

On the dielectric-dielectric boundary the normal component of electric field intensity should be same on both sides of the boundary. For the spherical boundary, *r*-component of electric field intensity is the normal component on the boundary. Hence,

$$-\varepsilon_i \left(\frac{\partial V_i}{\partial r}\right)\Bigg|_{r=a} = -\varepsilon_e \left(\frac{\partial V_e}{\partial r}\right)\Bigg|_{r=a}$$

or, $\varepsilon_i C_{3i} = \varepsilon_e \left(E_0 - \frac{2C_{4e}}{a^3}\right)$ …. 10.32

From eqns.(10.31) and (10.32)

$$C_{4e} = \frac{\varepsilon_e - \varepsilon_i}{2\varepsilon_e + \varepsilon_i} a^3 E_0$$

and $C_{3i} = \frac{3\varepsilon_e}{2\varepsilon_e + \varepsilon_i} E_0$

Therefore, the complete solutions for potential functions inside and outside the dielectric sphere are given by

$$V_i(r,\theta) = V_0 + \frac{3\varepsilon_e}{2\varepsilon_e + \varepsilon_i} E_0 r\cos\theta \quad \text{…. 10.33}$$

and $V_e(r,\theta) = V_0 + \left(r + \frac{\varepsilon_e - \varepsilon_i}{2\varepsilon_e + \varepsilon_i}\frac{a^3}{r^2}\right) E_0 \cos\theta$ …. 10.34

Noting that $r\cos\theta = z$, potential function inside the dielectric sphere can be written as

$$V_i(x,y,z) = V_0 + \frac{3\varepsilon_e}{2\varepsilon_e + \varepsilon_i} E_0 z \quad \text{…. 10.35}$$

Hence, electric potential within the dielectric sphere varies in only *z*-direction, i.e. the direction of the external field. Electric field intensity within the dielectric sphere will therefore have only the *z*-component, which is given by

$$E_{zi} = -\frac{\partial V_i}{\partial z} = -\frac{3\varepsilon_e}{2\varepsilon_e + \varepsilon_i} E_0 \quad \text{…. 10.36}$$

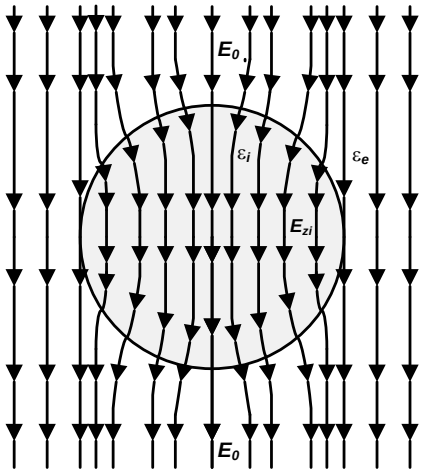

Fig.10.2 Electric field in and around dielectric sphere in uniform field

Eqn.(10.36) shows that the magnitude of electric field intensity within the dielectric sphere is constant. Typical field distribution in and around a dielectric sphere within a uniform external field is shown in Fig. 10.2.

Eqn.(10.36) also shows that if $\varepsilon_i < \varepsilon_e$, then $|E_{zi}| > E_0$. Consider the case of a spherical air bubble trapped within a moulded solid insulation of relative permittivity 4. If the magnitude of

electric field intensity in solid insulation at the location of the air bubble is E_0, then the magnitude of electric field intensity within the air bubble will be $1.33E_0$. The operating electric field intensity within solid insulation is usually kept at a higher value as the solid insulation has a higher dielectric strength and hence such increase in field intensity within the air bubble often causes partial discharge within the air bubble as the dielectric strength of air is much lower than solid insulation.

Cylinder in Uniform External Field

Consider a long cylindrical object of radius *a* within a uniform external field as shown in Fig.10.3. Since the boundary is a circle of *r=constant* on the *x-y* plane, hence the system is best described in cylindrical coordinates as shown in Fig.10.3. The uniform external field is given by $\vec{E}_0 = -E_0\hat{i}$ and the potential at any point due to the external field is given by $E_0 r\cos\theta = E_0 x$ with respect to the axis of the cylinder. In order to get the complete solution for electric field in this system, Laplace's equation in cylindrical coordinates as given in eqn.(10.37) needs to be solved.

$$\frac{1}{r}\frac{\partial}{\partial r}\left(r\frac{\partial V}{\partial r}\right)+\frac{1}{r^2}\frac{\partial^2 V}{\partial \theta^2}+\frac{\partial^2 V}{\partial z^2}=0 \qquad \text{…. 10.37}$$

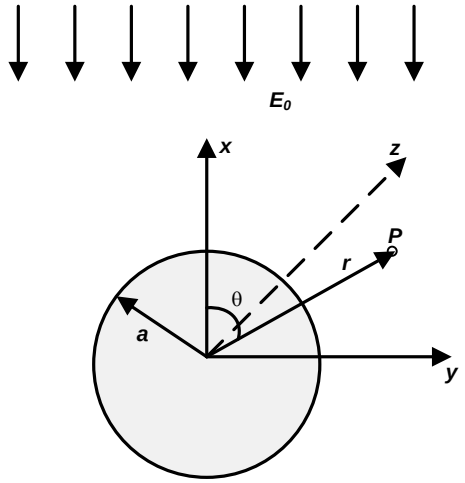

Fig.10.3 Cylinder in uniform external field

For this arrangement electric field distribution does not vary along the length of the cylinder, i.e. along *z*-coordinate. Hence, Laplace's equation reduces to

$$\frac{1}{r}\frac{\partial}{\partial r}\left(r\frac{\partial V}{\partial r}\right)+\frac{1}{r^2}\frac{\partial^2 V}{\partial \theta^2}=0 \qquad \text{…. 10.38}$$

Separating the terms of the LHS into functions of only one variable by multiplying r^2 with eqn.(10.38), it may be written that

$$r\frac{\partial}{\partial r}\left(r\frac{\partial V}{\partial r}\right)+\frac{\partial^2 V}{\partial \theta^2}=0 \qquad \text{…. 10.39}$$

The two terms on the LHS of eqn.(10.39) are functions of only one variable each, i.e. the first term is function of *r* only while the second term is function of θ only. The solution to eqn.(10.39) can be obtained as the product of two functions of which one is dependent only on *r* while the other is dependent only on θ.

Let the assumed solution be $V(r,\theta)=M(r)\,N(\theta)$ …. 10.40

The assumed solution is convenient as the boundary lies at *r=constant*.

Combining eqns.(10.39) and (10.40),

$$r\frac{\partial}{\partial r}\left(r\frac{\partial M(r)N(\theta)}{\partial r}\right)+\frac{\partial^2 M(r)N(\theta)}{\partial\theta^2}=0$$

or, $N(\theta)\left[r\frac{\partial}{\partial r}\left(r\frac{\partial M(r)}{\partial r}\right)\right]+M(r)\frac{\partial^2 M(r)N(\theta)}{\partial\theta^2}=0$

Dividing by $M(r)N(\theta)$,

$$\frac{r}{M(r)}\frac{d}{dr}\left(r\frac{dM(r)}{dr}\right)+\frac{1}{N(\theta)}\frac{d^2N(\theta)}{d\theta^2}=0 \qquad \text{…. 10.41}$$

The partial derivatives become total derivatives in eqn.(10.41) as each term is dependent on only one coordinate.

As in the case of sphere in uniform field, zero separation constant solution and equal and opposite separation constant solution are to be obtained separately in this case, too.

Determination of the zero separation constant solution:

The first term of eqn.(10.41) is $\frac{r}{M(r)}\frac{d}{dr}\left(r\frac{dM(r)}{dr}\right)=0$, where $M(r)$ is non-zero. So

$\frac{d}{dr}\left(r\frac{dM(r)}{dr}\right)=0$, or, $r\frac{dM(r)}{dr}=C_0$, or, $\frac{dM(r)}{dr}=\frac{C_0}{r}$

Integrating and incorporating constants of integration

$$M(r)=C_{10}\ln r+C_{20} \qquad \text{…. 10.42}$$

Next the second term of eqn.(10.41) is $\frac{1}{N(\theta)}\frac{d^2N(\theta)}{d\theta^2}=0$, where $N(\theta)$ is non-zero. So

$$N(\theta)=A_{10}\theta+A_{20} \qquad \text{…. 10.43}$$

But, from eqns.(10.42) and (10.43), it can be seen that there is discontinuity of potential at $r=0$ and $\theta=\infty$, which are not feasible in the given arrangement as potential must be a continuous function. Hence, $C_{10}=A_{10}=0$ in eqns.(10.42) and (10.43).

Therefore, $V(r,\theta)=C_{20}\,A_{20}=C_1$ …. 10.44

Determination of the equal and opposite separation constant solution:

The first term of eqn.(10.41) is $\frac{r}{M(r)}\frac{d}{dr}\left(r\frac{dM(r)}{dr}\right)=+p$, where p is a positive constant

or, $r^2\frac{d^2M(r)}{dr^2}+r\frac{dM(r)}{dr}=+pM(r)$ …. 10.45

Substituting $M(r)=Cr^n$ in eqn.(10.45), it may be obtained that

$n(n-1)+n=p$, or, $n=\pm\sqrt{p}$

Hence, $M(r)=\frac{C'}{r^{\sqrt{p}}}+C''r^{\sqrt{p}}$ …. 10.46

Again, the second term of eqn.(10.41) is $\frac{1}{N(\theta)}\frac{d^2N(\theta)}{d\theta^2}=-p$

or, $\frac{d^2N(\theta)}{d\theta^2}=-pN(\theta)$ …. 10.47

Substituting $N(\theta)=e^{a\theta}$ in eqn.(10.47), it may be obtained that

$a^2e^{a\theta}=-pe^{a\theta}$, or, $a=\pm i\sqrt{p}$

Hence, $N(\theta)=B\cos\left(\sqrt{p}\theta+\alpha\right)$ …. 10.48

Eqns.(10.46) and (10.48) lead to

$$V(r,\theta)=M(r)\,N(\theta)=\left(\frac{C_2}{r^{\sqrt{p}}}+C_3 r^{\sqrt{p}}\right)\cos\left(\sqrt{p}\theta+\alpha)\right) \quad \text{…. 10.49}$$

where, $C_2=C'B$ and $C_3=C''B$

From eqns.(10.44) and (10.49), the complete solution for potential function at all values of r and θ can be obtained as

$$V(r,\theta)=C_1+\left(\frac{C_2}{r^{\sqrt{p}}}+C_3 r^{\sqrt{p}}\right)\cos\left(\sqrt{p}\theta+\alpha)\right) \quad \text{…. 10.50}$$

The potential at large distance r ($r>>a$) from the cylinder is given by

$$V(r,\theta)=V_0+E_0\,r\cos\theta \quad \text{…. 10.51}$$

Matching eqns.(10.50) and (10.51), $\sqrt{p}=1$ and α=0.

Hence, the complete solution as given by eqn.(10.50) reduces to

$$V(r,\theta)=C_1+\left(\frac{C_2}{r}+C_3 r\right)\cos\theta \quad \text{…. 10.52}$$

Conducting Cylinder in Uniform Field

Comparing eqns.(10.51) and (10.52), $C_1=V_0$ and $C_3=E_0$.

So, $V(r,\theta)=V_0+\left(\frac{C_2}{r}+E_0 r\right)\cos\theta$

On the conductor surface, i.e. for $r=a$, $V(a,\theta)=V_0+\left(\frac{C_2}{a}+E_0 a\right)\cos\theta$ …. 10.53

But conducting cylinder surface is an equipotential and hence electric potential is independent of θ on the conductor surface.

So, from eqn.(10.53), $C_2=-E_0\,a^2$

Hence, the complete solution for electric potential in the domain $r>a$ is given by

$$V(r,\theta)=V_0+E_0\left(r-\frac{a^2}{r}\right)\cos\theta \quad \text{…. 10.54}$$

The r and θ components of electric field intensity could be obtained as follows

$$E_r=-\frac{\partial V}{\partial r}=-E_0\left(1+\frac{a^2}{r^2}\right)\cos\theta \quad \text{…. 10.55}$$

$$E_\theta=-\frac{1}{r}\frac{\partial V}{\partial \theta}=E_0\left(1-\frac{a^2}{r^2}\right)\sin\theta \quad \text{…. 10.56}$$

Eqn.(10.56) shows that for $r=a$, E_θ is zero, i.e. the tangential component of electric field intensity is zero on the cylindrical conductor surface as it is an equipotential surface.

Again, on the conducting cylinder surface, E_r is the normal component of electric field intensity, which is given by $E_r\big|_{r=a}=-2E_0\cos\theta$. Thus the maximum value of electric field intensity on the surface of the conducting cylinder is $2E_0$, i.e. twice the magnitude of uniform external field. Comparing this maximum electric field intensity with the value obtained for conducting sphere in uniform field, it may be seen that the enhancement of field intensity is more if the conducting object is spherical is shape.

Induced surface charge density on the surface of the conducting cylinder may be obtained as follows

$$\frac{\sigma_s}{\varepsilon_0} = E_r\Big|_{r=a} = -2E_0\cos\theta, \text{ or, } \sigma_s = -2\varepsilon_0 E_0\cos\theta \quad \text{…. 10.57}$$

Dielectric Cylinder in Uniform Field

Potential function valid for the region within the cylinder having dielectric of permittivity ε_I is

$$V_i(r,\theta) = C_{1i} + \left(\frac{C_{2i}}{r} + C_{3i}r\right)\cos\theta \quad \text{…. 10.58}$$

and the potential function valid for the region outside the cylinder having dielectric of permittivity ε_e is

$$V_e(r,\theta) = C_{1e} + \left(\frac{C_{2e}}{r} + C_{3e}r\right)\cos\theta \quad \text{…. 10.59}$$

The potential at large distance r ($r>>a$) from the cylinder

$$V(r,\theta) = V_0 + E_0 r\cos\theta \quad \text{…. 10.60}$$

where, V_0 is the potential at the location of the axis of the cylinder due to the external field. Comparing eqns.(10.59) and (10.60) for r$\to\infty$, $C_{1e} = V_0$, $C_{3e} = E_0$.

Hence, eqn.(10.59) can be rewritten as $V_e(r,\theta) = V_0 + \left(\frac{C_{2e}}{r} + E_0 r\right)\cos\theta$ …. 10.61

Inside the dielectric cylinder electric potential must be finite at all the points. Hence, from eqn.(10.58) $C_{1i} = V_0$, $C_{2i} = 0$. Hence, eqn.(10.58) can be rewritten as

$$V_i(r,\theta) = V_0 + C_{3i} r\cos\theta \quad \text{…. 10.62}$$

At any point on the dielectric cylinder surface, i.e. for $r=a$, electric potential as may be obtained from eqns.(10.61) and (10.62) must be unique. Hence,

$$\frac{C_{2e}}{a} + E_0 a = C_{3i}\, a \quad \text{…. 10.63}$$

From the boundary condition of normal component of electric flux density at $r=a$

$$-\varepsilon_i\left(\frac{\partial V_i}{\partial r}\right)\Big|_{r=a} = -\varepsilon_e\left(\frac{\partial V_e}{\partial r}\right)\Big|_{r=a}$$

or, $\varepsilon_i C_{3i} = \varepsilon_e\left(-\frac{C_{2e}}{a^2} + E_0\right)$ …. 10.64

From eqns.(10.63) and (10.64)

$$C_{2e} = \frac{\varepsilon_e - \varepsilon_i}{\varepsilon_e + \varepsilon_i} a^2 E_0$$

and $C_{3i} = \frac{2\varepsilon_e}{\varepsilon_e + \varepsilon_i} E_0$

Therefore, the complete solutions for potential functions inside and outside the dielectric cylinder are given by

$$V_i(r,\theta) = V_0 + \frac{2\varepsilon_e}{\varepsilon_e + \varepsilon_i} E_0 r\cos\theta \quad \text{…. 10.65}$$

and $V_e(r,\theta) = V_0 + \left(r + \frac{\varepsilon_e - \varepsilon_i}{\varepsilon_e + \varepsilon_i}\frac{a^2}{r}\right)E_0\cos\theta$ …. 10.66

As $r\cos\theta = x$, potential function inside the dielectric cylinder can be written as

$$V_i(x,y) = V_0 + \frac{2\varepsilon_e}{\varepsilon_e + \varepsilon_i} E_0\, x \qquad \text{…. 10.67}$$

Hence, electric potential within the dielectric cylinder varies in only *x*-direction, i.e. the direction of the external field. Electric field intensity within the dielectric cylinder will therefore have only the *x*-component, which is given by

$$E_{xi} = -\frac{\partial V_i}{\partial x} = -\frac{2\,\varepsilon_e}{\varepsilon_e + \varepsilon_i} E_0 \qquad \text{…. 10.68}$$

Similar to the case of dielectric sphere in uniform field, Eqn.(10.68) shows that the magnitude of electric field intensity within the dielectric cylinder is constant. Typical field distribution on the *x*-*y* plane in and around a dielectric cylinder within a uniform external field will be the same as that shown in Fig. 10.2.

As in the case of dielectric sphere in uniform field, for dielectric cylinder in uniform field also $|E_{zi}| > E_0$ if $\varepsilon_i < \varepsilon_e$. If a cylindrical air bubble is trapped within a moulded solid insulation of relative permittivity 4, then the magnitude of electric field intensity within the air bubble will be $1.6E_0$, where E_0 is the magnitude of electric field intensity in solid insulation at the location of the air bubble. Comparing this result with the corresponding value in the case of dielectric sphere, it may be seen that field enhancement is more if the gas cavity in liquid or solid insulation is cylindrical in shape.

Electrostatic Pressures on Boundary Surfaces

Introduction

There could be two different approaches towards the calculation of electrostatic force acting on any boundary. In the first approach, the macroscopic resultant force may be calculated by summing up the elementary electrostatic forces as obtained from Coulomb's law. On one hand this approach should always give correct result, but on the other hand in most of the practical cases it is very difficult, if not impossible, to perform such calculation as the actual distributions of charges are mostly unknown.
The second approach is based on the principle of energy conservation and the electrostatic forces are derived indirectly from energy relationship. This approach is advantageous in the sense that the forces can be calculated conveniently even by analytical methods. But the accuracy of the results obtained from this approach depends on the validity of the principle of energy conservation for the specific case under consideration. Some argue that this condition is not always satisfied and consequently this method can lead to wrong results in some cases. Although majority of the scientific community firmly believe that the principle of energy conservation has a general validity, and therefore this approach should always provide correct results. On the whole, it is better to suggest that one should use it with due circumspection and reservation by always verifying the results.

Mechanical Pressure on Conductor-Dielectric Boundary

As discussed in section 6.2, only same polarity charges reside on the boundary between a perfect conductor and a dielectric medium. These same polarity charges, residing on the surface of the conductor, exert repulsive forces on each other. These forces will be of such nature that the distance between the charges should increase. In other words, the surface area of the conductor-dielectric boundary will try to increase under the influence of these repulsive forces. Hence, the electrostatic force on the conductor-dielectric boundary always acts along the normal to the boundary directed from the conductor to the dielectric.
The force on a conductor-dielectric boundary could be calculated using the expression for energy density. If an elemental area ΔA on a conductor-dielectric boundary is depressed by a distance Δl, the increase in stored energy (ΔW) is equal to the work done against the electrostatic force acting on the conductor-dielectric boundary trying to swell the surface. Hence, considering the energy density of electric field within the dielectric to be W_E

$$\Delta W = W_E \, \Delta A \Delta l$$

Here, it has been assumed that the charge on the conductor surface remain unchanged even when the geometry is changed slightly. This assumption is valid when the conductor is an isolated one, i.e. it is not connected to a source that could alter its charge, e.g. a voltage source. Hence, the work done in depressing the boundary could be related directly to the energy content of electric field according to the law of conservation of energy.
If the electrostatic force acting against the depression of the surface is given by *F*, then the work done against this force is

$$F \, \Delta l = W_E \, \Delta A \Delta l \text{ , or, } F = W_E \, \Delta A \qquad \text{…. 8.1}$$

Electrostatic force per unit area is the mechanical pressure due to electrostatic field acting on the conductor-dielectric boundary, which is therefore given by

$$P_{mech}\big|_{cond} = \frac{F}{\Delta A} = W_E \qquad \text{…. 8.2}$$

Considering the surface charge density of the conductor-dielectric boundary to be σ,

$$P_{mech}\big|_{cond} = W_E = \frac{1}{2}\varepsilon E^2 = \frac{1}{2\varepsilon}D^2 = \frac{\sigma^2}{2\varepsilon} \quad \text{…. 8.3}$$

as $D = D_n = \sigma$, because $D_t = \varepsilon E_t$ is zero on the conductor surface, as E_t=0.

Electric Field Intensity exactly on the Conductor Surface

Dimensionally, the mechanical pressure acting on the charged conductor surface is equal to the product of surface charge density (σ) and the electric field intensity exactly on the conductor surface ($E_{surface}$), i.e. from eqn.(8.3)

$$P_{mech}\big|_{cond} = \sigma E_{Surface} = \frac{\sigma^2}{2\varepsilon}, \text{ or, } E_{Surface} = \frac{\sigma}{2\varepsilon} = \frac{\sigma}{2\varepsilon_r \varepsilon_0} \quad \text{…. 8.4}$$

From eqns.(6.8) and (6.10), $E_{just\ off\ the\ surface} = \frac{\sigma}{\varepsilon} = \frac{\sigma}{\varepsilon_r \varepsilon_0}$ …. 8.5

Therefore, $E_{just\ off\ the\ surface} = 2 \times E_{Surface}$ …. 8.6

Problem 8.1
A metallic sphere of 20cm radius is charged with 1μC, spread uniformly over the surface and is surrounded by a dielectric medium having a relative permittivity of 5. Find the electric field intensity just off the sphere and also on the sphere. Find also the mechanical pressure acting on the sphere.
Solution:
Sphere radius = 20 cm = 0.2m
Sphere surface area = $4\pi \times (0.2)^2$ = 0.5026 m^2
Therefore, surface charge density (σ) = $(1\times10^{-6}) / 0.5026 = 1.989\times10^{-6}$ C/m^2
Electric field intensity just off the sphere surface
= $(1.989\times10^{-6}) / (5\times8.854\times10^{-12}) = 44.94\times10^3$ V/m
Electric field intensity exactly on the sphere surface
= $(44.94\times10^3) / 2 = 22.47\times10^3$ V/m
Therefore, mechanical pressure acting on the sphere surface
= $1.989\times10^{-6}\times22.47\times10^3 = 0.0447$ N/m^2

Electrostatic Forces on the Plates of a Parallel Plate Capacitor

In order to get a simple analytical solution, consider that the distance between the plates (l) of the capacitor is much smaller than the area of the plates (A). In that case it may be assumed that the E-field between the plates is homogeneous, and the effect of the inhomogeneity of E-field at the edges, commonly known as fringing, may be neglected. The charge may also be assumed to be distributed uniformly over the plates, i.e. the charge density may be assumed to be known for the application of Coulomb's law.

Capacitance of the parallel plate capacitor (C) = $\frac{\varepsilon A}{l}$

Let, the potential difference between the two plates of the capacitor be V.

So, the uniformly distributed charge on the plates of the capacitor (Q_{plate}) = $C\times V = \frac{\varepsilon A V}{l}$

and the electric field intensity within the dielectric of the capacitor is $E = \frac{V}{l}$

As discussed in section 8.2.1, electric field intensity exactly on the plate surface is given by

$$E_{plate} = \frac{\sigma_{plate}}{2\varepsilon} = \frac{Q_{plate}}{2\varepsilon A} = \frac{1}{2\varepsilon A} \times \frac{\varepsilon AV}{l} = \frac{V}{2l} \quad \text{…. 8.7}$$

So from Coulomb's law, the electrostatic force acting on the capacitor plates is given by

$$F_{plate} = Q_{plate} E_{plate} = \frac{\varepsilon AV}{l} \times \frac{V}{2l} = \frac{1}{2} \varepsilon A \left(\frac{V}{l} \right)^2 \quad \text{…. 8.8}$$

Again, according to eqn.(8.2) mechanical pressure acting on the plates

$$P_{mech}\Big|_{plate} = W_E = \frac{1}{2} \varepsilon E^2 = \frac{1}{2} \varepsilon \left(\frac{V}{l} \right)^2 \quad \text{…. 8.9}$$

Hence, the electrostatic force acting on the capacitor plates is

$F_{Plate} = P_{mech}\Big|_{plate} \times A = \frac{1}{2} \varepsilon A \left(\frac{V}{l} \right)^2$, which is the same as that of eqn.(8.8)

Eqn.(8.8) is very useful because if the force could be measured when the voltage is unknown, then the voltage can be calculated from the above formula from the knowledge of the capacitor dimensions. In fact the measurement of voltage by electrostatic voltmeter is based on this principle.

Problem 8.2
For an air-filled parallel plate capacitor, the area of the plates is 50cm^2 and the separation distance between the plates is 5mm. What will be the maximum electrostatic force on the capacitor plates at standard temperature and pressure?
Solution
Breakdown strength of air at STP is 30kV/cm or 3×10^6 V/m. That will be the maximum possible electric field intensity within the parallel plate capacitor.
So the maximum electrostatic pressure on the capacitor plates is

$$P_{plate}\Big|_{\max} = \frac{1}{2} \times 8.854 \times 10^{-12} \times (3 \times 10^6)^2 = 39.84\, N/m^2$$

$$F_{plate}\Big|_{\max} = 39.84 \times 50 \times 10^{-4} = 0.199\, N$$

Mechanical Pressure on Dielectric-Dielectric Boundary

Mechanical pressure due to electrostatic field that act on a dielectric-dielectric boundary arise due to two reasons. The first one is the polarization of atoms and/or dipoles in the volume of the dielectric media under the action of electric field, while the second one is the change in the polarization vector that takes place at the boundary between two different dielectric media. These two mechanical pressures need to be discussed separately.

Mechanical Pressure due to Dielectric Polarization

Consider a homogeneous isotropic dielectric piece of small volume placed in vacuum within an electric field. The atoms and/or dipoles within this dielectric volume will be polarized under the action of the electric field. Since, each atom and/or dipole consists of positive and negative charge, it may be considered that under the action of the electric field a uniformly distributed cloud of negative charges is shifted through a small distance from a uniformly distributed cloud of positive charges. The same polarity charges by mutual repulsion develop

an outward force, which tends to swell the small dielectric volume into the surrounding vacuum.

The dielectric volume being small enough, it will not alter the electric field intensity due to the external field within which it is placed. But due to dielectric polarization the electric flux density within the dielectric volume will be higher due to higher permittivity of the dielectric compared to vacuum for the same electric field intensity.

In the absence of dielectric medium, energy density of electric field will be given by

$$W_E\big|_{vacuum} = \frac{1}{2}\varepsilon_0 E^2 \qquad \text{…. 8.10}$$

and in the presence of dielectric medium, energy density of electric field for the same electric field intensity within the same volume will be given by

$$W_E\big|_{dielectric} = \frac{1}{2}\varepsilon E^2 \qquad \text{…. 8.11}$$

Due to electrostatic repulsive force, if unit area of the surface of the small dielectric volume expands through a small distance *dl* in the normal direction, then the difference in stored energy is equal to the mechanical work done by the repulsive forces, if no heat energy is lost. Let the force on the dielectric boundary due to dielectric polarization be F_{pol}. Then the mechanical work done by F_{pol} is given by

$$Work\ Done = F_{pol} \times dl = \frac{1}{2}(\varepsilon - \varepsilon_0)E^2 \times dl \times 1$$

$$\text{or, } \frac{F_{pol}}{1} = \frac{1}{2}(\varepsilon - \varepsilon_0)E^2 \qquad \text{…. 8.12}$$

This force per unit area, i.e. mechanical pressure, acts normally on the boundary directed from the dielectric to vacuum.

When two different dielectric meet at a boundary, then the mechanical pressure by which each dielectric tends to push the boundary normally outward could be computed using eqn(8.12). The difference in these two pressures is the net pressure acting on the dielectric-dielectric boundary due to dielectric polarization.

The mechanical pressure on the boundary due to dielectric-1 alone, i.e. when dielectric-2 is replaced by vacuum, is given by

$$P_{mech}\big|_{dielctric1-vacuum} = \frac{1}{2}(\varepsilon_1 - \varepsilon_0)E_1^2 \qquad \text{…. 8.13}$$

This pressure given by eqn.(8.13) acts normally from dielectric-1 to vacuum on the boundary.

Again, the mechanical pressure on the boundary due to dielectric-2 alone, i.e. when dielectric-1 is replaced by vacuum, is given by

$$P_{mech}\big|_{dielctric2-vacuum} = \frac{1}{2}(\varepsilon_2 - \varepsilon_0)E_2^2 \qquad \text{…. 8.14}$$

This pressure given by eqn.(8.14) acts normally from dielectric-2 to vacuum on the boundary.

The difference in these two pressures as given by eqns.(8.13) and (8.14) is the net pressure acting on the boundary due to dielectric polarization. Considering the normal on the dielectric-dielectric boundary to be from dielectric-1 to dielectric-2,

$$P_{mech}\big|_{pol} = \frac{1}{2}\left[(\varepsilon_1 - \varepsilon_0)E_1^2 - (\varepsilon_2 - \varepsilon_0)E_2^2\right] \qquad \text{…. 8.15}$$

$$\text{or,} \qquad P_{mech}\big|_{pol} = \frac{1}{2}\left[(\varepsilon_1 - \varepsilon_0)\left(E_{1t}^2 + E_{1n}^2\right) - (\varepsilon_2 - \varepsilon_0)\left(E_{2t}^2 + E_{2n}^2\right)\right]$$

$$= \frac{1}{2}\left[\left(\varepsilon_1 E_{1t}^2 - \varepsilon_2 E_{2t}^2\right) + \left(\varepsilon_1 E_{1n}^2 - \varepsilon_2 E_{2n}^2\right) - \varepsilon_0\left(E_{1n}^2 - E_{2n}^2\right)\right]$$

$$= \frac{1}{2}\left[\left(\varepsilon_1 - \varepsilon_2\right)E_t^2 + \left(\frac{D_{1n}^2}{\varepsilon_1} - \frac{D_{2n}^2}{\varepsilon_2}\right) - \varepsilon_0\left(\frac{D_{1n}^2}{\varepsilon_1^2} - \frac{D_{2n}^2}{\varepsilon_2^2}\right)\right] \quad \text{…. 8.16}$$

$$= \frac{1}{2}\left[\left(\varepsilon_1 - \varepsilon_2\right)E_t^2 + \left(\frac{1}{\varepsilon_1} - \frac{1}{\varepsilon_2}\right)D_n^2 - \varepsilon_0\left(\frac{1}{\varepsilon_1^2} - \frac{1}{\varepsilon_2^2}\right)D_n^2\right]$$

as $E_{1t} = E_{2t} = E_t$ and $D_{1n} = D_{2n} = D_n$.

Mechanical Pressure on Surface Film at Dielectric-Dielectric Boundary

Consider a boundary between a homogeneous isotropic dielectric medium and vacuum as shown in Fig.8.1. For a boundary having no free charge, the boundary conditions are $E_{1t} = E_{2t}$ and $D_{1n} = D_{2n}$.

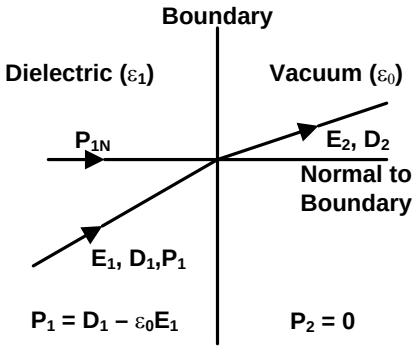

Fig.8.1 Change of polarization vector at dielectric-vacuum boundary

Within the dielectric medium $D_1 = \varepsilon_1 E_1 = \varepsilon_0 E_1 + P_1$, where P_1 is the polarization vector in the dielectric medium. Hence, $P_1 = D_1 - \varepsilon_0 E_1$.

On the other hand, within vacuum $D_2 = \varepsilon_0 E_2$ and hence, $P_2=0$.

Thus, as one crosses the boundary the polarization vector drops from a finite value within the dielectric medium to zero in vacuum. But this change in polarization vector cannot occur at one line of infinitesimal thickness representing the boundary. On the contrary, such change in polarization vector occurs within a thin film of finite but very small thickness within the dielectric medium just off the boundary.

Consequently, this boundary film needs to be studied closely. Since only a normal displacement of the boundary film will expand the boundary, hence only the normal components of electric flux density and polarization vector are considered. The normal component of electric flux density remains constant inside the boundary film. But, the normal component of electric field intensity as well as the normal component of polarization vector vary gradually and finally assume the values equal to those just outside the film on the vacuum side of the boundary. Such variation is schematically shown in Fig.8.2.

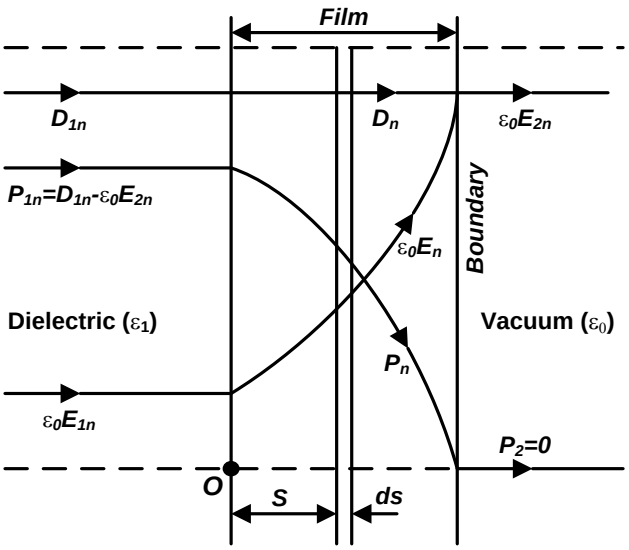

Fig.8.2 Variation of electric field quantities within the boundary film

Within the boundary film, the polarization vector is $P_n = D_n - \varepsilon_0 E_n$

Therefore, $dP_n = -\varepsilon_0 dE_N$ as D_n is constant within the film.

Now, consider a thin strip of thickness *ds* within the film such that the distance of the strip from the beginning of the film is *S*, as shown in Fig.8.2. Also consider that *ds* be the separation distance between the positive and negative charges of the atoms and/or dipoles within this strip. At a distance *S*, the negative charges of the atoms lie in a field of intensity E_n and at a distance $S + ds$, the positive charges lie in a field of $E_n + dE_n$. Hence, each dipole charge is subjected to a force per unit of dE_n towards right according to Fig.8.2. But the polarization vector being P_n, there are P_n charges per unit area. Thus the force per unit area, i.e. mechanical pressure, acting towards right on the thin strip is

$$dP_{mech}\big|_{film} = P_n\, dE_n = -\frac{1}{\varepsilon_0} P_n\, dP_n$$

So, total mechanical pressure acting on the entire film is

$$P_{mech}\big|_{film-dielectric-vacuum} = -\int_{Pn=P1n}^{Pn=0} \frac{1}{\varepsilon_0} P_n\, dP_n = \frac{P_{1n}^2}{2\varepsilon_0} = \frac{(D_{1n} - \varepsilon_0 E_{1n})^2}{2\varepsilon_0}$$

As $D_{1n} = \varepsilon_1 E_{1n}$, $P_{mech}\big|_{film-dielectric-vacuum} = \dfrac{(\varepsilon_1 - \varepsilon_0)^2}{2\varepsilon_0} E_{1n}^2$ …. 8.17

Thus, when two dielectric media meet at a boundary, the normal pressure that acts on the boundary film from dielectric-1 to dielectric-2 may be computed following the same logic as in the case of eqns. (8.13), (8.14) and (8.15). So,

$$P_{mech}\big|_{film} = \frac{1}{2\varepsilon_0}\left[(\varepsilon_1 - \varepsilon_0)^2 E_{1n}^2 - (\varepsilon_2 - \varepsilon_0)^2 E_{2n}^2\right] \quad \text{…. 8.18}$$

Total Mechanical Pressure on Dielectric-Dielectric Boundary

The total mechanical pressure on the boundary between two dielectric media pushing the boundary from dielectric-1 to dielectric-2 is the sum of eqns.(8.15) and (8.18). So,

$$P_{mech}\big|_{dielectric} = \frac{1}{2}\left[(\varepsilon_1 - \varepsilon_0)E_1^2 - (\varepsilon_2 - \varepsilon_0)E_2^2 + \frac{(\varepsilon_1 - \varepsilon_0)^2 E_{1n}^2}{\varepsilon_0} - \frac{(\varepsilon_2 - \varepsilon_0)^2 E_{2n}^2}{\varepsilon_0}\right] \quad \text{…. 8.19}$$

Noting that $E_1^2 = E_{1t}^2 + E_{1n}^2$, $E_2^2 = E_{2t}^2 + E_{2n}^2$, $E_{1t} = E_{2t}$ and $D_{1n} = D_{2n}$, eqn.(8.19) may be rewritten as

$$P_{mech}\big|_{dielectric} = \frac{1}{2}\left[(\varepsilon_1 - \varepsilon_0)(E_{1t}^2 + E_{1n}^2) - (\varepsilon_2 - \varepsilon_0)(E_{2t}^2 + E_{2n}^2) + \frac{(\varepsilon_1^2 - 2\varepsilon_1\varepsilon_0 + \varepsilon_0^2)E_{1n}^2}{\varepsilon_0} - \frac{(\varepsilon_2^2 - 2\varepsilon_2\varepsilon_0 + \varepsilon_0^2)E_{2n}^2}{\varepsilon_0} \right]$$

$$= \frac{1}{2}\left[\varepsilon_1 E_{1t}^2 - \varepsilon_2 E_{2t}^2 - \varepsilon_1 E_{1n}^2 + \varepsilon_2 E_{2n}^2 + \frac{\varepsilon_1^2 E_{1n}^2}{\varepsilon_0} - \frac{\varepsilon_2^2 E_{2n}^2}{\varepsilon_0} \right]$$

$$= \frac{1}{2}\left[\frac{(\varepsilon_1 E_{1t})^2}{\varepsilon_1} - \frac{(\varepsilon_2 E_{2t})^2}{\varepsilon_2} - \frac{(\varepsilon_1 E_{1n})^2}{\varepsilon_1} + \frac{(\varepsilon_2 E_{2n})^2}{\varepsilon_2} \right]$$

$$= \frac{1}{2}\left[\frac{D_{1t}^2}{\varepsilon_1} - \frac{D_{2t}^2}{\varepsilon_2} - \frac{D_{1n}^2}{\varepsilon_1} + \frac{D_{2n}^2}{\varepsilon_2} \right] \quad \text{…. 8.20}$$

Eqn.(8.20) may also be written as

$$P_{mech}\big|_{dielectric} = \frac{1}{2}\left[(\varepsilon_1 - \varepsilon_2)E_t^2 + \left(\frac{1}{\varepsilon_2} - \frac{1}{\varepsilon_1} \right) D_n^2 \right] \quad \text{…. 8.21}$$

as $E_{1t} = E_{2t} = E_t$ and $D_{1n} = D_{2n} = D_n$.

Eqn.(8.21) can be used to find the mechanical pressure acting on the conductor-dielectric boundary, by considering $\varepsilon_1 = \infty$ for the conductor and noting the boundary conditions on the conductor-dielectric boundary as E_t=0 and hence D=D_n. Then putting $\varepsilon_2 = \varepsilon$ for the dielectric surrounding the conductor in eqn.(8.21)

$P_{mech}\big|_{cond} = \frac{D^2}{2\varepsilon}$, which is the same as eqn.(8.3).

Problem 8.3

There is a paper insulated transformer coil immersed in oil. ε_r for paper=3 and ε_r for transformer oil=2.1. There is a normal electric stress of 25 kV/cm and a tangential electric stress of 10kV/cm just within the paper at the paper-oil boundary. Calculate the total mechanical pressure acting on the paper-oil boundary.

Solution

Given: E_{1n} = 25kV/cm = 25×10^5V/m and E_{1t} = 10kV/cm = 10^6V/m

So, $D_{1n} = \varepsilon_{r1}\varepsilon_0 E_{1n} = 3\times\varepsilon_0\times25\times10^5 = 75\times\varepsilon_0\times10^5$ V/m

Total mechanical pressure acting on the paper-oil boundary

$$= \frac{1}{2}\left[(3-2.1)\times\varepsilon_0\times(10^6)^2 + \frac{1}{\varepsilon_0}\left(\frac{1}{2.1} - \frac{1}{3} \right)(75\times\varepsilon_0\times10^5)^2 \right] = 39.56 \text{ N/m}^2.$$

Problem 8.4

A rectangular slab of porcelain (ε_r=5) is placed in air within an electric field such that the surface of the porcelain slab is perpendicular to the electric field lines. Find the maximum possible mechanical pressure acting on the porcelain-air boundary at standard temperature and pressure.

Solution

Since the boundary is perpendicular to the electric field lines in air, hence on the air side of the boundary, E_t=0. Again the maximum value of electric field intensity in air is 30kV/cm at standard temperature and pressure. So, on the air side of the boundary $E_{n\text{-}max}$ = 30kV/cm or 3×10^6V/m.

So, the maximum possible mechanical pressure acting on the porcelain-air boundary is

$$= \frac{1}{2\varepsilon_0}\left(\frac{1}{1}-\frac{1}{5}\right)\times(\varepsilon_0)^2\times\left(3\times10^6\right)^2 = 31.9\,N/m^2$$

Two Dielectric Media in series between a Parallel Plate Capacitor

Consider a parallel plate capacitor having two dielectric media in series between the plates such that the boundary between the dielectric media is parallel to the plates, as shown in Fig.8.3. In this case, electric field lines will be perpendicular to the boundary. According to the boundary condition, normal component of electric flux density will be same in both the dielectric media, but the magnitude of electric field intensity will be different in the two dielectrics. Further, since the tangential component of electric field is zero because the electric flux lines are perpendicular to the boundary, hence $D=D_n$.

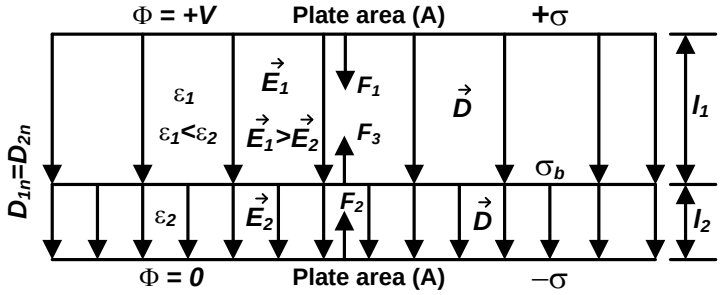

Fig.8.3 Two dielectric media in series between a parallel plate capacitor

Let, the potential difference across the dielectric-1 (ε_1) is V_1 and that across the dielectric-2 (ε_2) is V_2. Then

$$V = V_1 + V_2 = E_1 l_1 + E_2 l_2 = \frac{D}{\varepsilon_1} l_1 + \frac{D}{\varepsilon_2} l_2$$

or, $D = \dfrac{\varepsilon_1 \varepsilon_2}{\varepsilon_2 l_1 + \varepsilon_1 l_2} V$

Hence, $E_1 = \dfrac{D}{\varepsilon_1} = \dfrac{\varepsilon_2}{\varepsilon_2 l_1 + \varepsilon_1 l_2} V$ and $E_2 = \dfrac{D}{\varepsilon_2} = \dfrac{\varepsilon_1}{\varepsilon_2 l_1 + \varepsilon_1 l_2} V$ …. 8.22

Mechanical pressure acting on the plates will be equal to energy density of electric field just off the plates, i.e. $\frac{1}{2}\varepsilon E^2$. Considering the area of the plates to be A,

Mechanical force acting on the top plate (F_1) = $\dfrac{1}{2}\varepsilon_1 E_1^2 A = \dfrac{1}{2}\varepsilon_1\left(\dfrac{\varepsilon_2}{\varepsilon_2 l_1 + \varepsilon_1 l_2}\right)^2 V^2 A$

or, $F_1 = \dfrac{1}{2\varepsilon_1}\left(\dfrac{\varepsilon_1 \varepsilon_2}{\varepsilon_2 l_1 + \varepsilon_1 l_2}\right)^2 V^2 A = \dfrac{F}{\varepsilon_1}$, where $F = \dfrac{1}{2}\left(\dfrac{\varepsilon_1 \varepsilon_2}{\varepsilon_2 l_1 + \varepsilon_1 l_2}\right)^2 V^2 A$ …. 8.23

Similarly, mechanical force acting on the bottom plate (F_2) = $\dfrac{1}{2}\varepsilon_2 E_2^2 A = \dfrac{F}{\varepsilon_2}$ …. 8.24

The force F_1 acts on the top plate directed towards dielectric-1, while the force F_2 acts on the bottom plate directed towards dielectric-2. Thus F_1 and F_2 are in opposite direction and $F_1 > F_2$ as $\varepsilon_1 < \varepsilon_2$.

So it appears that there is a resultant unidirectional reaction-less force acting on the capacitor. But this is not true, because the force acting on the boundary surface between the two dielectric media has to be taken into account, too.

From eqn.(8.21) the mechanical force on the dielectric-dielectric boundary is given by

$$F_3 = \frac{1}{2}\left(\frac{1}{\varepsilon_2} - \frac{1}{\varepsilon_1}\right) D^2 A = \frac{1}{2}\left(\frac{1}{\varepsilon_2} - \frac{1}{\varepsilon_1}\right)\left(\frac{\varepsilon_1 \varepsilon_2}{\varepsilon_2 l_1 + \varepsilon_1 l_2}\right)^2 V^2 A = \frac{F}{\varepsilon_2} - \frac{F}{\varepsilon_1} \qquad \text{…. 8.25}$$

In eqn.(8.21) the mechanical pressure is assumed to be acting from dielectric-1 to dielectric-2. As $\varepsilon_1 < \varepsilon_2$, F_3 as per eqn.(8.25) is negative indicating that the force F_3 acts towards the dielectric of smaller permittivity, i.e. towards dielectric-1.

Thus net electrostatic force acting on the capacitor $= F_1 - F_2 + F_3 = \frac{F}{\varepsilon_1} - \frac{F}{\varepsilon_2} + \left(\frac{F}{\varepsilon_2} - \frac{F}{\varepsilon_1}\right) = 0$

Two Dielectric Media in parallel between a Parallel Plate Capacitor

Consider a parallel plate capacitor having two dielectric media in parallel between the plates such that the boundary between the dielectric media is perpendicular to the plates, as shown in Fig.8.4. In this case, electric field lines will be tangential to the boundary. According to the boundary condition, tangential component of electric field intensity will be same in both the dielectric media, but the magnitude of electric flux density will be different in the two dielectrics.

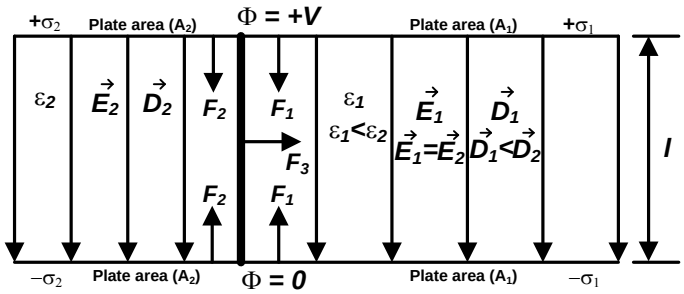

Fig.8.4 Two dielectric media in parallel between a parallel plate capacitor

In this case, $E_1 = E_2 = \frac{V}{l}$, $D_1 = \varepsilon_1 E_1$ and $D_2 = \varepsilon_2 E_2$

The mechanical force acting on the part of the plate in contact with dielectric-1 is given by

$$F_1 = \frac{1}{2}\varepsilon_1 E_1^2 A_1 = \frac{1}{2}\varepsilon_1 \left(\frac{V}{l}\right)^2 A_1 \qquad \text{…. 8.26}$$

The forces acting on the two plates within the section of the capacitor containing dielectric-1 will be equal to F_1 but will act in opposite directions.

The mechanical force acting on the part of the plate in contact with dielectric-2 is given by

$$F_2 = \frac{1}{2}\varepsilon_2 E_2^2 A_2 = \frac{1}{2}\varepsilon_2 \left(\frac{V}{l}\right)^2 A_2 \qquad \text{…. 8.27}$$

The forces acting on the two plates within the section of the capacitor containing dielectric-2 will be equal to F_2 but will act in opposite directions. If $A_1 = A_2$, then $F_2 > F_1$ as $\varepsilon_2 > \varepsilon_1$. But the net force on the capacitor plates will always be zero due to the presence of equal and opposite forces on the plates.

But there will be mechanical force acting on the boundary between the two dielectric media, which according to eqn.(8.21) is given by

$$F_3 = \frac{1}{2}(\varepsilon_1 - \varepsilon_2) E^2 A_b = \frac{1}{2}(\varepsilon_1 - \varepsilon_2)\frac{V^2}{l^2} A_b \qquad \text{…. 8.28}$$

where, A_b = area of the dielectric-dielectric boundary.
As stated earlier, in eqn.(8.21) the mechanical pressure is considered to be acting from dielectric-1 to dielectric-2. As $\varepsilon_1<\varepsilon_2$, F_3 as per eqn.(8.28) is negative, which indicates that the force F_3 acts towards the dielectric of smaller permittivity, i.e. from dielectric-2 to dielectric-1.

Electrostatic Pump

The mechanical force acting on the dielectric-dielectric boundary, as discussed in section 8.5 above, can be demonstrated practically with the help of the arrangement shown in Fig.8.5, which is also known as electrostatic pump.

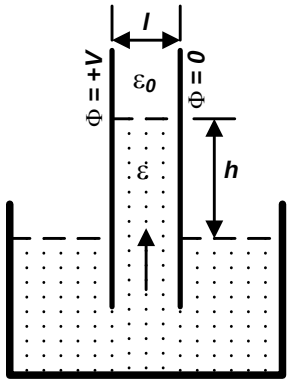

Fig.8.5. Demonstration of electrostatic pump

If a charged parallel plate capacitor with air between the plates is partially submerged in a liquid dielectric as shown in Fig.8.5, then the mechanical force on liquid-air boundary within the capacitor will act from the liquid dielectric to air, as the permittivity of air is smaller than the permittivity of liquid dielectric. Hence, this mechanical force will push the liquid up between the plates against the force of gravity. When the electrical force on the boundary and the weight of the liquid column between the capacitor plates become equal, then the upward movement of the liquid dielectric between the plates stops, and the surface of the liquid dielectric between the capacitor plates remains at a higher level than the surface of the liquid dielectric in the container.
As per eqn.(8.28), the mechanical force on the liquid-air boundary acting towards air is

$$F_{dielectric-boundary} = \frac{1}{2}(\varepsilon-\varepsilon_0)\frac{V^2}{l^2}A_b = \frac{1}{2}(\varepsilon-\varepsilon_0)\frac{V^2}{l^2}l\times l_w = \frac{1}{2}(\varepsilon-\varepsilon_0)\frac{V^2}{l}l_w \qquad \text{…. 8.29}$$

where, l_w = width of the plates normal to the plane of the paper, l = separation distance between the capacitor plates and V = potential difference between the capacitor plates.
The gravitational force on the liquid column between the capacitor plates is

$$F_{gravity} = \rho h l_w l g \qquad \text{…. 8.30}$$

where, h = height of the liquid column between the capacitor plates, ρ = density of the liquid dielectric and g = acceleration due to gravity.
At equilibrium $F_{gravity} = F_{dielectric\text{-}boundary}$, i.e.

$$\rho h l_w l g = \frac{1}{2}(\varepsilon-\varepsilon_0)\frac{V^2}{l}l_w$$

or, $$h = \frac{1}{2\rho g}(\varepsilon-\varepsilon_0)\left(\frac{V}{l}\right)^2 = \frac{1}{2\rho g}(\varepsilon-\varepsilon_0)E^2 \qquad \text{…. 8.31}$$

In the case of electrostatic pump, for a given liquid dielectric and for fixed dimensions of the capacitor, the height of the liquid column between the capacitor plates can be controlled by controlling the voltage applied across the plates.

Problem 8.5

A parallel plate capacitor with air between the plates is submerged into transformer oil in a container in such a way that the top surface of transformer oil in the container is perpendicular to the capacitor plates. The potential difference between the capacitor plates is 15kV and the separation distance between the plates is 6mm. Density of transformer oil is 860kg/m^3. Calculate the height of the transformer oil column between the capacitor plates if ε_r for transformer oil = 2.1. What will be height of the liquid column if transformer oil is replaced by water for which density is 1000kg/m^3 and ε_r is 80.

Solution

Given: ρ_{oil} = 860kg/m^3, ε_r of oil = 2.1, V = 15kV = 15×10^{3}V and l = 6mm = 6×10^{-3}m

Acceleration due to gravity (g) = 9.81 m/s^2

So, $h_{oil} = \frac{1}{2 \times 860 \times 9.81} \times (2.1-1) \times 8.854 \times 10^{-12} \times \left(\frac{15 \times 10^3}{6 \times 10^{-3}} \right)^2 = 3.6mm$

If transformer is replaced by water, then ρ_{water} = 1000kg/m^3, ε_r of water = 80

So, $h_{water} = \frac{1}{2 \times 1000 \times 9.81} \times (80-1) \times 8.854 \times 10^{-12} \times \left(\frac{15 \times 10^3}{6 \times 10^{-3}} \right)^2 = 222.3mm$

Conformal Mapping

Introduction

Analytical solutions to many field problems, particularly Dirichlet problems, can be obtained using methods like Fourier Series and integral transforms. These methods are applicable only for simple regions and the solutions are either infinite series or improper integrals, which are difficult to evaluate. Closed form solutions to many Dirichlet problems can be obtained using conformal mapping, which is a similarity transformation. If a function is harmonic, i.e. it satisfies Laplace's equation $\vec{\nabla}^2 f = 0$, then the transformation of such a function via conformal mapping is also harmonic. Hence, equations in relation to any field that can be represented by a potential function can be solved with the help of conformal mapping. However, conformal mapping can only be employed in two dimensional fields. If the solution for potential field is required in three dimensional cases, then conformal mapping is applicable to only those configurations where the potential field is translationally invariant along any one of the three axes. The two dimensional potential fields that can be solved by conformal mapping are static electric fields, static magnetic fields, static electric flow fields, stationary thermal flow fields, stationary hydrodynamic flow fields to name a few. According to Riemann Mapping Theorem any two regions with same connectivity may be conformally mapped to one another. But in practical applications conformal mapping is used only in those cases where the maps take simpler, explicit forms, so that one may carry out actual calculations with those maps.

As the application of conformal mapping is limited to variables which solve the Laplace's equation for two dimensional fields, one such variable of practical interest is the electrostatic potential in a region of space that is free of charges. This chapter, therefore, focuses on application of conformal mapping to determine electrostatic potential field by solving two dimensional Laplace's equation.

Basic Theory of Conformal Mapping

Conformal transformation is based on the properties of analytic functions. Let, $z = x + iy$ be a complex variable such that the real and imaginary parts x and y are real valued variables, and $f(z) = u(z) + iv(z) = u(x, y) + iv(x, y)$ be a complex valued function such that the real and imaginary parts u and v are real and single valued functions of real valued variables x and y.

If the derivative of *f(z)* exists at a point *z*, then the partial derivatives of *u* and *v* exist at that point and obey the Cauchy-Riemann equations as follows.

$$\frac{\partial u}{\partial x} = \frac{\partial v}{\partial y} \text{ and } \frac{\partial u}{\partial y} = -\frac{\partial v}{\partial x} \quad \text{…. 11.1}$$

A function *f(z)* is analytic at a point z_0 if its derivative $f'(z)$ exists not only at z_0 but at every point in the neighborhood of z_0. It can also be shown that if *f(z)* is analytic, the partial derivatives of *u* and *v* of all orders exist and are continuous functions of *x* and *y*. So,

$$\frac{\partial^2 u}{\partial x^2} = \frac{\partial}{\partial x}\left(\frac{\partial u}{\partial x}\right) = \frac{\partial}{\partial x}\left(\frac{\partial v}{\partial y}\right) = \frac{\partial^2 v}{\partial x \partial y} = \frac{\partial}{\partial y}\left(\frac{\partial v}{\partial x}\right) = \frac{\partial}{\partial y}\left(-\frac{\partial u}{\partial y}\right) = -\frac{\partial^2 u}{\partial^2 y}$$

or, $$\frac{\partial^2 u}{\partial x^2} + \frac{\partial^2 u}{\partial y^2} = 0 \quad \text{…. 11.2}$$

In the same way one may get, $\frac{\partial^2 v}{\partial x^2}+\frac{\partial^2 v}{\partial y^2}=0$ …. 11.3

Eqns.(11.2) and (11.3) show that both the functions *u(x,y)* and *v(x,y)* satisfy Laplace's equation.

Any function that has continuous second order partial derivatives and satisfies Laplace's equation is called a Harmonic function. Thus both the real part, *u(x,y)*, and imaginary part, *v(x,y)*, of the complex function *f(z)* are harmonic functions. If the function *f(z) = u(x,y)+iv(x,y)* is analytic, then *u(x,y)* and *v(x,y)* are conjugate harmonic functions. If one of two harmonic functions is known, then the other can be found using Cauchy-Riemann equations.

Thus both the conjugate harmonic functions *u(x,y)* and *v(x,y)* can be used to find the potential since they satisfy Laplace's equation.

Mapping of Shapes

From a different point of view, the complex function *f(z)* can be considered as a tool for change of variables, i.e. a transformation from the complex *z*-plane to the complex *w*-plane, as shown in Fig.11.1, where

$z=x+iy$ and $w=u+iv$

It can also be shown that if the function *f* is analytic at a point $z=z_0$ on the *z*-plane, where the first order derivative $f'(z_0)$ is non-zero, there exists a neighborhood of the point w_0 in the *w*-plane in which the function *w=f(z)* has a unique inverse *z=F(w)*. The functions *f(z)* and *F(w)*, therefore, define a change of variables from (*x,y*) to (*u,v*) and from (*u,v*) to (*x,y*), respectively.

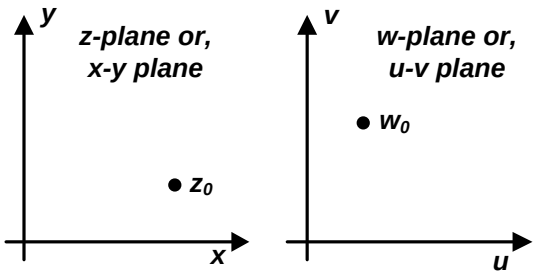

Fig.11.1 Mapping between *z*-plane and *w*-plane

On the *z*-plane, $dz=dx+i\,dy$ and on the *w*-plane $dw=du+i\,dv$

So, $|dz|^2=dx^2+dy^2$ …. 11.4

and $|dw|^2=du^2+dv^2$ …. 11.5

Then, on the *z*-plane, square of the length element can be written as

$dl^2=dx^2+dy^2=|dz|^2$ …. 11.6

and, on the *w*-plane, square of the length element can be written as

$dL^2=du^2+dv^2=|dw|^2$ …. 11.7

Therefore, from eqns.(11.6) and (11.7), it may be written that

$\frac{dL}{dl}=\left|\frac{dw}{dz}\right|$ …. 11.8

Thus, in the neighborhood of each point in *z*-plane, if *w(z)* is analytic and have a non-zero derivative, i.e. finite slope at that point, then the ratio of length elements in two planes remains constant. The net result of this transformation is to change the dimensions in equal

proportions and rotate each infinitesimal area in the neighborhood of that point. In general, a linear transformation $w = f(z) = a\,z + b$, where a and b are complex numbers, rotates by $arg(a)$ in the anti-clockwise direction, dilates or compresses by $|a|$ and translates by b. Thus the ratio of linear dimensions, which may also be represented as the angle, is preserved. As a result, conformal mapping is isogonic because it preserves angles. Hence, all curves in the z-plane that intersect each other at particular angles are mapped into curves in the w-plane that intersect each other at exactly the same angles. This property is most useful for electric field analysis as the equipotentials and the field lines, which are normal to each other in z-plane, are mapped to corresponding curves in w-plane, which are also mutually orthogonal.

Furthermore, $f'(z)F'(w) = \left|\frac{dw}{dz}\right|\left|\frac{dz}{dw}\right| = 1$, which means that the inverse mapping is also conformal. Because of this uniqueness and conformal property of inverse mapping, solution obtained in the w-plane can be mapped back to z-plane.

When infinitesimally small region is considered, then every shape in the z-plane is transformed into a similar shape in the w-plane, e.g. a rectangle in the z-plane remains a rectangle in w-plane. However, shape will not be preserved in general, particularly in a large scale as the value of $\left|\frac{dw}{dz}\right|$ may vary considerably at different points in the z-plane. As a result rotation and scaling will vary from one point in the z-plane to its neighboring point and hence the similarity of shape is not achieved for large regions.

At this juncture, it is pertinent to mention that conformal mapping does not provide a solution to any arbitrary problem. Another question that arises is why one should use conformal mapping instead of numerical methods. The answer to this question is two-fold: firstly analytical solutions to field problems provides insight and secondly it provides useful approximations to difficult problems, which in many cases is valuable to practicing engineers.

Preservation of Angles in Conformal Mapping

As shown in Fig.11.2, two curves A and B intersect each other at an angle α at the point z_i in the z-plane. With the help of the tangent vectors to the curves, the angle between the curves could be computed. Let, t_{zA} and t_{zB} be the tangent vectors to the curves A and B, respectively. Then from the law of cosines it may be written that

$$\alpha = \cos^{-1}\left(\frac{|t_{zA}|^2 + |t_{zB}|^2 - |t_{zA} - t_{zB}|^2}{2|t_{zA}||t_{zB}|}\right) \quad \text{…. 11.9}$$

The corresponding transformed curves A' and B' intersect at an angle β in the w-plane. Let, t'_{wA} and t'_{wB} be the tangent vectors to the curves A' and B', respectively. Then β can be obtained as

$$\beta = \cos^{-1}\left(\frac{|t'_{wA}|^2 + |t'_{wB}|^2 - |t'_{wA} - t'_{wB}|^2}{2|t'_{wA}||t'_{wB}|}\right) \quad \text{…. 11.10}$$

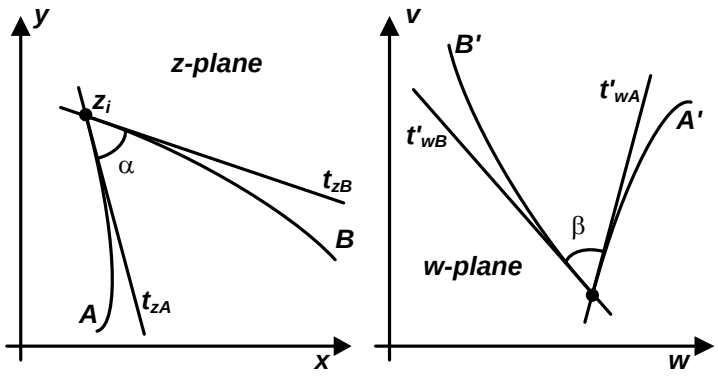

Fig.11.2 Preservation of angles in conformal mapping

Let, a curve is parameterized in *z*-plane by *z=z(p)* and the complex analytic function *w=f(z(p))* defines the mapped curve in the *w*-plane. Then application of chain rule to *w=f(z(p))* gives $t'_w = f'(z(p))t_z(p)$. Since the curves intersect in *z*-plane at $z=z_i$, then $t'_{wA} = f'(z_i)t_{zA}$ and $t'_{wB} = f'(z_i)t_{zB}$. Since $f'(z_i)\neq 0$, hence eqn.(11.10) can be re-written as

$$\beta = \cos^{-1}\left(\frac{\left|f'(z_i)t_{zA}\right|^2 + \left|f'(z_i)t_{zB}\right|^2 - \left|f'(z_i)t_{zA} - f'(z_i)t_{zB}\right|^2}{2\left|f'(z_i)t_{zA}\right|\left|f'(z_i)t_{zB}\right|}\right) \quad \text{…. 11.11}$$

In eqn.(11.11), the absolute value $\left|f'(z_i)\right|^2$ cancels from the numerator and denominator and eqn.(11.11) gets reduced to

$$\beta = \cos^{-1}\left(\frac{\left|t_{zA}\right|^2 + \left|t_{zB}\right|^2 - \left|t_{zA} - t_{zB}\right|^2}{2\left|t_{zA}\right|\left|t_{zB}\right|}\right) \quad \text{…. 11.12}$$

From eqns.(11.9) and (11.10), $\alpha = \beta$, which proves that angles are preserved in conformal mapping.

Problem 11.1

For the point *z=1+i* in the *z*-plane, find the mapped point in the *w*-plane under the linear transformation *w=(1+i)z +(2 +2i).*

Solution

The given transformation function $w = f(z) = (1+i)z + (2+2i) = \sqrt{2}e^{i\frac{\pi}{4}}z + (2+2i)$

Hence, the transformation of the point (*1+i*) in the *z*-plane to the corresponding point in the *w*-plane can be obtained in three steps as shown in Fig.11.3.

Step-1: The length *OP* $\left(\left|z\right|\right)$ is multiplied by $\left|1+i\right| = \sqrt{2}$ to get the length *AB* as shown in Fig.11.3(b).

Step-2: The length *AB* is rotated by an angle ($\pi/4$) in the anti-clockwise direction to get the length *AC*, as shown in Fig.11.3(c).

Step-3: The point *C* is then translated by (*2+2i*) to get the point *P′* (*2+4i*) in the *w*-plane which is the conformally mapped point corresponding to the point *P* in the *z*-plane.

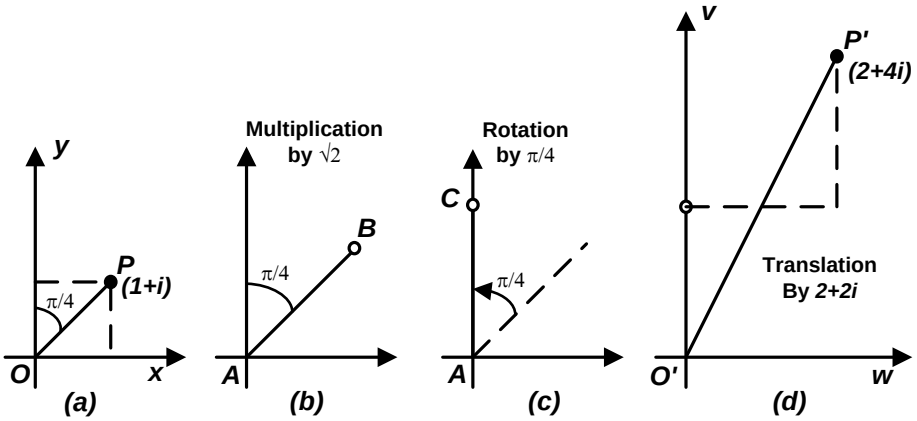

Fig.11.3 Pertaining to Problem 11.1

Problem 11.2

Let Ω be the rectangular region in the *z*-plane bounded by *x=1*, *y=1*, *x=3* and *y=2*. Find the mapped region Ω' in the *w*-plane under the linear transformation *w=(1+i)z +(2 +2i)*.

Solution

Given, $w=f(z)=(1+i)z + (2+2i) = (1+i)(x+iy) + (2+2i) = (x-y+2) + i\,(x+y+2)$

Hence, $u = x-y+2$ and $v = x+y+2$

Therefore, for $x=1$, $u = -y+3$ and $v = y+3$ or, $u+v = 6$, i.e. the line $x=1$ in the *z*-plane is mapped to the straight line $u+v=6$ in the *w*-plane.

Similarly, for $y=1$, $u = x+1$ and $v = x+3$ or, $u-v = -2$

For $x=3$, $u = -y+5$ and $v = y+5$ or, $u+v = 10$

For $y=2$, $u = x$ and $v = x+4$ or, $u-v = -4$

So, the four straight lines in the *z*-plane defined by *x=1*, *y=1*, *x=3* and *y=2* are mapped to four straight lines defined by *u+v = 6*, *u-v = -2*, *u+v = 10* and *u-v = -4*, respectively, in the *w*-plane. The mapping is shown in Fig.11.4. Under the linear transformation *w=az+b*, where *a=1+i* and *b=2+2i*, it may be seen that the rectangular region Ω in the *z*-plane is translated by *b(=2+2i)*, rotated by an angle 45^0 (*=arg(a)=arg(1+i)*) in the anti-clockwise direction and dilated by $\sqrt{2}(=|a|=|1+i|)$ to another rectangular region Ω' in the *w*-plane.

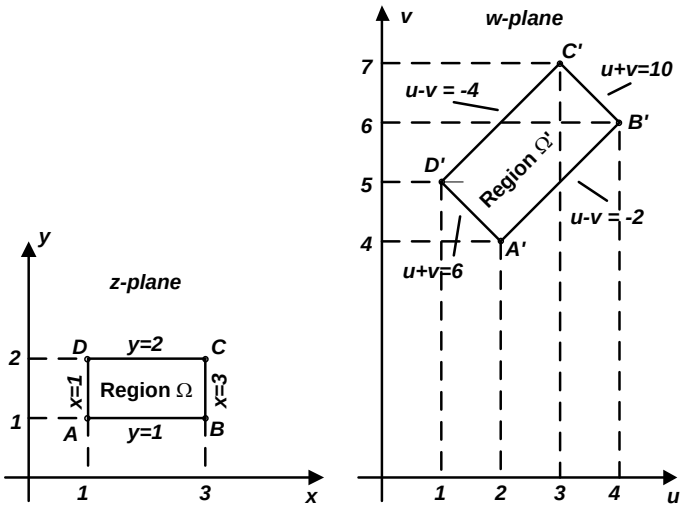

Fig.11.4 Pertaining to Problem 11.2

Concept of Complex Potential

Let, $\phi(x, y)$ be a harmonic function in a domain Ω. It is possible to define a harmonic conjugate function, $\psi(x, y)$, uniquely by Cauchy-Riemann equations in the same domain. Thus an analytic function of $z = x + iy$ in the domain Ω can be written as

$$F(z) = \phi(x, y) + i\psi(x, y) \quad \text{…. 11.13}$$

Consequently, *F(z)* conformally maps the curves in the *z*-plane onto the corresponding curves in the *w*–plane and vice-versa preserving the angles during mapping.

Since, both the real and imaginary parts of *F(z),* viz. $\phi(x, y)$ and $\psi(x, y)$, are harmonic functions, they satisfy Laplace's equation and hence either one of these two could be used to find potential. Thus the complex analytic function *F(z)* is known as complex potential. Laplace's equation is one of the most important partial differential equations in engineering and physics. The theory of solutions of Laplace's equation is known as Potential Theory. The concept of complex potential relates potential theory closely to complex analysis.

If $\phi(x, y)$ is considered to be real potential, then $\phi(x, y) = const$ represents equipotential lines in the *z*-plane. Since, $\phi(x, y)$ and $\psi(x, y)$ are orthogonal, hence, $\psi(x, y) = const$ represents electric field lines in the *z*-plane. For example, consider the complex potential function as $F(z) = Az + B = Ax + B + iAy$. Then the equipotential lines corresponding to $\phi(x, y) = Ax + B = const$ are straight lines parallel to *y*-axis and the electric field lines corresponding to $\psi(x, y) = Ay = const$ are straight lines parallel to *x*-axis.

The introduction of the concept of complex potential is advantageous in the following ways: i) it is possible to handle equipotential and electric field lines simultaneously and ii) Dirichlet problems with difficult geometry of boundaries could be solved by conformal mapping by finding an analytic function *F(z)* which maps a complicated domain Ω in the *z*-plane onto a simpler domain Ω' in the *w*-plane. The complex potential $F'(w)$ is solved in the *w*-plane by satisfying Laplace's equation along with the boundary conditions. Then the complex potential in the *z*-plane can be obtained by inverse transform from which the real potential is obtained as $\phi(x, y) = \mathrm{Re}\{F(z)\}$. This is a practicable way of solution as harmonic functions remain harmonic under conformal mapping.

Procedural Steps in Solving Problems using Conformal Mapping

1) Find an analytic function *w=F(z)* to map the original region Ω in the *z*-plane to the transformed region Ω' in the *w*-plane. The region Ω' should be a region for which explicit solutions to the problem at hand are known.
2) Transfer the boundary conditions from the boundaries of the region Ω in the *z*-plane to the boundaries of the transformed region Ω' in the *w*-plane.
3) Solve the problem and find the complex potential $F'(w)$ for the transformed region Ω' in the *w*-plane.
4) Map the solution $F'(w)$ for the region Ω' in the *w*-plane back to the complex potential *F(z)* for the region Ω in the *z*-plane through inverse mapping.

The steps are schematically shown in Fig.11.5. The most important step is to find an appropriate mapping function *w=F(z),* which fits the problem at hand. Once the right mapping function has been found, the problem is as good as solved.

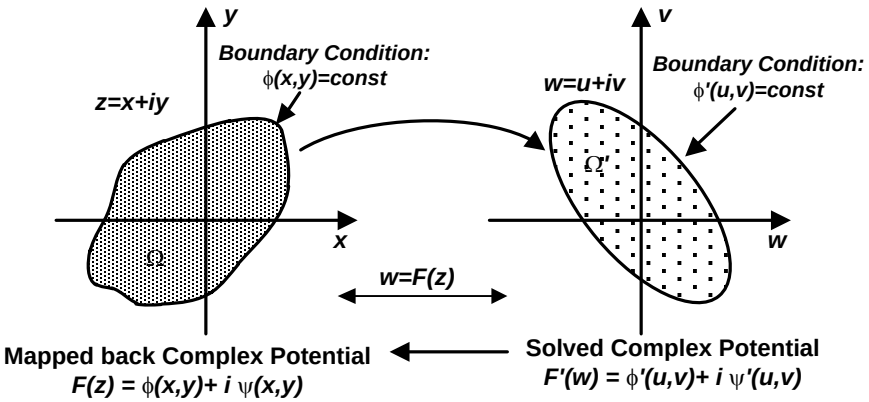

Fig.11.5 Schematic representation of solution of potential problem by conformal mapping

Applications of Conformal Mapping in Electrostatic Potential Problems

Conformal mapping is a powerful method for solving boundary value problems in two-dimensional potential theory through transformation of a complicated region into a simpler region. Electric potential satisfies Laplace's equation in charge free region. Therefore, electrostatic field that satisfies Laplace's equation in a two-dimensional region in *xy*-plane, will also satisfy Laplace's equation in any plane to which the region may be transformed by an analytic complex potential function *F(z)*. For each value of complex $z = x + iy$, there is a corresponding value of complex $w = F(z)$. In other words, for every point in the *z*-plane, there is a corresponding point in the *w*-plane. As a result, the locus of any point in the *z*-plane will trace another path in *w*-plane. Let, the locus in the *z*-plane maps onto a path $\phi'(u,v) = const$ in the *w*-plane, which corresponds to an equipotential and may also be the surface of a conductor. Then the problem can be solved in the *w*-plane incorporating the appropriate boundary condition, i.e. the value of the conductor potential, and the results can be mapped back to *z*-plane to get the real potential and then the electric field lines can be obtained from the conjugate harmonic function. This section discusses some of the applications of conformal mapping in solving two-dimensional electrostatic potential problems.

Conformal Mapping of Co-Axial Cylinders

The cross-sectional view of a single-core cable is shown in Fig.11.6, where the co-axial cylindrical conductors are of infinite length in the direction normal to the plane of the paper. Hence, the field varies only in the cross-sectional plane and is translationally invariant in the direction of the length of the cable. Let, the cross-sectional plane of the cable be the *x*-*y* plane or the *z*-plane. Then the field in the region between the two cylindrical conductors can be found by conformal mapping. Let, the radii of the inner and the outer conductors be r_1 and r_2, respectively, and the potential of the inner and the outer conductors be *V* and zero respectively.

Consider the complex analytical function for conformal mapping be

$$w = u + iv = C_1 \ln(z) + C_2 \qquad \text{.... 11.14}$$

where, $z = x+iy = re^{i\theta}$ such that $r = \sqrt{x^2 + y^2}$ and $\theta = \tan^{-1}(y/x)$

So, $u + iv = C_1 \ln(re^{i\theta}) + C_2 = C_1 \ln r + C_2 + iC_1\theta$

or, $u = C_1 \ln(r) + C_2$ and $v = C_1\theta$ 11.15

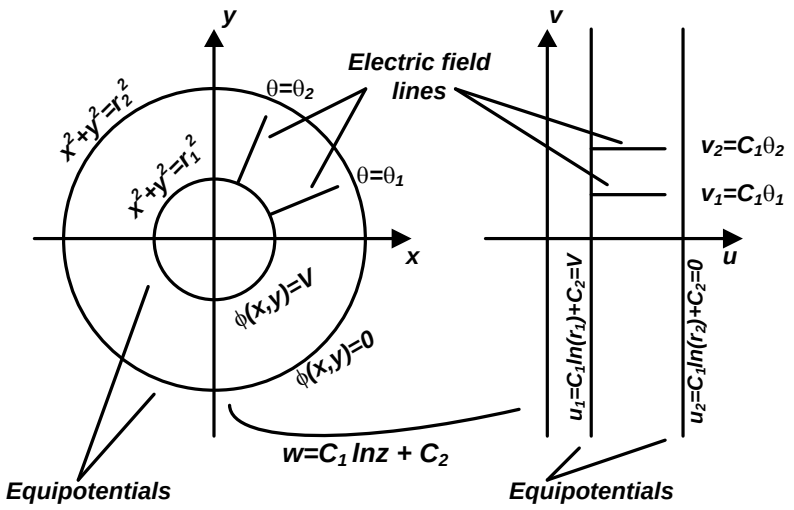

Fig.11.6 Conformal mapping of co-axial cylinders

For the inner conductor, $x^2+y^2=r_1^2$ and hence it maps to a straight line $u_1 = const$ parallel to *v*-axis in the *w*-plane. Similarly, the outer conductor for which $x^2+y^2=r_2^2$ maps to another straight line $u_2 = const$ parallel to *v*-axis in the *w*-plane, as shown in Fig.11.6. In other words, the field within the two cylindrical conductors in the *z*-plane is conformally mapped to field between two infinitely long parallel plates, i.e. the field within a parallel-plate capacitor, in the *w*-plane. From Fig.11.6 it may be seen that the orthogonality of the equipotentials in the form of circles and electric field lines in the form of radial lines in the *z*-plane are maintained in the *w*-plane, where the equipotentials are straight lines parallel to *v*-axis and the electric field lines are straight lines parallel to *u*-axis.

From the boundary conditions on the conductor surfaces

$$C_1 \ln r_1 + C_2 = V \qquad \text{.... 11.16}$$

and $C_1 \ln r_2 + C_2 = 0$ 11.17

From eqns. (11.16) and (11.17),

$$C_1 = -\frac{V}{\ln \frac{r_2}{r_1}} \quad \text{and} \quad C_2 = \frac{V \ln r_2}{\ln \frac{r_2}{r_1}} \qquad \text{.... 11.18}$$

The potential at any radius *r* is given by $u = C_1 \ln r + C_2$. Correspondingly, in the *z*-plane

$$\phi(x,y) = -\frac{V \ln r}{\ln \frac{r_2}{r_1}} + \frac{V \ln r_2}{\ln \frac{r_2}{r_1}} = \frac{V \ln \frac{r_2}{r}}{\ln \frac{r_2}{r_1}} \qquad \text{.... 11.19}$$

Then, $E_r(x,y) = -\frac{\partial \phi}{\partial r} = \frac{V}{r \ln \frac{r_2}{r_1}}$ 11.20

Eqn.(11.20) gives the value of electric field intensity at any radius *r*, which is the same as the one given by eqn.(4.30).

Conformal Mapping of Non Co-Axial Cylinders

Fig.11.7 shows two non co-axial cylinders in the *z*-plane, such that for the outer cylinder C_2, $|z|=1$. Radius of the inner cylinder C_1 is (1/5) and its center is located at a distance of (1/5) from the center of the larger cylinder. In this case also the length of the two cylinders is taken to be infinite in the direction normal to the plane of the paper. Hence, the field in the space between the two cylinders does not vary in the direction of the length of the cylinders. So the cross-sectional plane is shown to be the *z*-plane in Fig.11.7. The inner cylinder is at a potential of *V* while the outer cylinder is earthed. Direct solution of the field between the two cylinders is difficult in the *z*-plane. However, it is possible to conformally map the non co-axial cylinders in the *z*-plane onto two co-axial cylinders in the *w*-plane keeping the boundary conditions, i.e. boundary potentials, same.

In this transformation, the unit radius outer circle C_2 in the *z*-plane is mapped onto a unit radius circle C'_2 in the *w*-plane in such a way that the inner circle C'_1 becomes concentric with a radius r_i, as shown in Fig.11.7. The mapping function for this linear fractional transformation is

$$w=\frac{z-k}{k\,z-1} \qquad \text{…. 11.21}$$

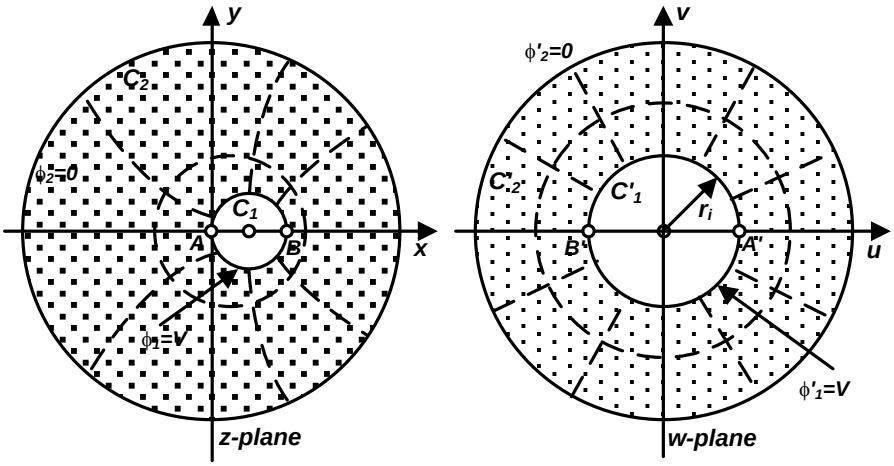

Fig.11.7 Conformal mapping of non co-axial cylinders

As shown in Fig.11.7, the two points on the inner circle $A(0,0)$ and $B(\frac{2}{5},0)$ in the *z*-plane are mapped onto two points $A'(r_i,0)$ and $B'(-r_i,0)$ on the inner circle in the *w*-plane.

Hence, from eqn.(11.21) for the points $A(0,0)$ and $A'(r_i,0)$ $\quad r_i=\frac{0-k}{0-1}=k$

and for the points $B(\frac{2}{5},0)$ and $B'(-r_i,0)$ $\quad -r_i=\frac{\frac{2}{5}-k}{\frac{2k}{5}-1}=\frac{2-5r_i}{2r_i-5}$

or, $r_i^2-5r_i+1=0$, or, r_i=4.79 and 0.208.

But, r_i cannot be greater than 1 and hence, r_i= 0.208. Therefore, $k = r_i = 0.208$.

Thus the mapping function for this problem is $w=\frac{z-0.208}{0.208\,z-1}$ …. 11.22

Writing the complex potential function in the *w*-plane as $F'(w) = a \ln w + b$, the real part of the complex potential can be written as

$$\phi'(u,v) = \mathrm{Re}\{F'(w)\} = a \ln|w| + b \quad \text{…. 11.23}$$

Two conditions on boundary potentials in the *w*-plane are as follows: i) $\phi' = 0$ for $|w| = 1$ and ii) $\phi' = V$ for $|w| = r_i$

Application of first boundary condition on eqn.(11.23) yields

$a \ln 1 + b = 0$, or, $b = 0$

Similarly, applying the second boundary condition on eqn.(11.23) one would get

$a \ln r_i + b = V, or \ \ln 0.208 = V$, or, a = -0.6368V

Thus the desired solution for complex potential in the *z*-plane is

$$F(z) = -0.6368V \ln \frac{z - 0.208}{0.208z - 1} \quad \text{…. 11.24}$$

The real potential within the two cylinders is then given by

$$\phi(x,y) = \mathrm{Re}\{F(z)\} = -0.6368V \ln \left| \frac{z - 0.208}{0.208z - 1} \right| \quad \text{…. 11.25}$$

If the potentials are $+V$ and $-V$ instead of V and 0, then from the first boundary condition

$a \ln 1 + b = -V$, or b = -V

and from the second boundary condition $a \ln r_i + b = V$, or, $a \ln 0.208 - V = V$ or, a = -1.273V

Hence, the desired solution for complex potential in the *z*-plane is

$$F(z) = -1.273V \ln \frac{z - 0.208}{0.208z - 1} - V = V\left(-1.273 \ln \frac{z - 0.208}{0.208z - 1} - 1 \right) \quad \text{…. 11.26}$$

The real potential within the two cylinders is then given by

$$\phi(x,y) = \mathrm{Re}\{F(z)\} = V\left(-1.273 \ln \left| \frac{z - 0.208}{0.208z - 1} \right| - 1 \right) \quad \text{…. 11.27}$$

Conformal Mapping of Unequal Parallel Cylinders

Fig.11.8 shows two unequal parallel cylinders in the *z*-plane, such that for the larger cylinder $C_2, |z| = 1$. Radius of the smaller cylinder C_1 is (1/2) and its center is located at a distance of (7/2) from the center of the larger cylinder. In this case also the length of the two cylinders is taken to be infinite in the direction normal to the plane of the paper. Hence, the field in the space between the two parallel cylinders does not vary in the direction of the length of the cylinders. So the cross-sectional plane is shown to be the *z*-plane in Fig.11.8. The smaller cylinder is at a potential of V while the larger cylinder is earthed. It is possible to map these two parallel cylinders onto two co-axial cylinders in the *w*-plane as follows.

In this transformation, too, the unit radius larger circle C_2 in the *z*-plane is mapped onto a unit radius circle C'_2 in the *w*-plane in such a way that the smaller circle C'_1 becomes concentric with a radius r_i, as shown in Fig.11.8. The mapping function for this linear fractional transformation is also

$$w = \frac{z - k}{k z - 1} \quad \text{…. 11.28}$$

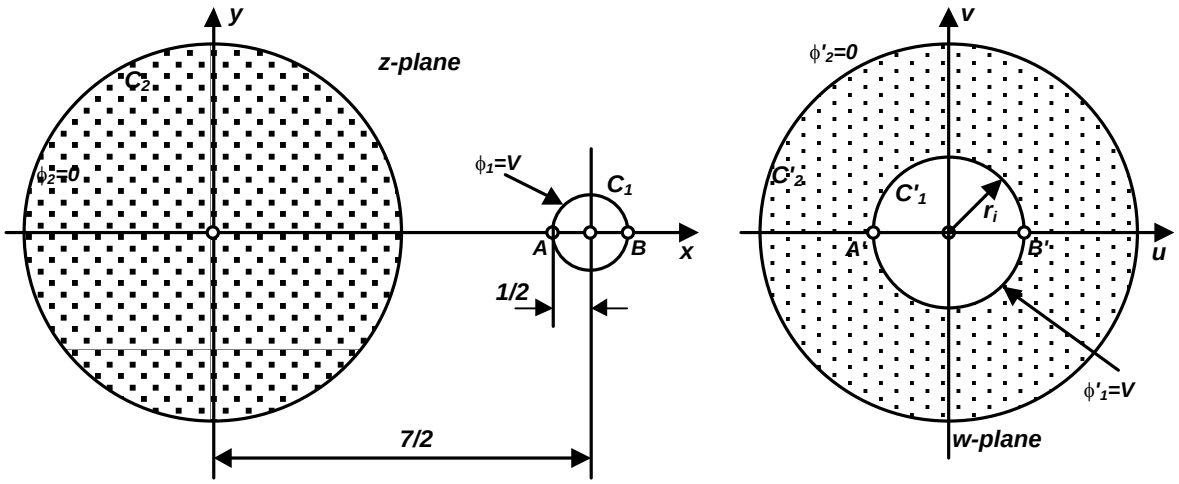

Fig.11.8 Conformal mapping of two unequal parallel cylinders

However, as shown in Fig.11.8, the two points on the inner circle $A(3,0)$ and $B(4,0)$ in the z-plane are mapped onto two points $A'(-r_i,0)$ and $B'(r_i,0)$ on the inner circle in the w-plane.

Hence, from eqn.(11.26) for the points $A(3,0)$ and $A'(-r_i,0)$ $\quad -r_i = \dfrac{3-k}{3k-1}$

and for the points $B(4,0)$ and $B'(r_i,0)$ $\quad r_i = \dfrac{4-k}{4k-1} = \dfrac{k-3}{3k-1}$

or, $7k^2 - 26k + 7 = 0$, or, k = 3.42 and 0.292.

For k=3.42, r_i=0.046 and for k=0.292, r_i=21.84.

But r_i cannot be greater than 1 in the w-plane, so the solution is k=3.42 and r_i=0.046.

Writing the same complex potential function in the w-plane as $F'(w) = a \ln w + b$, as in section 11.5.2, and applying the same boundary conditions for potential, as shown in Fig.11.8,

b=0 and $a = \dfrac{V}{\ln r_i} = \dfrac{V}{\ln 0.046} = -0.3247V$

Thus the desired solution for complex potential in the z-plane is

$$F(z) = -0.3247V \ln \frac{z-3.42}{3.42z-1} \qquad \text{…. 11.29}$$

The real potential between the two unequal parallel cylinders is then given by

$$\phi(x,y) = \mathrm{Re}\{F(z)\} = -0.3247V \ln \left| \frac{z-3.42}{3.42z-1} \right| \qquad \text{…. 11.30}$$

If the potentials are $+V$ and $-V$ instead of V and 0, then from the first boundary condition $a \ln 1 + b = -V$, or b = $-V$

and from the second boundary condition $a \ln r_i + b = V$, or, $a \ln 0.046 - V = V$ or, a = -0.6494V

Hence, the desired solution for complex potential in the z-plane is

$$F(z) = -0.6494V \ln \frac{z-3.42}{3.42z-1} - V = V\left(-0.6494 \ln \frac{z-3.42}{3.42z-1} - 1 \right) \qquad \text{…. 11.31}$$

The real potential between the two unequal parallel cylinders is then given by

$$\phi(x,y) = \mathrm{Re}\{F(z)\} = V\left(-0.6494 \ln \left| \frac{z-3.42}{3.42z-1} \right| - 1 \right) \qquad \text{…. 11.32}$$

Conformal Mapping of Equal Parallel Cylinders

With reference to Fig.11.8, if the radius of the cylinder-1, i.e C_1, is taken to be unity, then k=2.906 and r_i=0.064

Hence, if the potentials of the two cylinders are V and 0, respectively, then the desired solution for complex potential in the z-plane is

$$F(z) = -0.3638V \ln\frac{z-2.906}{2.906z-1} \quad \text{…. 11.33}$$

The real potential between the two equal parallel cylinders is then given by

$$\phi(x,y) = \mathrm{Re}\{F(z)\} = -0.3638V \ln\left|\frac{z-2.906}{2.906z-1}\right| \quad \text{…. 11.34}$$

If the potentials of the two cylinders are $+V$ and $-V$, respectively, then the desired solution for complex potential in the z-plane is

$$F(z) = -0.7276V \ln\frac{z-2.906}{2.906z-1} - V = V\left(-0.7276 \ln\frac{z-2.906}{2.906z-1} - 1\right) \quad \text{…. 11.35}$$

The real potential between the two equal parallel cylinders is then given by

$$\phi(x,y) = \mathrm{Re}\{F(z)\} = V\left(-0.7276 \ln\left|\frac{z-2.906}{2.906z-1}\right| - 1\right) \quad \text{…. 11.36}$$

Graphical Field Plotting

Introduction

Most of the practical problems have such complicated geometry that no exact method of finding the electric field is possible or feasible and approximate techniques are the only ones which can be used. Out of the several approximate techniques, numerical techniques are now extensively used to determine electric field distribution with high accuracy. Numerical techniques, which are widely used, will be discussed in details in the later chapters. In this chapter, experimental and graphical field mapping methods are discussed. Experimental field mapping involve special equipments such as electrolytic tank, a device for fluid flow, conducting paper and associated measuring system. The other mapping method is a graphical one and needs only paper and pencil. In both these methods, the exact value of the field quantities could not be determined, but accuracy level which is sufficient for practical engineering applications could be achieved. Graphical field plotting is economical compared to experimental method and is also capable of providing good accuracy when used with skill. Accuracy of the order of 5 to 10% in capacitance determination could be achieved even by a non-expert simply by following the rules.

Experimental Field Mapping

Experimental method of field mapping is based on the analogy of stationary current field with static electric field, as presented in Table 12.1, rather than directly on measurement of electric field. If the medium between electrodes is isotropic, then volume conductivity and dielectric constant do not vary with position. Then current density (J) in stationary current field and electric field intensity (E) and electric flux density (D) in static electric field will be in the same direction. In other words, current density and electric field lines are the same. Thus for a given electrode system, if a slightly conducting material, e.g. conducting paper or an electrolyte, is placed instead of a dielectric material between the electrodes, then electric field lines and equipotential lines will remain the same.

It is well known that if one travels along a line through an electric field and measures electric scalar potential V as one goes, then the negative of the rate of change of V is equal to the component of electric field intensity E in the direction of travel. In other words,

$$\vec{E} = -\frac{\partial V}{\partial l}\hat{u}_l \qquad \text{…. 12.1}$$

If $-\frac{\partial V}{\partial l}$ is maximum, then it gives the value of E itself. If electric potential does not change with position, then the path of travel is at right angles to the electric field and is along an equipotential. Thus electric field could be mapped by a voltmeter that will measure potential difference and two metal rods acting as probes. The probes are connected to the terminals of the voltmeter and are placed in various positions in an electric field to monitor the potential differences between the positions of the two probes.

Table 12.1 Analogy between static electric field and stationary current field

Static Electric Field	Stationary Current Field
Electric Flux	Electric Current
$\vec{D} = \varepsilon \vec{E}$	$\vec{J} = \kappa \vec{E}$
Dielectric constant	Volume conductivity
$Q = \oint_S \vec{D}.d\vec{s}$	$I = \oint_S \vec{J}.d\vec{s}$

For the determination of equipotential lines one probe is kept still, while the other probe is moved. In whichever position of the moving probe the voltmeter registers a zero reading; the potential of the moving probe is same as that of the standstill probe. By marking each such position, equipotentials could be traced.

For tracing electric field lines the two probes are kept at a constant separation distance and one probe is rotated around the other. The position of the rotating probe where the voltmeter registers a maximum reading, the electric field is changing at its maximum rate. Hence, the electric field at that location of the rotating probe is parallel to the line joining the two probes. By repeating this measurement process at several positions, the electric field could be mapped.

Since a real-life voltmeter draws a current, however small it may be, measurement of the potential differences using voltmeter could not be done with vacuum or air as the medium. In practice, measurement is carried out for the electric field that is set up in a medium, which is slightly conducting.

Commonly slightly conducting paper, e.g. paper impregnated with carbon, is used. Since the paper is slightly conducting, the electric field due to the charged electrodes is almost the same as the one that would be produced in air or vacuum with similar geometry. At the same time the paper is sufficiently conducting to supply the small current needed by the voltmeter.

Alternately electrolytic tank setup is used which consists of a specially fabricated insulating tray. A large sheet of laminated graph paper is pasted on the base plate of the tray. The tray is then half-filled with an electrolyte and the height of the electrolyte is kept same throughout the tray. Metallic electrodes are placed in the electrolytic tank, which are shaped to conform to the boundaries of the problem, and appropriate potential difference between the electrodes is maintained.

Field Mapping using Curvilinear Squares

Field mapping by curvilinear squares is a graphical method based on the orthogonal property of a pair of conjugate harmonic functions and also on the geometric considerations. This method is suitable for mapping only those fields in which there is no variation of field in the direction normal to the plane of the sketch, i.e. the field is two-dimensional in nature. Many practical electric field problems may be considered as two dimensional, e.g. the co-axial cylindrical system or a pair of long parallel wires. In these cases the field remains same in all cross-sectional planes. It is a fact that no real system is infinitely long, but the idealization is a useful one for electric field analysis and visualization.

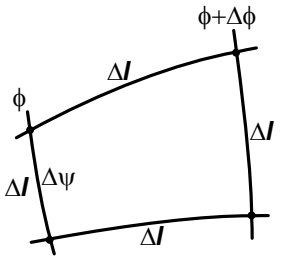

Fig.12.1 A typical curvilinear square

In this method the field region of interest is discretized into a network of curvilinear squares formed by flux or field lines and equipotentials. Curvilinear square is a planar geometric figure which is different from a true square as its sides are slightly curved and slightly unequal, but which approaches a true square as its dimensions become small. A typical curvilinear square is shown in Fig. 12.1. The field map thus obtained is unique for a given problem and helps in understanding the behaviour of electric field through visualization. The method of curvilinear square is capable of handling problems with complicated boundaries. A curvilinear field map is also independent of field property coefficients and could be directly applied from one physical field to another if an analogy exists between the concerned fields.
Theoretically curvilinear field mapping is based on Cauchy-Riemann relations, which ensures that the Laplace's equation is satisfied by a conjugate pair of harmonic functions in any orthogonal coordinate system. Hence, this method utilizes the fieldline coordinate representation of electric field such that electric field is always tangent to the fieldlines and depends only on the distribution of fieldlines and equipotentials.

Foundations of Field Mapping

Construction of field map using curvilinear squares is based on some significant features of electric field as described below:
i) A conductor boundary is one of the equipotentials.
ii) Equipotential and electric field intensity (or electric flux density) are normal to each other. As a conductor boundary is an equipotential, hence electric field intensity and electric flux density vectors are always perpendicular to the conductor boundaries.
iii) Electric flux lines (often termed as streamlines) originate and terminate on charges. Hence, in the case of a homogeneous and charge free dielectric medium, electric flux lines originate and terminate on conductor boundaries.
Fig.12.2 shows two coaxial cylindrical conductor boundaries having a specified potential difference (V) and extending 1m into the plane of the paper. A field line is considered to leave the boundary with more positive electric potential making an angle of 90^0 with the boundary at the point X. If the line is extended following the rule that it is always perpendicular to the equipotentials and if the dielectric medium is considered to be homogeneous and charge free, then the fieldline will terminate normally on the boundary of the less positive conductor at the point X' as shown in Fig.12.2. In a similar manner, another fieldline could be drawn in such a way that it starts from the point Y on the more positive conductor boundary and terminates on the point Y' on the less positive conductor boundary. As the fieldlines are drawn perpendicular to the equipotentials everywhere, electric field intensity and hence electric flux density will be tangent to a fieldline everywhere on it. Consequently, no electric flux can cross any fieldline thus drawn. Therefore, if there is a charge of ΔQ on the surface of the conductor between the points X and Y, then a flux of $\Delta\psi = \Delta Q$ will originate in this region and must terminate on the surface of the other conductor boundary between the points X' and Y'. Such a pair of fieldlines is known as a

"*flux tube*" as it seems to carry flux from one conductor to the other without losing any flux in between the two conductors. For simplification of interpretation of the field map, another flux tube *YZ* may be drawn in such a way that the same amount of flux is carried in the flux tubes *XY* and *YZ*. The method of determination of dimensions of the curvilinear square for drawing such flux tubes is described in the next section.

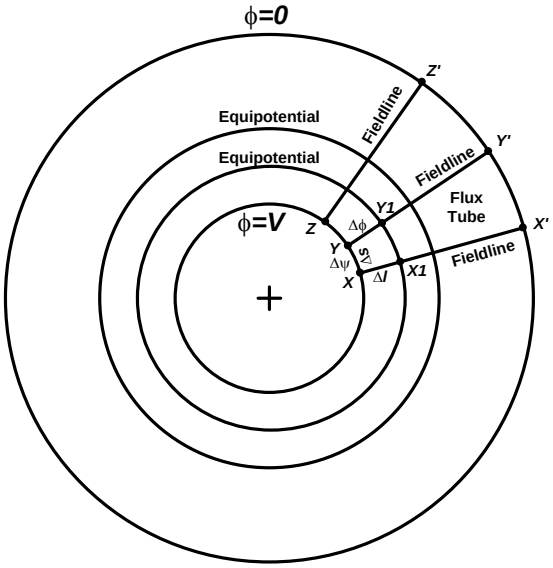

Fig.12.2 Field map between two co-axial cylinders

Sketching of Curvilinear Squares

Considering the length of the line joining the points *X* and *Y* to be Δs, the flux in the tube *XY* to be $\Delta\psi$ and the depth of the tube to be 1m into the paper, the electric flux density at the midpoint of this line is then given by

$$D = \frac{\Delta\psi}{\Delta s} \qquad \text{…. 12.2}$$

So, considering the permittivity of dielectric medium to be ε, electric field intensity at the midpoint of the line *XY* is then given by

$$E = \frac{1}{\varepsilon}\frac{\Delta\psi}{\Delta s} \qquad \text{…. 12.3}$$

Alternately, electric field intensity could also be determined from the potential difference between the points *X* and *X1* lying on the same fieldline on two equipotentials as shown in Fig.12.2.

Considering the length of the line joining the points *X* and *X1* to be Δl and the potential difference between the two consecutive equipotentials to be $\Delta\phi$, electric field intensity at the midpoint of the line *X-X1* is then given by

$$E = \frac{\Delta\phi}{\Delta l} \qquad \text{…. 12.4}$$

Considering Δs and Δl to be small, the two values of electric field intensity as given by eqns. (12.3) and (12.4) may be taken to be equal. Hence,

$$\frac{1}{\varepsilon}\frac{\Delta\psi}{\Delta s} = \frac{\Delta\phi}{\Delta l}$$

or, $$\frac{\Delta l}{\Delta s} = \varepsilon\frac{\Delta\phi}{\Delta\psi} \qquad \text{…. 12.5}$$

For sketching the field map, consider the following: a) homogeneous dielectric having a constant permittivity ε, ii) constant amount of electric flux per tube, i.e. $\Delta\psi$ is constant, and iii) constant potential difference between two consecutive equipotentials, i.e. $\Delta\phi$ is constant. Then from eqn.(12.5), $\frac{\Delta l}{\Delta s} = constant$. In other words, the ratio of the distance between fieldlines as measured along an equipotential and the distance between equipotentials as measured along a fieldline must be maintained constant and not the individual lengths. The simplest ratio of lengths that can be maintained is unity, so that $\Delta l = \Delta s$. Then the field region is divided into curvilinear squares by the fieldines and equipotentials.

The field map thus obtained is composed of curvilinear squares of the same kind such that each square has the same potential difference across it and also has the same amount of flux through it. For a given $\Delta\phi$ and $\Delta\psi$, the sides of a curvilinear square are thus inversely proportional to electric field intensity. For a non-uniform field electric field intensity varies with location and hence Δl and Δs vary with the strength of electric field. In the region of higher field strength, Δl and Δs are to be kept small, i.e. the squares are to be made smaller in size where the magnitude of the field intensity is high. On the other hand, the squares are made larger in size in the field region where the field intensity is low.

It may be recalled that the product of electric charge and electric potential difference is the energy of electric field. Moreover, electric charge and electric flux has a one to one correspondence. Thus for a field map if $\Delta\phi$ and $\Delta\psi$ are kept constant, then their product remains constant and hence, energy of electric field remains constant. Therefore, curvilinear squares having the same ratio as give by eqn.(12.5) have the same energy stored in electric field regardless of the size of the square. A curvilinear square can thus be scaled up or down keeping the energy stored in the curvilinear square unaltered as long as the ratio given by eqn.(12.5) remains unaltered.

Construction of Curvilinear Square Field Map

The fieldines and equipotentials are typically drawn on the original sketch which shows the conductor boundaries. Arbitrarily one fieldline is begun from a point on the surface of the more positive conductor with a suitable value of Δl and an equipotential is drawn perpendicular to the fieldline with a value of $\Delta s = \Delta l$. Then another fieldline is added to complete the curvilinear square. The field map is then gradually extended throughout the field region of interest. As the field map is extended, the condition of orthogonality of fieldline and equipotential should be kept paramount, even if this results in some squares with ratios other than unity. Construction of a satisfactory field map using curvilinear squares is a trial and error process that involves continuous adjustment and refinement. Typically the field maps are started as a course map having large curvilinear squares. Then the field map is fine tuned through successive subdivisions to form a dense field map having higher accuracy. In the process of subdivision, the lengths between consecutive fieldlines as well as equipotentials are kept equal. Before starting the construction of a field map, it is a judicious practice to examine the geometry of the system and take advantage of any symmetry that may exist in the system under consideration. This is because of the fact the lines of symmetry serve as boundaries with no flux crossing and thereby separate regions of similar field maps.

Capacitance Calculation from Field Map

Once the field map is drawn, it is possible to determine the capacitance per unit length between the two conductors using the field map. It is well known that capacitance between

two conductors having a potential difference of V is given by $C=\frac{Q}{V}$, where Q is the charge on the conductor. Applying Gauss's law on a Gaussian surface enclosing the conductor having more positive potential, $Q=\psi$, where ψ is the flux coming out of the conductor. Thus, $C=\frac{\psi}{V}$.

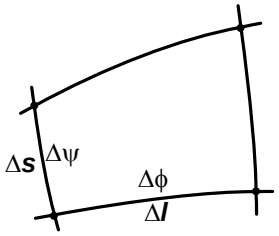

Fig.12.3 An isolated curvilinear rectangle

To calculate the capacitance with the help of curvilinear rectangle, consider first an isolated curvilinear rectangle as shown in Fig.12.3. Let the flux through it be $\Delta\psi$ and the potential difference across it be $\Delta\phi$. Considering the curvilinear rectangle to be small, the flux density may be assumed uniform within the curvilinear rectangle so that

$$\Delta\psi=\varepsilon E\,\Delta s\times 1 \qquad \text{…. 12.6}$$

where, the depth is taken to be 1m into the plane of the field map.

Electric field intensity (E) and the potential difference $\Delta\phi$ are related as

$$\Delta\phi=E\times\Delta l \qquad \text{…. 12.7}$$

Combining eqns. (12.6) and (12.7)

$$\Delta\psi=\varepsilon\,\Delta s\times\frac{\Delta\phi}{\Delta l}$$

Therefore, the capacitance of the small curvilinear rectangle, which may be taken as a small field cell, is given by

$$\Delta C=\frac{\Delta\psi}{\Delta\phi}=\varepsilon\,\frac{\Delta s}{\Delta l} \qquad \text{…. 12.8}$$

The total amount of flux (ψ) emanating from one conductor and terminating on the other conductor may be obtained by adding all the small amounts of flux ($\Delta\psi$) through each flux tube so that

$$\psi=\sum_{N_\psi}\Delta\psi=N_\psi\,\Delta\psi \qquad \text{…. 12.9}$$

where, $\Delta\psi$ is assumed to be same for each flux tube and N_ψ is the number of flux tubes in parallel, i.e. the number of curvilinear rectangles in parallel.

The total potential difference between the two conductors (V) may be obtained by adding all the small amounts of potential differences ($\Delta\phi$) between consecutive equipotentials starting from one conductor and finishing at the other conductor, i.e.

$$V=\sum_{N_\phi}\Delta\phi=N_\phi\,\Delta\phi \qquad \text{…. 12.10}$$

where, $\Delta\phi$ is assumed to be same between any two consecutive equipotentials and N_ϕ is the number of equipotentials (including the two conductors) minus one, i.e. the number of curvilinear rectangles in series between the two conductors.

Thus capacitance per unit length of the two conductors is given by

$$C = \frac{\psi}{V} = \frac{N_\psi}{N_\phi}\frac{\Delta\psi}{\Delta\phi} = \frac{N_\psi}{N_\phi}\frac{\varepsilon\Delta s}{\Delta l} = \varepsilon\frac{N_\psi}{N_\phi} \quad \text{…. 12.11}$$

where, $\Delta s = \Delta l$, considering the ratio of the lengths to be unity, i.e. considering curvilinear squares.

Hence, determination of capacitance from the field map involves counting of curvilinear squares in two directions, one in series between the two conductors and the other in parallel around either conductor.

Field Mapping in Multi-dielectric Media

From eqn.(12.5), it may be seen that for the same value of electric flux per tube and same potential difference between two consecutive equipotentials,

$$\frac{\Delta l}{\Delta s} \propto \varepsilon \quad \text{…. 12.12}$$

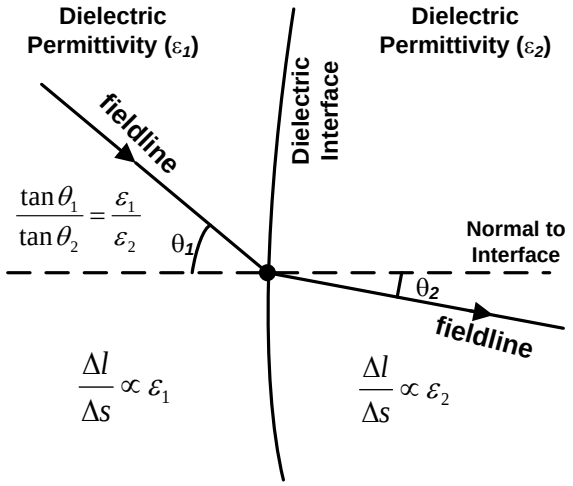

Fig.12.4 Mapping in two-dimensional configuration with multi-dielectric media

Thus in the case of a two dielectric configuration as shown in Fig.12.4, the ratio of the sides of curvilinear element is to be made proportional to the relative permittivity of the dielectric medium in which the field map is drawn. In other words, curvilinear rectangles are to be used.

Moreover, the deviation of the fieldlines takes place at the boundary between the two dielectric media, as shown in Fig.12.4, which is given for charge free dielectric media by

$$\frac{\tan\theta_1}{\tan\theta_2} = \frac{\varepsilon_1}{\varepsilon_2} \quad \text{…. 12.13}$$

For two-dimensional configurations comprising multi-dielectric media, the field map is first drawn in the field region where there is only one dielectric media. Then the directions of the fieldlines are changed at the boundary between the two dielectric media according to eqn.(12.13). Subsequently the ratio of the sides of the curvilinear rectangles is changed as per eqn.(12.12) and the field map is extended into the field region comprising a different dielectric medium. In this way the field map could be obtained in configurations comprising several dielectric media.

Field Mapping in Axi-Symmetric Configuration

Consider a curvilinear rectangle in an axi-symmetric configuration as shown in Fig.12.5. Let the radial distance of the centroid of the curvilinear rectangle from the axis of rotational symmetry be *r*.

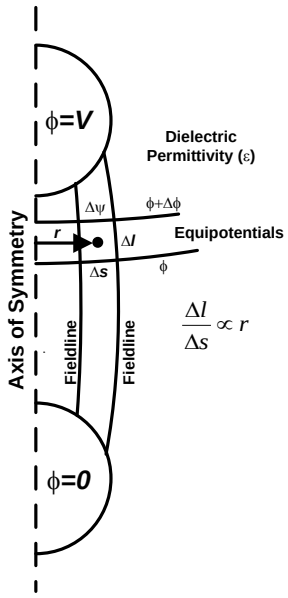

Fig.12.5 Field mapping in axi-symmetric configuration

Considering the flux through the rectangle to be $\Delta\psi$ and assuming the square to be small, the electric flux density can be taken to be uniform within the rectangle and is given by

$$D=\frac{\Delta\psi}{2\pi r\Delta s}$$

or, $$E=\frac{\Delta\psi}{2\pi\varepsilon r\Delta s} \quad \text{…. 12.14}$$

Alternately, electric field intensity as obtained from the potential difference between two consecutive equipotentials, which are the two sides of the rectangle perpendicular to the fieldlines, is given by

$$E=\frac{\Delta\phi}{\Delta l}$$

Considering a small curvilinear rectangle, these two values of electric field intensity could be taken as same such that

$$\frac{\Delta\psi}{2\pi\varepsilon r\Delta s}=\frac{\Delta\phi}{\Delta l}$$

or, $$\frac{\Delta l}{\Delta s}=2\pi\varepsilon r\frac{\Delta\phi}{\Delta\psi} \quad \text{…. 12.15}$$

Considering i) homogeneous dielectric having a constant permittivity ε, ii) constant amount of electric flux per tube, i.e. $\Delta\psi$ is constant, and iii) constant potential difference between two consecutive equipotentials, i.e. $\Delta\phi$ is constant,

$$\frac{\Delta l}{\Delta s}\propto r \quad \text{…. 12.16}$$

Hence, to draw field maps in axi-symmetric configurations comprising a homogeneous dielectric, the ratio of the sides of the curvilinear rectangles is to be increased in direct proportion to the radial distance of the square from the axis of rotational symmetry.

For axi-symmetric configurations comprising multiple dielectric media, eqn.(12.16) is to be rewritten in the light of eqn.(12.15) as

$$\frac{\Delta l}{\Delta s} \propto \varepsilon r \qquad \text{…. 12.17}$$

So for multi-dielectric media in axi-symmetric configurations, the ratio of the sides of the curvilinear rectangles is to be increased not only in direct proportion to the radial distance of the square from the axis of rotational symmetry, but also in direct proportion to the relative permittivity of the dielectric medium in which the field map is drawn. The directions of the fieldlines at the boundary between the two dielectric media are to be changed according to eqn.(12.13).